ABSTRACT

JI, MIKYOUNG LEE. Superoxide Reductase from the Hyperthermophilic Archaeon *Pyrococcus furiosus*: its Function, Regulation, and Biotechnological Applications. (Under the direction of Amy M. Grunden.)

The anaerobic hyperthermophilic archaeon, *Pyrococcus furious*, possesses a system for the detoxification of reactive oxygen species, which is different from the classical defense mechanisms present in aerobes. *P. furiosus* employs a novel enzyme system centered on the enzyme superoxide reductase (SOR), which reduces superoxide molecules to hydrogen peroxide without producing oxygen. Surprisingly, *P. furiosus* SOR, unlike many *P. furiosus* enzymes, was shown to function at low temperature ($<25^{o}$ C). A model for superoxide reduction by SOR was proposed where the electrons used by SOR to reduce superoxide are supplied by a small iron containing protein, rubredoxin (Rd), and Rd is reduced by the oxidoreductase, NAD(P)H-rubredoxin oxidoreductase (NROR). The first objective of this study was to evaluate the validity of the proposed superoxide reduction pathway by using the recombinant SOR, Rd and NROR enzymes in an *in vitro* assay as well as to demonstrate *in vivo* function via complementation studies in superoxide detoxification deficient *Escherichia coli* strains. The second objective was to investigate the transcriptional expression levels of genes that are involved in the SOR-centered superoxide reduction pathway in order to determine how these genes are expressed and regulated in response to various oxidative stresses. The third objective was to evaluate the efficacy of the biotechnological application of this superoxide detoxification system by expressing SOR in plant cells, which enhanced their survival at high temperature and from drought indicating that it functions successfully *in vivo*. The fourth objective of this study was the characterization of glutathione reductase (GR) from

a psychrophile, *Colwellia psychrerythraea*, which is stable at low temperatures and protects cells from free radicals by serving as a reductant. The *C. psychrerythraea* GR gene was cloned into an *E. coli*-based recombinant expression system. Recombinant *C. psychrerythrae* GR was expressed and purified. The recombinant GR showed significant activity at low temperature (4°C). The *P. furiosus* superoxide reduction system genes and GR from *C. psychrerythraea* can be engineered into plants (Arabidopsis) to aid in combating damage caused by oxidative stress when plants undergo rapid changes in temperature, high light or UV exposure, or drought conditions.

Superoxide Reductase from the Hyperthermophilic Archaeon *Pyrococcus furiosus*: its Function, Regulation, and Biotechnological Applications

by

Mikyoung Lee Ji

A dissertation submitted to the Graduate faculty of
North Carolina State University
In partial fulfillment of the
Requirements for the degree of
Doctor of Philosophy

Microbiology

Raleigh, N.C.

2007

APPROVED BY:

---	---
Dr. Amy M. Grunden (Chair of Advisory committee)	Dr. Hosni M. Hassan
---	---
Dr. Wendy F. Boss	Dr. Jonathan W. Olson

DEDICATION

I would like to dedicate this work to my mother, Haeok Lee, who gave me motivation, strength and encouragement. Without her support, this work couldn’t be accomplished.

BIOGRAPHY

Mikyoung Lee Ji was born to Haeok and Hunyoung Lee in Seoul, Korea on October 10th 1961. She received her primary education in Seoul, Korea. She entered Kyunghee University at Seoul, Korea in 1980 and majored in microbiology. She married Chueng Ji in 1983 and moved to Palo Alto, California where she had her first son, Stephen Ji. In 1985, she continued to study microbiology at San Jose University in San Jose, CA. Her family moved to Brooklyn, New York in 1986 where she transferred to Brooklyn City College. Her family moved to Raleigh, NC in 1987, and she finally received her Bachelors degree in microbiology in December 1988 from North Carolina State University. She stayed at home raising her family from 1989 to 2000 and she had two more children, Lisa and David. In 2000, Mikyoung was admitted to the Masters of Microbiology program at North Carolina State University and transferred to Masters of Science program in 2001 and finished it in 2003 under the direction of Dr. Amy Grunden. She continued her graduate career by entering the Ph.D. program in the Microbiology department at North Carolina State University in 2003 again under the direction of Dr. Grunden.

ACKNOWLEDGEMENTS

First of all, I would like to thank God who gave me strength. I am very thankful to my family who understands, supports, and encourages me all the time. I would like to give special appreciation to Amy Grunden, my advisor, who trained me as a scientist with endless patience and excellent guidance. Without these people, I couldn't accomplish this work.

I would like to thank to all of our lab graduate students, Alice Lee, Drew Devine, Casey Theriot, Oscar Tirado-Acevedo, and Xuelian Du who helped all the time and gave me useful information. I am thankful to Dr. Boss, Dr. Hassan, and Dr. Olson who served as my committee members. I would like to thank the following collaborators for my studies: Dr. Hosni Hassan, Dr. Ryan Fink, Dr. Jose Bruno-Barcena, Dr. Wendy Boss, Dr. Yangju Im, Dr. Mike Adams, Dr. Frank Jenny, and Dr. Mike Weinberg. I also appreciate the help ofundergraduate researchers Callie Barnwell and Andy Capps. Lastly, I really appreciate the Department of Microbiology for giving me an opportunity to further my education in the area of microbiology

TABLE OF CONTENTS

LIST OF FIGURES……xiii

LIST OF TABLES……...….xviii

CHAPTER 1. Literature Review…….1

1.1 Aerobic organisms and oxygen toxicity……...…….2

1.2 Oxidative damage……..……5

1.3 Cellular antioxidant defense……..7

1.3.1 Superoxide dismutase ……..……7

1.3.2 Catalase……8

1.3.3 Ascorbate and Ascorbate Peroxidase…….....……..10

1.3.4 Glutathione and Glutathione Reductase..……..…….10

1.3.5 Glutathione Peroxidase……11

1.3.6 Low molecular weight antioxidant compounds…….12

1.4 Anaerobic organisms and oxygen toxicity……...14

1.5 Hydrothermal vent system and vent microbes……...……..15

1.6 Superoxide reductase……...……17

1.6.1 History of the study of superoxide reductase ……..…17

1.6.2 The structure of SOR…….18

1.6.3 Proposed model of SOR reduction for detoxification of reactive oxygen……18

1.6.4 In vitro reconstitution and in vivo complementation studies of the *P. furiosus* superoxide detoxification system……20

1.6.5 Transcriptional analysis of the *P. furiosus* oxygen detoxification system……22

1.6.6 Production of thermostable *P. furiosus* SOR *in* plant cells: a real world application of superoxide reductase……23

1.7 Glutathione reductase and *Colwellia psychrerythraea*……24

1.8 Literature cited...…….…….....37

CHAPTER 2 In vitro reconstitution and in vivo complementation studies of the *P. furiosus* superoxide detoxification system……..……..... 48

Abstract……..49

2.1 Introduction……...…….50

2.2 Materials and Methods……...54

2.2.1 Construction of the rNROR expression vector for the *in vitro* reconstitution experiments……54

2.2.2 Expression and purification of recombinant NROR…….55

2.2.3 Enzyme assays……..……56

2.2.4 Bacterial strains and plasmids for the *in vivo* complementation study……..58

2.2.5 Construction of compatible recombinant *P. furiosus* SOR and Rd expression plasmids for use in the *in vivo* study……58

2.2.6 Expression of recombinant *P. furiosus* SOR and Rd proteins in *E. coli* strain JM105……...59

2.2.7 Cloning and Expression of recombinant *P. furiosus* NROR proteins in *E. coli* strain JM105…….60

2.2.8 The use of the *P. furiosus* SOR enzyme assay to verify the SOR activity of the complemented strains……...…60

2.2.9 *In vivo P. furiosus* SOR-Rd complementation studies using the *E.coli sodA, sodB, norV* deficient strains……62

2.3 Results……63

2.3.1. Expression and purification of recombinant NROR for the *in vitro* reconstitution experiments……63

2.3.2. Catalytic properties of recombinant NROR...……63

2.3.3. Reconstitution of a recombinant NADPH-dependent, superoxide reduction pathway……..64

2.3.4. Analyzing the *in vitro* reconstitution of the SOR pathway by measuring hydrogen peroxide production…….64

2.3.5. Construction of compatible recombinant *P. furiosus* SOR and Rd plasmids and their co-expression in *E. coli*……...65

2.3.6. *P. furiosus* SOR showed high activity in the *sodA, sodB* deficient strain and *sodA, sodB,* and *norV* mutant strain …….66

2.3.7. Co-expression of *P. furiosus* SOR and Rd in *E. coli* wild type strain NC 905 limits its growth in M63 minimal media lacking amino acid supplementation …….68

Conclusion…….70

Literature cited……..…….85

CHAPTER 3. Transcriptional regulation of genes in the *P. furiosus* superoxide detoxification pathway……87

Abstract……..88

3.1 Introduction……89

3.2 Materials and Methods…….91

3.2.1 Growth conditions, treatment of cells and RNA extraction for QRT-PCR……...91

3.2.2 Primer design and optimization of RT-PCR……..92

3.2.3 Standard curves and quantification of real time PCR……..93

3.3 Results and discussion……..……..…..94

3.3.1 Generation of gene-specific standard curves……...….94

3.3.2 Relative quantification of expression of the superoxide detoxification pathway genes……..…….94

3.3.3 Expression levels of the superoxide detoxification pathway genes as determined by quantitative reverse transcriptase PCR……95

3.3.4 Effects of oxidative stress on the growth of *P. furiosus*…….....97

Literature cited.....…….……...106

CHAPTER 4. Production of a thermostable archaeal superoxide reductase in plant cells……109

Abstract……....110

4.1 Introduction……..111

4.2 Materials and Methods…….114

4.2.1 Vector construction……..114

4.2.2 Transformation into *Nicotiana tabacum*1……114

4.2.3 Determination of gene expression in *Nicotiana tabacum*1……..115

4.2.4 Immunoblotting…….....116

4.2.5 SOR assays in NT1 cell culture……...116

4.2.6 Temperature challenge experiments of wild type and transgenic tobacco cell culture……...118

4.2.7 Production of monoclonal antibodies specific for *P. furiosus* SOR and Rd…….119

4.2.7.1 Construction of *P. furiosus* SOR and Rd expression plasmids……...119

4.2.7.2 Overexpression and purification of recombinant *P. furiosus* SOR and Rd……..119

4.2.8 Generation of Arabidopsis plants expressing *P. furiosus* SOR...120

4.2.8.1 Transformation of the *P. furiosus* SOR-expression plasmid into Arabidopsis……120

4.2.8.2 Reverse-Transcriptase PCR…….....121

4.2.8.3 Immunoblot analysis……121

4.2.8.4 SOR enzyme activity assays……121

4.2.8.5 Heat Stress Experiments……..121

4.2.8.6 Drought Stress Experiments……..……..122

4.2.8.7 SOR activity gel……...122

4.3. Results and discussion……123

4.3.1 *Pyrococcus furiosus* SOR is expressed as a fusion with GFP in tobacco cell culture……..……123

4.3.2. SOR expressed in transgenic tobacco cells has heat-stable activity…….124

4.3.3. Recombinant SOR protects transgenic tobacco cells from heat stress……125

4.3.4 Cloning, protein over-expression and purification of recombinant *P. furiosus* SOR and Rd for antibody production……...…126

4.3.5 *P. furiosus* SOR is expressed as a fusion with GFP in Arabidopsis……..127

4.3.5.1 Detection of SOR expressed in Arabidopsis through visualization of GFP fluorescence……..…….127

4.3.5.2 *P. furiosus* SOR is successfully produced and functional in Arabidopsis as demonstrated by RT-PCR, immunoblot assay, enzyme assay and heat stress experiments……128

4.3.5.3 SOR transgenic plants exhibited drought tolerance…….130

Conclusion……...……132

Literature cited..……..…….152

CHAPTER 5 Cloning, expression, and purification of recombinant *Colwellia psychrerythraea* glutathione reductase.....155

Abstract……156

5.1 Introduction……....……..……157

5.2 Materials and methods.....161

5.2.1 Cloning of GR into the pBAD (His_6 tag) plasmid.....161

5.2.2 Protein over-expression and purification of the recombinant His_6-tagged *C. psychrerythraea* GR.....161

5.2.3 Cloning of *C. psychrerythraea* glutathione reductase into the IMPACT expression system vector.....163

5.2.3.1 PCR amplification and cloning.....163

5.3.3.2 Protein over-expression and purification of GR.....163

5.2.4 Enzyme assay of *C. psychrerythraea* GR.....164

5.2.5 *E. coli gor* mutant strain construction.....165

5.3 Results and discussion.....166

5.3.1 Cloning the *C. psychrerythraea* GR in the pBAD-HisA vector..166

5.3.2 Over-expression of *C. psychrerythraea* His_6-GR in *E. coli* at various induction temperatures.....167

5.3.3. Purification and activity analysis of recombinant *Colwellia psychrerythraea* His_6-GR Protein…….....168

5.3.4 Purification and enzyme activity analysis of an unmodified recombinant *C. psychrerythraea* GR.....169

5.3.5 Construction of the *E. coli* GR mutant strains.....171

5.4 Conclusion.....173

5.5 Future work.....173

Literature cited.....187

APPENDIX. Evaluation of the impact of small affinity tags on the expression and activity of recombinant *P. furiosus* NROR.....190

A1 Introduction.....191

A2 Materials and methods.....194

A2.1 Construction of Tagged NROR Vectors.....194

A2.1.1 pET24dBam construction.....194

A2.1.2 pET24dAla and pET24dMAGS construction.....194

A2.2 Screening the clones.....195

A2.3 Cloning *P. furiosus* NROR into the pET24sMAGS and pET24dAla vectors.....195

A2.4 NROR protein over-expression in BL21(DE3).....196

A2.5 Large-scale NROR purification using anion exchange columns.197

A2.6 rNROR Enzyme Assay.....197

A2.7 Purification of recombinant Ala-tagged NROR 198

A3 Results and Discussions.....200

A3.1 Cloning and screening the pET24dAla and pET24dMAGS expression vectors.....200

A3.2 *P. furiosus* NROR can be expressed as fusions with different types of tags.....200

A3.3 Enzyme activity for the various tagged forms of *P. furiosus* rNROR…….....201

A3.4 Large-scale purification of recombinant *P. furiosus*.....203

Literature cited 217

LIST OF FIGURES

CHAPTER 1. Literature Review

Figure1-1 Model of lipid peroxidation…….27

Figure 1-2a Ascorbate-glutathione cycle in chloroplasts of higher plants……..…...28

Figure 1-2b Glutathione redox cycle in mammalian cells……...28

Figure 1-3 The catalytic mechanism proposed for reduction of hydroperoxides by glutathione peroxidase……...29

Figure 1-4 Network of low molecular mass antioxidants……30

Figure 1-5 Model structure of *Desulfovibrio vulgaris* (Dv) superoxide reductase..31

Figure 1-6 A standard SOD assay of *P. furiosus* superoxide reductase ……..32

Figure 1-7. A model for the detoxification of oxygen in the hyperthemophilic, anaerobe *P. furiosus* ……...33

Figure 1-8. Common oxygen detoxification enzymes present in aerobes ……34

Figure 1-9 Oxygen detoxification enzymes in most of anaerobes……35

Figure 1-10 The *E.coli* FL-Rd *(norV)* and NROR *(norW)* operon…….36

CHAPTER 2. In vitro reconstitution and in vivo complementation studies of the *P. furiosus* superoxide detoxification system

Figure 2-1 SDS-12% polyacrylamide gel electrophoresis of purified *P. furiosus* rNROR……...78

Figure 2-2 Reduction of *P. furiosus* superoxide reductase by recombinant NROR via rubredoxin……79

Figure 2-3 Restriction site analysis and PCR verification for the cloned *P. furiosus* Rd…….80

Figure 2-4 Complementation study of the ability of *P. furiosus* SOR to restore growth of an *E. coli sodA, sodB, norV* mutant in M63 glycerol minimal medium without amino acid supplementation ……81

Figure 2-5 *P. furiosus* SOR in pTrc99A and Rd in modified pACYC184 co-expression in *E. coli* JM105…….. 82

Figure 2-6 *P. furiosus* NROR protein expression in JM105……83

Figure 2-7 Model of the pathway for detoxification of reactive oxygen species in *P. furiosus*……..84

CHAPTER 3. Transcriptional regulation of genes in the *P. furiosus* superoxide detoxification pathway

Figure 3-1 Model of the pathway for detoxification of reactive oxygen species in *P. furiosus*……..…….....101

Figure 3-2. Organization of genes involved in the *P. furiosus* SOR reduction system……...……102

Figure 3-3 Standard curves for the genes involved in the superoxide reduction pathway and their equations……103

Figure 3-4 Relative expression of genes involved in the *P. furiosus* superoxide reduction pathway under various oxidative-stress conditions…….104

Figure 3-5 Growth of *P. furiosus* cultures exposed to various oxidative stresses.105

CHAPTER 4 Production of a thermostable archaeal superoxide reductase in plant cells

Figure 4-1 Model of the pathway for detoxification of reactive oxygen species in *P. furiosus*……136

Figure 4-2 SOR expression construct used in this study……...…137

Figure 4-3 RT-PCR analysis shows that SOR mRNA is produced in the transgenic NT1 cells……...138

Figure 4-4 Western analysis indicates that the GFP–SOR fusion protein is produced in NT1 cell culture……...139

Figure 4-5 Heat resistance in suspension cultured cell lines of wild-type (NT1) and tobacco cells expressing either GFP or SOR……140

Figure 4-6 Restriction site analysis for the *P. furiosus* SOR expression plasmids……..141

Figure 4-7 Restriction site analysis for the *P. furiosus* Rd expression plasmids...142

Figure 4-8 Protein purification of *P. furiosus* SOR……...143

Figure 4-9. Protein purification of *P. furiosus* Rd……..144

Figure 4-10 Detection of SOR expressed in Arabidopsis through visualization of GFP fluorescence…….145

Figure 4-11 RT-PCR analysis showing that SOR mRNA is produced in the transgenic Arabidopsis……146

Figure 4-12 Western blot analysis for *P. furiosus* SOR in transgenic Arabidopsis plants ……...147

Figure 4-13 Gel for detection of *P furiosus* SOR activity in *N. crassa*……...148

Figure 4-14 The effects of heat-stress on Arabidopsis seed germination……149

Figure 4-15 Survival rate of 10-day old Arabidopsis seedlings……..150

Figure 4-16 Responses of Arabidopsis plants to drought stress……..151

CHAPTER 5 Cloning, expression, and purification of recombinant *Colwellia psychrerythraea* glutathione reductase

Figure 5-1 The synthesis and structure of GSH and GSSG…….…...178

Figure 5-2 Restriction enzyme analysis of glutathione reductase from 34H cloned into the pBAD-HisA vector……..179

Figure 5-3 PCR verification of *C. psychrerythraea* GR insert in the pBAD-HisA vector……180

Figure 5-4 *C. psychrerythraea* His_6-GR tagged protein over-expression analysis for protein expression induced at various temperatures…….181

Figure 5-5 Protein purification of *C. psychrerythraea* GR in His_6-GR…….182

Figure 5-6 Restriction analysis of GR from *C. psychrerythraea* in IMPACT vector ……..183

Figure 5-7 Protein purification of the recombinant form of *C. psychrerythraea* GR expressed using the IMPACT system (untagged GR)……..184

Figure 5-8 Alignment of the amino acid sequence of *C. psychrerythraea* GR with other Grs from other organisms……. …..185

Figure 5-9 PCR verification of *E. coli gor* mutant (MJ500)……...186

APPENDIX **The impact of the small affinity tags by attaching various tags to recombinant form of *P. furiosus* NROR protein**

Figure A1 pET24dBam expression vector map…….….205

Figure A2 pET24(a-d) vector map and cloning/expression region…….206

Figure A3 Restriction site analysis for pET24dAla…….…..…….207

Figure A4 PCR verification to screen the pET24MAGS construct……208

Figure A5 Restriction site analysis for pNROR-MAGS clone……...……209

Figure A6 Restriction analysis for pNROR-Ala clone……210

Figure A7 Protein over-expression of *P. furiosus* His_6-NROR, MAGS-NROR, and Ala_6-NROR in *E. Coli* strain BL21(DE3)…… 211

Figure A8 Protein purification of the various recombinant forms of *P. furiosus* rNROR…….…….212

Figure A9 Stages of purification Ala_6-rNROR……...213

Figure A10a Purified Ala_6-rNROR stored in 50mM MOPS buffer pH at 6.5……214

Figure A10b Purified Ala_6-rNROR stored in 50mM Tris buffer pH at 8…...……214

LIST OF TABLES

CHAPTER 2 In vitro reconstitution and in vivo complementation studies of the *P. furiosus* superoxide detoxification system

Table 2-1 Bacterial strains and plasmids used in this study……..72

Table 2-2 Reconstitution of recombinant *P. furiosus* NROR……...73

Table 2-3 *In vitro* reconstitution of *P. furiosus* NAD(P)H- dependant superoxide reduction pathway……..……74

Table 2-4 SOR specific activities for various *E. coli* strains grown in M63 without amino acid supplementation……...……...…….……...…75

Table 2-5 Relative growth level of various *E. coli* strains in amino acid deficient M63-glycerol minimal media……..76

Table 2-6 Relative growth levels of various *E. coli* strains in LB media…….…....77

CHAPTER 3. Transcriptional regulation of genes in the *P. furiosus* superoxide detoxification pathway

Table 3-1 Growth conditions used for oxidative stress treatments of *P. furiosus*...98

Table 3-2 Primers used for qRT quantification experiments evaluating expression of the superoxide detoxification genes…….....99

Table 3-3 Generation times of *P. furiosus* cultures in response to various stress conditions……...100

CHAPTER 4 **Production of a thermostable archaeal superoxide reductase in plant cell biotechnological applications**

Table 4-1 SOR activity of transgenic tobacco cell culture strains……..….133

Table 4-2 Reconstitution of heat-stable SOR activity from transgenic tobacco cell culture……..134

Table 4-3 SOR activity of transgenic Arabidopsis plants……135

CHAPTER 5 **Cloning, expression, and purification of recombinant *Colwellia psychrerythraea* glutathione reductase**

Table 5-1 *E. coli* strains used for GR disruption…….…….174

Table 5-2 Sequences and features of primers used in construction of the disrupted GR mutation in *E. coli* strains…….…….175

Table 5-3 His_6-GR enzyme activity…….176

Table 5-4 Enzyme activity for the unmodified *C. psychrerythraea* rGR…..….177

APPENDIX **The impact of the small affinity tags by attaching various tags to recombinant form of *P. furiosus* NROR protein**

Table A1 Quantification of FAD content in the different tagged recombinant NROR enzymes…….215

Table A2 Reconstitution of the different recombinant tagged-NROR proteins..216

CHAPTER 1

Literature Review

1.1 Aerobic organisms and oxygen toxicity

The paradox of aerobic life, or the 'Oxygen Paradox', is that most living organisms except anaerobic microbes cannot exist without oxygen, yet oxygen is inherently dangerous to organisms (29). The atmosphere of planet earth was anaerobic until two and a half billion years ago. The process known as photosynthesis suddenly supported the ability to release molecular oxygen into Earth's atmosphere, causing one of the largest environmental changes in the history of our planet. The organisms assumed responsible for oxygenating the atmosphere were the cyanobacteria, which are known to have evolved the ability to turn water, carbon dioxide, and sunlight into oxygen and sugar, and are still around today as the blue-green algae and the chloroplasts in all green plants (35, 105). The accumulation of oxygen in the atmosphere changed the environment of the earth and the selection pressure on ancient microbes by development of novel and new pathways in their metabolism as well as increased mutation rates. It made possible a highly exergonic respiratory chain based on O_2 as a terminal electron acceptor, an event that is widely held to have been closely coincident with the development of complex eukaryotic life (30). Oxygen is used by many enzymes as substrates as well. For example, in kidney there are about thirty enzymes that use oxygen for metabolizing different compounds like amines, prostaglandins, purines, amino acids, carnitine, etc. (78).

The dangerous effects for the oxygen molecules relate to the two unpaired electrons with parallel spins ('triplet' ground state) rendering dioxygen rather unreactive toward other molecules. However, when the electrons are added one at a time, there is a time between collisions for the inversion of electron spins. As a result, the route of molecular reduction is series of univalent electron transfers, which can generate reactive intermediates (40). The reductive environment within cells provides ample opportunities for oxygen to undergo univalent

reduction. Thus, the superoxide anion radical, hydrogen peroxide and the extremely reactive hydroxyl radical are common intermediates of partially reduced forms of oxygen species in an aerobic environment, and these agents appear to be responsible for oxygen toxicity (63).

Tetravalent reduction of oxygen to water in a respiring cell is carried out by cytochrome c oxidase without releasing reactive oxygen species. However, a small chance of partial reduction of oxygen molecules can produce superoxide radicals. NADH dehydrogenase II, succinate dehydrogenase, fumarate reductase, and sulphite reductase are members of electron transport chains and they utilize flavin redox moieties that are adept at univalent electron transfer reactions, which can produce superoxide (61). The primary sites of superoxide production in the mammalian system are at the flavin cofactors of redox enzymes (61, 80, 81). Reduced flavin transfers a single electron to molecular oxygen, forming flavosemiquinone and superoxide. The flavosemiquinone undergoes spin inversion further generating hydrogen peroxide (61). In vertebrates, the rate of generation of ROS is tightly associated with the rate of oxygen consumption and is proportional to the number of mitochondria (6). In rat liver and pigeon heart, at physiological oxygen concentrations, about 1-4% of the O_2 consumed is transformed to ROS due to leakage from the electron transport chain (78). In *E. coli*, less than 1% of the electrons that flow through are leaked from electron transport chain (61).

Due to the low redox potential of superoxide molecules, its activity as an oxidant is kinetically restricted and its biological relevance is probably minor because it is a poor electrophile at physiological pH (61). However, in 1976, Boehm *et al.* had determined the impact of superoxide in *E. coli* cells. Hyperbaric oxygen created growth defects when they were grown in minimal media lacking branched amino acids (17). It was shown in the study that dihydroxyacid dehydratase was the specific step that could cause the failure of the branched

amino acid chain pathway. Later Carlioz and Touati also established that the same phenomenon occurred in an *E. coli* SOD mutant suggesting that superoxide damaged the dihydroxyacid dehydratase (21). Dihydroxyacid dehydratase uses a [4Fe-4S] cluster for substrate dehydration. When the cluster is exposed to superoxide, the catalytic iron attracts the superoxide anion, and the cluster undergoes univalent oxidation leading to loss of a ferrous atom, generating a [3Fe-4S] cluster instead (37). Inactivation of the iron sulfur cluster by superoxide attack can also be found in the metabolic enzymes aconitase A and B (46), fumarase A and B (71), 6-phosphogluconate dehydratase (45) and serine dehydratase (57) in *E. coli*.

Univalent reduction of superoxide anions generates hydrogen peroxide. Hydrogen peroxide is not a radical because it has no unpaired electrons. Numerous enzymes (peroxidases) use hydrogen peroxide as a substrate in oxidation reactions involving the synthesis of complex organic molecules. For example, in plants, lignification of cell walls involves the synthesis of the phenyl propanoid precursors of lignin, and hydrogen peroxide is required for their subsequent polymerization (24). However, when it is catalyzed with a metal reductant, highly reactive hydroxyl radicals are generated via the Fenton reaction. Hydroxyl radicals are formed when ferrous iron transfers an electron to H_2O_2 as shown below:

$$\mathbf{Fe^{2+} + H_2O_2 \rightarrow Fe^{3+} + {\bullet}OH + OH^-}$$

In a mixture of iron salts and H_2O_2, hydroxyl radicals, which are the strongest oxidant agents known, are generated, and they can react with organic molecules at diffusion-limited rates. This strong oxidant can react non-specifically with cellular components such as lipids, proteins, and DNA resulting in damage and potentially cell death.

1.2 Oxidative damage

Lipid peroxidation is one of the most significant kinds of cellular damage attributed to oxygen toxicity. Polyunsaturated fatty acids (PUFAs) serve as excellent substrates for lipid peroxidation because of the presence of active bis-allylic methylene groups. Initiation of lipid peroxidation in a membrane or free fatty acid starts with the attack by any oxygen species, such as hydroxyl radicals, superoxide anion, or preexisting lipid hydroperoxide that has sufficient reactivity to abstract a hydrogen atom (51, 69, 121). Since a hydrogen atom has only one electron, this leaves behind an unpaired electron on the carbon atom. The carbon radical in a polyunsaturated fatty acid tends to be stabilized by a molecular rearrangement to produce a conjugated diene, which rapidly reacts with O_2 to give a hydroperoxy radical ($ROO^{\cdot}$) (55). Hydroperoxy radicals abstract hydrogen atoms from other lipid molecules and so continue the chain reaction of lipid peroxidation (propagation) (Figure 1). The hydroperoxyl radical can abstract a hydrogen atom from a number of *in vivo* sources, such as DNA and proteins, to form the primary oxidation product, a lipid hydroperoxide ($ROOH^{\cdot}$) (50, 52).

Protein oxidation can cause site-specific amino acid modifications, cleavage of the polypeptide chain, formation of cross-linked protein aggregation, altered electrical charge, modified gene transcription and increased susceptibility to proteolysis (106, 112, 115, 116). Inhibition of activity and loss of function of the proteins are a common biological impact of protein oxidation (43). The two amino acids that are perhaps the most prone to oxidative attack are cysteine and methionine, both of which contain susceptible sulfur atoms. Reactive oxygen species can abstract an H atom from cysteine residues to form a thiyl radical that will cross-link to a second thiyl radical to form disulfide bridges (61, 104). Under *in vitro* conditions, H_2O_2

oxidizes the thiolated anion of free cysteine to form sulphenic acid, and this derivatives reacts with additional thiols to form a disulfide bond as shown below.

Cys-SH ←→Cys-S^- + H^+

Cys-S^- +H_2O_2 → Cys-SOH +OH^-

Cys-SOH + Cys-SH → Cys-SS-Cys +H_2O

With Met residues, the major product under biological conditions is methionine sulfoxide (126). These two amino acid residues are distinguished from other oxidative protein modification targets in that the cells have mechanisms to protect from the oxidative damage of Met and Cys by possessing reverse oxidation enzymes, such as the glutathione or thioredoxin redox system and methionine sulfoxide reductase. It is thought that disulfide bond formed by hydrogen peroxide between cysteine residues is responsible for activation of the transcription factor, OxyR in *E. coli* (78), and Yap1 (9) in yeast, which serve important regulatory functions in the cells. Reversible oxidation/reduction of methionine may protect proteins from more damaging forms of oxidative modification (*e.g.*, carbonyl formation) (118).

Other forms of free radical attack on proteins are not reversible. For example, the oxidation of iron-sulfur clusters by superoxide destroys enzymatic function (61). Many amino acids undergo specific irreversible modifications when a protein undergoes metal catalyzed oxidation. The reduced form of a protein-bound transition metal (e.g., Fe^{+2}, Cu^{+1}) reacts with hydrogen peroxide in a Fenton reaction to form a hydroxyl radical that rapidly oxidizes an amino acid residue at or near the cation binding site of the protein (114, 116). For example, tyrosine is readily cross-linked to form bityrosine products. Histidine, lysine, proline, arginine, and serine form carbonyl groups (aldehydes and ketones) on their side chains.(117).

Either by the consequence of endogenous metabolism or by exogenous sources of reactive oxygen species, DNA damage can cause deleterious effects to cells including: mutagenesis, carcinogenesis, aging and a number of neurological disorders (7). *In vitro* neither hydrogen peroxide alone nor superoxide cause DNA strand breaks under physiological conditions since they are relatively mild oxidants, and therefore, their toxicity *in vivo* is most likely the result of Fenton reactions with a metal catalyst. In *E. coli*, active forms of hydroxyl radicals from hydrogen peroxide, DNA-bound iron, and NADH oxidation can drive the lesion of DNA (63). The oxidative damage of DNA can occur in the sugar back bone and bases resulting in the fragmentation of sugar residue, loss of bases and strand breaks within the DNA chain and cross-linking of DNA to protein (98).

1.3 Cellular antioxidant defense

Oxidative stress has been defined as an imbalance between oxidants and antioxidants in favor of the former, resulting in an overall increase in cellular levels of reactive oxygen species (70). Cells have antioxidant defenses that protect cells from oxidative damage and toxicity by removing the excessive formation of reactive oxygen species. These defenses can be divided into two categories, enzymatic and non-enzymatic. Enzymatic antioxidants to be discussed include superoxide dismutase, catalase, glutathione peroxidase, and ascorbate peroxidase. Non-enzymatic antioxidants under review include vitamin E, vitamin C, glutathione, thioredoxin, lipoic acid, and coenzyme Q.

1.3.1 Superoxide dismutase

Superoxide dismutase (SOD) was first isolated by Mann and Keilis, and its catalytic function was discovered by McCord and Fridovich (82). SOD is now known to catalyze the dismutation of superoxide to hydrogen peroxide and oxygen as follows:

$$2\,O_2^- + 2H^+ \rightarrow H_2O_2 + O_2$$

In mammalian cells, two forms of isozymes exist, manganese SOD (Mn-SOD), and copper/zinc SOD (Cu/Zn-SOD). Mn-SOD, an 80 kDa tetramer, which contains a manganese prosthetic group, is present in the mitochondria most likely to protect mitochondrial proteins, membranes, and DNA from O_2^- generated as a result of the mitochondrial respiratory chain (128). The Cu/Zn-SOD, a 32-kDa dimer, containing copper and zinc prosthetic groups, is present in the cytoplasm (82). In plants, there are three distinct types of SOD classified on the basis of the metal cofactor: the Cu/Zn - SOD, the Mn-SOD, and the iron (Fe-SOD) isozymes (14). The Mn-SOD is found in the mitochondria. Some Cu/Zn-SOD isozymes are found in the cytosol, others in the chloroplasts of higher plants. The Fe-SOD isozymes are often not detected in plants, but when detected, Fe-SOD is usually associated with the chloroplast compartment (18).

There are three known SODs in *E. coli*: MnSOD, FeSOD and CuZnSOD. The iron-containing enzyme (FeSOD) and manganese-containing enzyme (MnSOD) are located in the cytoplasm and the copper-zinc-containing enzyme (CuZnSOD) is in the periplasmic space (56). MnSOD is a basic dimeric protein having a molecular weight (M.W.) of 22.9 kDa per subunit, while FeSOD is an acidic dimeric protein having a M.W. of 21.1 kDa per subunit (16, 41, 134). The copper-zinc superoxide dismutase (CuZnSOD) in *E. coli* is a homodimer a M.W. of 15.7 kDa per subunit (64). All forms of SOD dismutates O_2^- operate via a ping-pong mechanism whereby the transition metal prosthetic group is reduced by O_2^-, forming O_2. The metal in the prosthetic group is then immediately re-oxidized by another O_2^- molecule, resulting in the production of H_2O_2 (42).

1.3.2 Catalase

All catalases, whether of eukaryote, prokaryote, or archaeal origin, catalyze the same reaction:

$$2H_2O_2 \rightarrow 2H_2O + O_2$$

It dismutates hydrogen peroxide to water and oxygen. Its antioxidant role is to remove the risk of hydroxyl radical formation from H_2O_2 via the Fenton reaction catalyzed by Cu or Fe ions (40). Despite a considerable diversity, heme-containing catalases are most prevalent among the eukaryotic organisms. In mammalian cells, the predominant subcellular localization is in peroxisomes, perhaps because of the large number of H_2O_2-producing oxidases found in these organelles, while lower levels are also found in mitochondria and the cytosol (97). In plants, catalase is only present in peroxisomes and is an efficient catalyst when hydrogen peroxide is in low concentration. However, during high oxidative stress in cells, proliferation of peroxisomes are observed suggesting that it is responsible for removing the excess hydrogen peroxide production (77, 87). In prokaryotes, multiple forms of diverse catalases are present. They can be categorized into four groups according to their heme contents, subunit sizes, and sequences (110): 1) monofunctional 'typical' catalases (because of their similarity to eukaryotic catalases) 2) monofunctional 'atypical' catalases (because of differences from the typical catalases) 3) bifunctional (catalase/peroxidase) catalase and 4) non-heme containing catalases. Another property of the catalases is the multiplicity of isozymes. It is common that several isozymes are present in an organism, and many of them are not characterized yet.

Despite its importance in protection from reactive oxygen species, catalase is not necessary for cell growth under normal conditions in *E. coli* (73) and *Bacillus subtilis* (74). However, it is known that catalase is important in providing a selective advantage in numerous organisms. In the presence of hydrogen peroxide, cell survival is enhanced in catalase proficient strains compared to catalase-deficient strains (133). The *katEkatG* mutant of *E. coli*, had no

assayable catalase activities in the extract and showed increased (about 20 fold) sensitivity to killing by H_2O_2 when compared with its parental strain (109, 133).

1.3.3 Ascorbate and ascorbate peroxidase

L-ascorbic acid (vitamin C) is an important hydrophilic antioxidant in eukaryotes. It is a major antioxidant in mammalian cells. It reduces α-tocopherol as well as peroxides and ROS such as superoxide (15). The vitamin C serves mainly to prevent lipid hydroperoxide formation by reducing α-tocopherol radicals formed upon reaction with lipid peroxyl radicals (20, 85), protecting lipids in cell membranes by this mechanism. In its action as an antioxidant, ascorbate is rapidly oxidized to dehydroascorbate, which shows little antioxidant activity. Dehydroascorbate may be reduced back to ascorbate via a GSH-dependent reductase (Figure 1-2b) (103). In plants, ascorbic acids play an essential role in scavenging of H_2O_2 in plant leaves. Different isoforms of ascorbic acids are active in chloroplasts, cytosol, and microsomes (110).

Ascorbate peroxidase (APX) detoxifies hydrogen peroxide using ascorbate for reduction. In the chloroplasts, SOD and APX exist in both soluble and thylakoid-bound forms. Superoxide generated at the membrane surface can thus be trapped and converted immediately to H_2O_2 to be scavenged by the membrane bound ascorbate peroxidase. Two enzymes are involved in the regeneration of reduced ascorbate, mono-dehydro-ascorbate reductase that uses NAD(P)H directly to recycle ascorbate and dehydro-ascorbate reductase (Figure 1-2a).

1.3.4 Glutathione and Glutathione reductase

Glutathione (GSH) is a tripeptide (Glu-Cys-Gly) whose antioxidant function is facilitated by the sulfydryl group of cysteine. On oxidation, the sulfur forms a thiyl radical that reacts with a second oxidized glutathione forming a disulfide bond (GSSG). In plant cells, one of the essential roles of GSH is that it detoxifies reactive oxygen species via the ascorbic acid-GSH-cycle and

glutathione reductases (96). It participates in the regeneration of ascorbate from dehydro-ascorbate via the enzyme dehydro-ascorbate reductase. In such reactions, GSH is oxidized to glutathione disulfide (GSSG). GSH is regenerated by glutathione reductase (GR) in a NADPH-dependent reaction (Figure 1-2a). Foyer and Halliwell proposed that hydrogen peroxide was dissipated in the chloroplast by the coupling of ascorbate and glutathione redox cycling as shown in figure 1-2a (53). Many of the details of this pathway have been established and the enzymes characterized by K. Asada. It is referred to as the Halliwell-Asada pathway. Additional functions and background information about GSH and GR in plants and bacteria will be discussed in a later chapter of this study. In mammals, GSH quenches reactive oxygen species, which involves GR and glutathione peroxidase via a NADPH dependent redox cycle. A comparison of the Ascorbate-glutathione cycle in chloroplasts of higher plants and the glutathione redox cycle in mammalian cells that operates in detoxifying reactive oxygen species is shown in Figure 1-2.

1.3.5 Glutathione peroxidase

Glutathione peroxidase (GPx) catalyzes the reduction of H_2O_2 using glutathione (GSH) as substrate or it reduces organic peroxides (ROOH), which are potential radical forming species within the cell to the corresponding alcohols and water. Glutathione, a nonenzymatic antioxidant, provides the reducing equivalents needed by GPx to carry out the following reduction reaction:

ROOH (HOOH) + 2GSH → ROH + GSSG + H_2O

There are at least four different GPx enzymes in mammals (GPx1–4), all of them containing selenocysteine (122). GPx1 and GPx4 are both cytosolic enzymes abundant in most tissues. The catalytic mechanism proposed for reduction of hydroperoxides by GPx involves oxidation of the active site selenate (Se^-) to selenenic acid (SeOH). Upon addition of one molecule of GSH, the selenenic acid is transformed to a selenenyl sulfide adduct with glutathione (Se-SG), which can

be regenerated to the active selenate and glutathione disulfide (GSSG) by addition of a second molecule of GSH. Thus, in the reaction, two molecules of GSH are oxidized to GSSG that subsequently can be reduced by glutathione reductase, the major mammalian GSSG-reducing enzyme (Figure1-3)(33, 38, 97). In higher plants, this enzyme has not been well studied, but recently there have been reports of characterization of tomato cDNAs encoding glutathione peroxidase-like proteins (31). In prokaryotes, GPx activity has not been studied except for the enzyme from one prokaryote, *Neisseria meningitidis* (90, 91). Inactivation of the gene for GPx in *N. meningitidis* increases the sensitivity of the resulting mutants to oxidative stress induced by paraquat (methyl viologen) (90).

1.3.6. Low molecular weight antioxidant compounds: Ascorbate (vitamin C), α-Tocopherol (vitamin E), Ubiquinone (coenzyme Q), Lipoic acid (Lipoate), and Thioredoxin.

Liposoluble tocopherol and ubiquinone are found in cell membranes, the water-soluble antioxidants ascorbate and glutathione are localized mainly in the cytoplasm. Despite these separate localizations in the cell, the low molecular weight antioxidants are not independent of each other; they function to reduce each other and restore their active form. They form a close association, which is also described as an anti-oxidative network (Figure1-4) (103). The tocopherols, specifically α-tocopherol (vitamin E) are known as membrane stabilizing antioxidants containing a hydroxyl group which donates a hydrogen atom to reduce unpaired electrons, e.g., peroxyl radicals and a hydrophobic chain which allows for penetration into membranes (23). Tocopherol, the primary lipid soluble small molecule antioxidant, and vitamin C, the terminal water soluble small molecule antioxidant, cooperate to protect lipids and lipid structures against peroxidation of the lipid bilayer (20). Lipid peroxidation oxidizes the tocopherol, generating tocopheroxyl radical on the surface of the membrane bilayers. It reacts

with ascorbate in the aqueous phase to function as a free radical chain-breaking antioxidant. Glutathione regenerates oxidized ascorbate (dehydroascorbate) to ascorbate using NADPH as reducing power (120). α-Lipoic acid, or its reduced form, dihydrolipoate, reacts with reactive oxygen species such as superoxide radicals, hydroxyl radicals, hypochlorous acid, peroxyl radicals, and singlet oxygen. It also protects membranes by interacting with vitamin C and glutathione, which may in turn recycle vitamin E (99). Ubiquinone exerts its main natural function in mitochondria as a part of the electron transport chain, but it is also present in low concentrations in the cytoplasm and in cell membranes where it functions as an antioxidant by preventing lipid peroxidation (34). Regeneration of ubiquinone is performed by lipoamide dehydrogenase (131) and to some extent also by the other members of this family of enzymes, including glutathione reductase and thioredoxin reductase (131).

Thioredoxins (Trx) are proteins with oxidoreductase activity and are ubiquitous in all forms of life ranging from archaea to humans. It interacts with a broad range of proteins by a redox mechanism based on reversible oxidation of 2 cysteine thiol groups to a disulfide, accompanied by the transfer of 2 electrons and 2 protons. The net result is the covalent interconversion of a disulfide and a dithiol. In general, Trx modulates the signal transduction properties of ROS via reduction of the intracellular disulfides induced by ROS and by lowering the levels of ROS directly (97). Thioredoxin reductase (TR) catalyzes reduction of oxidized thioredoxin (trx) by NADPH using the cofactor FAD and its redox-active disulfide. Reduced thioredoxin then directly reduces the disulfide in a variety of substrate proteins. Thioredoxins can also act as electron donors to such enzymes as peroxidase and ribonucleotide reductase (58).

1.4 Anaerobic organisms and oxygen toxicity

The first discovery of anaerobic organism in history originated in 1683 when the Dutch scientist Antonio Van Leeuwenhoek described the morphological shape of bacteria isolated from his teeth. His description of the spiral shapes of the bacteria was the first known example of an anaerobic organism. Italian biologist, Spallanzani was the next to study anaerobes. He discovered that life could exist without air by preparing cultures that had been evacuated using the vacuum pump he designed. Louis Pasteur was an important influence on the origin of anaerobic microbiology. In 1861, he observed that yeast could thrive under anaerobic conditions in fermenting cultures. He postulated the Pasteur Effect, which stated that oxygen could be the inhibiting effect on the process of fermentation and he classified microorganisms into 'aerobic', 'facultative' and 'anaerobic' according to their requirements of oxygen for growth (10).

Obligate anaerobes are sensitive to oxygen because they are qualitatively different from aerobes in that their metabolism operates upon highly reduced substrates (62). Anaerobes use low potential redox moieties to deliver electrons to low potential acceptors to ferment effectively (61). They often use terminal flavin reductases to reoxidize their dinucleotide pool. Since flavin moieties are particularly reactive with oxygen, the rate of intracellular superoxide formation may be very high (80). Most of the essential redox enzymes in central metabolic pathways in anaerobes contain iron sulfur clusters, which are hypersensitive to oxygen. The large group of dehydratases such as aconitase, fumarase, and dihydroxyacid dehydratase and the group of ferredoxin-dependant dehydrogenases such as pyruvate:ferredoxin oxidoreductase (PFOR) are good examples of [Fe-S] cluster-containing enzymes. They are rapidly inactivated when exposed to oxygen because of oxidation of the clusters (3). In archaea, a family of ferredoxin-dependent enzymes that oxidize glycerol aldehyde-3-phosphate, formaldehyde, and glyceraldehyde contain

tungsten and pterin cofactors as well as iron-sulfur clusters, which are all irreversibly damaged by oxygen in vitro (61). More specifically, when anaerobic organisms are exposed to oxygen, low potential redox enzymes, such as flavins generate flavosemiquinone, superoxide, and even hydrogen peroxide by transferring a single electron to molecular oxygen. The abundant formation of superoxide and hydrogen peroxide causes the inactivation of iron sulfur clusters of essential enzymes in central metabolism, which can explains the hypersensitivity to oxygen in anaerobic organisms.

With the discovery in 1969 by McCord and Fridovich of copper zinc superoxide dismutase from blood (82) , the necessity of the presence of SOD in aerobic organisms was recognized. McCord *et al.* (83) established the correlation between oxygen tolerance and the production of SOD, indicating that obligate anaerobes lacked of any SOD activity while aerobic and aerotolerent organisms had activity (83). Their study suggested that SOD was the single most important enzyme for enabling organisms to survive in the presence of molecular oxygen. They theorized that obligate anaerobes are hypersensitive to oxygen due to a deficiency of SOD. However, most of the anaerobic organisms, which often lack SOD, show various degrees of tolerance to oxygen when they are occasionally exposed to oxygen in their environments.

1-5 Hydrothermal vent systems and vent microbes

The 1977 discovery of hydrothermal vents and the spectacular communities living on/within them has been considered an extraordinary scientific observation. Hydrothermal vents are found along the mid-ocean ridge and rift system at sea floor-spreading centers. Vents form when volcanic activity adds to diverging plates and seawater gets into cracks in the plates. Then the heated water mixes with minerals and metals returning to the ocean floor as jets of hydrothermal fluid. The hydrothermal fluids cool in contact with cold and oxygen containing

seawater. The resulting metal precipitates, create chimneys of metal deposits (94). Researchers once thought that no living organisms could survive around hydrothermal vents located on the ocean floor since the environment was judged to be too extreme for life. However, extensive communities of organisms such as six foot, red-tipped tube worms, large white clams, yellow mussels and pale crabs that congregate around hydrothermal vents were discovered (27). Vent fluids contain gases, especially hydrogen sulfide, and vent microbes can utilize hydrogen sulfide as their energy source. Microbes from the vents serve as the primary food source for clams, mussels and other invertebrates, thereby forming the base of a food web in this ecosystem (27, 124).

The microbes found in the hydrothermal vents including *Pyrococcus furiosus* are predominantly anaerobic hyperthermophilic species that can grow above 80^{o}C (27, 119). *P. furiosus*, isolated from a marine volcano in Italy, is classified as a strict anaerobic hyperthermophilic heterotroph, which grows optimally at 100°C and ferments carbohydrates and peptides producing organic acids, CO_2, H_2, and H_2S as by-products (36). *P. furiosus* is classified as a member of the domain Archaea, which was identified as the third domain of life based on the 16S rRNA sequence derived phylogenetic trees developed by Carl Woese (130). Phylogenetic trees constructed using 16S rRNA homology have indicated that thermophiles are in the most deeply rooted and shortest lineages, and are therefore regarded as the most primitive and slowest evolving organisms (119).

Interestingly, studies have shown that certain anaerobic hyperthermophilic microbes including *P. furiosus* that live within the erupting hydrothermal vent could survive for a substantial amount of time even with exposure to cold, oxygen containing seawater in their environment (59). Actually, most anaerobes show various degrees of tolerance to oxygen in an

environment transiently exposed to air, even though they generally lack SOD and/or catalase enzymes in their genomes. These findings suggest that some anaerobes may possess reactive oxygen species detoxification mechanisms to ensure their survival during transient oxygen exposure. Therefore, there has been much interest in determining what mechanism(s) other than SOD and catalase may be used by these anaerobes to detoxify oxygen.

1.6 Superoxide reductase

1.6.1 History of the study of superoxide reductase

The discovery of the novel enzymes to detoxify the superoxide molecules in anaerobes began with isolation of two iron-sulfur containing proteins named desulfoferrodoxin (Dfx) from *Desulfovibrio desulfuricans* (92) and neelaredoxin (Nlr) from *Desulfovibrio gigas* (22) in the early 1990's. Upon comparison of their amino acid sequences and UV-visible spectroscopic properties, it was determined that these proteins shared a common domain called a mononuclear iron site (2). Later it was found out that these domains are the active sites where superoxide is bound (26, 132). The enzyme's function was first studied in 1996 in the laboratory of Danièle Touati. Dfx was cloned from *Desulfovibrio baarsii* and it showed complementation of SOD activity in *E. coli* SOD deficient mutants suppressing the deleterious effect of the superoxide toxicity (102). Later Nlr from *Treponema pallidum* (76) and *D. gigas* (113) were also shown to complement the *E. coli sodA sodB* mutant showing *in vivo* activity to remove superoxide toxicity. Liochev and Fridovich (72) proposed that Dfx catalyzes the reduction of superoxide rather than dismutation at the expense of cellular reductant such as NAD(P)H. Later, the Dfx enzyme was confirmed as an oxidoreductase by Lombard *et al.* (75).

1.6.2. The structure of SOR

Superoxide reductases are present in most known anaerobes and have been classified into three different classes, distinguished by the presence or absence of an N-terminal domain (108). SORs from the three classes share a conserved C-terminal domain, a single iron-containing active site coordinated by four equatorial histidine nitrogen atoms and an axial cysteinyl sulfur atom, designated as center II (Figure 5) (22, 92). The first class, also called desulfoferrodoxins (Dfx), was isolated from *Desulfovibrio vulgaris* and *Desulfovibrio desulfuricans* (92). They have two mononuclear iron centers (center I and center II) (Fig. 1-5). In addition to the C-terminal domain (center II), class I SORs also have an iron in the N-terminal domain (center I), which is coordinated by four conserved cysteine residues in a distorted tetrahedral coordination. The second class of SORs is called neelaredoxins (Nlr). Class II SORs only have center II and lack the N-terminal domain (center I). SORs from *Pyrococcus furiosus* (132) and *Archaeoglobus fulgidus* (1) belong to this family. The SOR from *Treponema pallidum* is an example of the third class of SOR. It has an extended non-iron N terminal domain of unknown function (67, 76). Only the reduced form of the iron-containing active site (center II) among these three classes is able to react with the superoxide anion $O_2^{\bullet -}$, leading to the formation of the ferric state of the enzyme. Therefore, the presence of an electron donor is necessary to regenerate the ferrous active form and complete the catalytic cycle of the enzyme. Recently, several groups have clearly established rubredoxin as the proximal electron donor to SORs in the case of *P. furiosus* (49, 65), *T. pallidum* (13), *D. vulgaris*(28), and *A. fulgidus* (107) SORs.

1.6.3. Proposed model of SOR reduction for detoxification of reactive oxygen

In 1999, Jenny *et al*. (65) identified SOD activity in *P. furiosus*. The putative SOD was a protein of M.W. of 14.3 kDa containing 124 amino acids. This putative SOD had high

homology to the Dfx and Nlr enzymes of the sulfate reducing bacteria. High SOD activity was measured by a standard SOD assay at 25^{o}C. However, there is a fundamental difference in terms of enzyme properties. In the assay, an increasing amount of bovine SOD inhibited cytochrome c reduction, which means that bovine SOD reduces the superoxide, and a similar pattern was observed in the case of the putative SOD in *P. furiosus.* However, when an excess amount of bovine SOD is added to the reaction mix, no further effect had been observed, while an excess amount of *P. furiosus* "SOD" caused oxidation of the reduced cytochrome c (Figure 1-6). Therefore, it was realized that *P. furiosus* "SOD" is an oxidoreductase, not a dismutase and has accordingly been named superoxide oxidoreductase (SOR).

P. furiosus rubredoxin (Rd) is a small Fe-containing redox protein (~5.3kDa) located adjacent to SOR gene in the genome. Even though it had been purified in several anaerobic organisms and characterized, its physiological function was not determined until *P. furiosus* NAD(P)H:rubredoxin oxidoreductase (NROR) was characterized. The native form of NROR in *P. furiosus* is a monomer with a M. W. of ~45 kDa, and it contains one flavin adenine dinucleotide (FAD) per molecule (79). Its physiological role was identified as catalyzing the reduction of rubredoxin in *P. furiosus* (79). The role of Rd was subsequently determined as a physiological electron carrier for SOR reduction (65). Homologs of *P. furiosus* SOR were not found in the genomes of any aerobic organism but were present in those of most anaerobes (65). In 1999, the detoxification mechanism for removal of reactive oxygen molecules in anaerobes was proposed by Jenny *et al.* In this model superoxide is reduced to hydrogen peroxide by SOR, which receives the necessary electrons from Rd. Rd is ultimately reduced by NAD(P)H via NROR (65) (Figure1-7). At the time the model was originally developed, it was thought that further conversion of hydrogen peroxide to water molecules occurred via peroxidases since

genes encoding peroxidases had been identified in the *P. furiosus* genome (65). Later, it was found that the hydrogen peroxide is reduced to water by a peroxidase known as rubrerythrin reductase (Rr) (127).

Most of the *P. furiosus* enzymes are not very active below 80°C, but SOR, NROR, and Rd are still active at low temperature (< 25°C), which would obviously be advantageous for the ROS detoxification in *P. furiosus* since *P. furiosus* lives in an environment in which it would periodically encounter oxygen-containing cold seawater. SOD and SOR can be distinguished from one another in that SOD generates one half mole of oxygen and one-half mole of hydrogen peroxide per superoxide molecule (Figure 1-8) while SOR produces only one mole of hydrogen peroxide (Figure 1-9). The generation of oxygen by SOD would be disadvantageous to anaerobes because this oxygen could potentially produce yet more superoxide as a result of cellular metabolism, and it is known that some of the enzymes in the fermentation pathways of anaerobes have reaction centers and iron-sulfur clusters that are especially sensitive to damage by superoxide. The hydrogen peroxide generated by SOR is a strong oxidant that is easily reduced within anaerobic cells where cellular reducing agents are abundant (12).

1.6.4 In vitro reconstitution and in vivo complementation studies of the *P. furiosus* superoxide detoxification system

In order to test the feasibility of the proposed model for oxygen detoxification in *P. furiosus*, enzymatic reactions involving SOR, Rd, NROR had to be shown to function together to reduce superoxide to hydrogen peroxide *in vitro* as well as *in vivo*. There had been accumulating evidence that reduced Rd mediated the reduction of SOR (65) and that NROR could reduce Rd in an NAD(P)H dependant reaction (79). Since the recombinant form of NROR (rNROR) of *P. furiosus* was cloned (49), and rSOR (25) and rRd (3) were available from previous studies, *in*

vitro reconstitution of an recombinant superoxide reduction pathway has been performed to demonstrate that NADPH can serve as an electron source for superoxide reduction to peroxide. Additionally, *P. furiosus* SOR was shown to complement an *E. coli* strain deficient in SodA and SodB, restoring the deleterious growth defect.(66). Due to the fact that the *P. furiosus* genetic system is not well established and that it has the homologs of genes involved in the *P. furiosus* SOR pathway, *E. coli* can be an amenable choice to investigate the *in vivo* studies.

E. coli contains the *norV* and *norW* genes that encode a flavorubredoxin (Fl-Rd, *norV*) and NADH:(flavo) rubredoxin reductase (NROR, *norW*), respectively which are involved in nitric oxide reduction under anaerobic conditions. NorV and NorW show high homology to the sequences of *P. furiosus* Rd and NROR, respectively (In this study, Figure 1-10) (49). In *E. coli*, *norV* and *norW* have overlapping coding regions suggesting that they likely comprise a single transcriptional unit (44, 60). *E. coli* flavorubredoxin (*norV*) belongs to a family of flavinproteins, called A type flavoproteins. It is suggested in *E. coli* that the NADH-dependent flavorubredoxin reductase (NorW) is responsible for supplying two electrons to the diferric center via the rubredoxin domain, and these electrons are ultimately used for nitric oxide reduction (44). Based on the sequence and functional similarities that exist between *E. coli* NorV and NorW and *P. furiosus* Rd and NROR, respectively, knockout mutants of these genes in *E. coli* have been constructed for use in complementation experiments with the *P. furiosus* homologs. These complementation experiments ultimately will be able to test whether these enzymes participate in SOR-mediated oxygen detoxification *in vivo.* To fully verify *P. furiosus* SOR reduction pathway *in vivo*, complementation of additional *P. furiosus* genes involved in the SOR reduction pathway in *E. coli* strains can demonstrate the proposed *P. furiosus* SOR reduction pathway.

In this work, the *P. furiosus* SOR centered superoxide reduction pathway was studied to test the feasibility of the proposed model of the anaerobic oxygen detoxification mechanism using *in vitro* as well as *in vivo* methods. The complete enzymatic SOR centered superoxide reduction pathway is proven in *in vitro* reaction by reconstitution experiments. The complementation studies of *P. furiosus* genes involved in the SOR reduction pathway, which were evaluated utilizing an *E. coli* complementation system will be discussed in a section devoted to the *in vivo* studies.

1.6.5 Transcriptional analysis of the *P. furiosus* oxygen detoxification system

In order to understand the oxygen detoxification system in *P. furiosus*, it is valuable to analyze the transcriptional expression levels when *P. furiosus* is exposed to various sources of oxidative stress. Even though there are a few studies mentioning transcriptional expression of genes of the *P. furiosus* SOR reduction system (111, 127, 129), no clear quantitative transcriptional analysis has been performed on the system yet. Real-time PCR is a technique to analyze the mRNA expression levels, which allows the quantification of rare transcripts and small changes in gene expression (123). In this study, the four most important genes (SOR, Rd, NROR, Rr) involved in the *P. furiosus* SOR reduction system were chosen to investigate the transcriptional expression against the various sources of ROS by using quantitative real time PCR methods. Interestingly, Rr, Rd, and SOR are organized as a single transcriptional unit in the *P. furiosus* genome. *P. furiosus* cultures were exposed to various environmental sources of ROS, such as air, and free radical generating antibiotics, and the resulting SOR, Rr, Rd, and NROR transcript levels were determined using quantitative real time PCR methods.

1.6.6 Production of thermostable *P. furiosus* SOR *in* plant cells: a real world application of superoxide reductase

There are many sources of reactive oxygen species in plants. It can be produced endogenously resulting from processes such as photosynthesis and aerobic respiration (106). The major ROS-scavenging mechanisms of plants include superoxide dismutase (SOD), ascorbic peroxidase (APX), and catalase (CAT) (88). SOD removes superoxide and decreases the risk of hydroxyl radical formation from superoxide. There have been three isozymes of SOD identified, Mn-SOD, Cu/Zn-SOD, and Fe-SOD in various plants. Mn-SOD is predominantly found in mitochondria and peroxisomes. Cu/Zn-SOD is located mainly in cytosolic fraction as well as chloroplastic and mitochondria fractions. Fe-SOD is predominantly detected in chloroplasts (8). H_2O_2 is eliminated from plant cells by the action of catalases and peroxidases. Ascorbate peroxidase (APX) is one of the most important antioxidant enzymes of plants that detoxify hydrogen peroxide using ascorbate for reduction. The ascorbate peroxidase (APX) family of isoenzymes is crucial in maintaining H_2O_2 content at nontoxic concentrations in many of the compartments of the cell. Catalase is largely restricted to the peroxisomes, but it is necessary during stress when high levels of ROS are produced (88).

There is increasing evidence for considerable interlinking between the responses to heat stress and oxidative stress. Drought and low temperature can cause significant ROS production (4). Overexpression of radical scavenging enzymes, such as SOD and GR, have resulted in an increased resistance to drought, ozone, low temperature, and high light stress (84, 101, 125). These experiments indicate that modification of ROI scavenging systems can lead to significant changes in oxidative stress tolerance and provide some indication that these approaches can be used to improve plant performance (4).

In this work, we have shown that the *P. furiosus* SOR gene can be expressed in plants and that it produces a functional protein that retains thermal stability characteristic of the native enzyme. Furthermore, the recombinant SOR fusion protein is distributed throughout the cytosol and nucleus of the plant cells, and enhances the survival of the transgenic plant cells to short-term, high temperature exposures. This study proves that genes from an archaeal source can be successfully expressed in a plant system and reveals a new mechanism for dampening ROS signals, and thus, potentially identifying ROS-dependent pathways in plant cells (3).

1.7 Glutathione reductase and *Colwellia psychrerythraea*

Glutathione, a low molecular weight antioxidant, protects cells from toxins such as free radicals by serving as a reductant. The sulfhydryl of GSH can be used to reduce peroxides formed during oxygen transport. The resulting oxidized form of GSH consists of two molecules disulfide bonded together (GSSG). Utilization of GSH results in its conversion to the disulfide form, (GSH), the major non-protein sulfhydryl in living organisms. Glutathione (GSH) is involved in various cellular functions. GSH takes part in many different intra-cellular processes, including maintenance of reduced thiol groups, protection from oxygen-induced cell damage, and generation of deoxyribonucleotide precursors for DNA synthesis. It is regenerated in an NADPH-dependent reaction catalyzed by glutathione reductase (47)..

The active site of glutathione reductase (GR) is a redox-active disulfide bond which acts with the bound FAD (100). It is responsible for maintaining the GSH/GSSG ratio in the cellular homeostasis. This enzyme uses NAD(P)H as its source of electrons. Glutathione comes mainly from the pentose phosphate shunt, which is the predominant source of GSH reducing power. In *E. coli*, GR is a member of the dimeric FAD-containing thiol reductase family. One surprising aspect of glutathione metabolism is that the ratio of reduced to oxidized glutathione does not

appear to change significantly in mutants that lack glutathione reductase (128). *E. coli* may, therefore, contain alternative glutathione reductases. Candidate proteins that might also be able to reduce glutathione include putative homologs of GR encoded in the chromosome. Alternatively, there may be some cross-talk between the glutathione and other thiol-mediated molecules.

In plants, numerous functions of GSH have been known. It regulates sulfur allocation within the cell and acts as regulator of gene expression (95). The reduced form of GSH may act as an important redox buffer, preventing enzyme inactivation by protecting protein thiol groups (5, 53, 54). The ascorbate-glutathione cycle has been demonstrated to remove hydrogen peroxide by ascorbate peroxidase in the chloroplast stroma and to protect the thiol-modulated enzymes of the Benson-Calvin cycle from oxidative inactivation (32, 48, 53, 68). In this pathway, glutathione acts as a recycled intermediate in the reduction of H_2O_2 using electrons derived from H_2O (39). Efficient recycling of glutathione is ensured by GR activity. Since GR is considered to be a key enzyme in maintaining the redox status of the cell during oxidative stress, it has attracted researchers working on a wide range of organisms (5, 110)

Colwellia psychrerythraea is an arctic marine bacterium which thrives at temperatures below 5^{o}C and can survive at subzero temperatures. It is classified as a facultative anaerobic gamma proteobacteria, obtained from stably cold marine environments, including deep sea, and Arctic and Antarctic sea ice (19). The genome of this marine psychrophilic bacterium was recently completed, and it has been used as a model for the study of life in permanently cold environments (86). The genomic analysis revealed several key biochemical adaptations that support its survival in cold environments. *C. psychrerythraea* produces extracellular biofilm, synthesizes polyunsaturated fatty acids to prevent the membrane rigidity, and possesses enzymes

able to degrade high molecular weight organic compounds, all features characteristic of psychrophilic bacteria (86). It is suggested that the psychrophilic life style is most likely conferred not by a unique set of genes but by a collection of synergistic changes in overall genome content and amino acid composition of proteins (86).

C. psychrerythraea can be faced with great deal of reactive oxygen species (ROS) by their own metabolism as well as by exposure to its environment, which can be a high UV-light environment. The production of extra polyunsaturated fatty acids which is known to be more susceptible to ROS than saturated fatty acids can result in the lipid peroxidation damaging the cell membrane (55). In addition to the intracellular formation of ROS, there is extracellular ROS formation within brine channels of sea ice where high concentrations of hydrogen peroxide (500 nmol l^{-1}) was measured (89, 93). In order to cope with the oxygen toxicity, several antioxidants are present including SODs and catalases in its genome (86).

Under certain environmental stresses such as exposure to extreme temperatures, radiation, and dehydration, plants face the challenges of protecting protein structure and preventing cellular damage. *C. psychrerythraea* can utilize the activity of GR as a protection mechanism under cold conditions to promote the formation of adducts between thiol groups of intracellular proteins and glutathione. *C. psychrerythraea* GR, which is stable under cold temperature and responsible for continuous production of the reduced glutathione (GSH), could be engineered into plants to aid in combating oxidative stress under low-temperature/freezing conditions. Since GR from *C. psychrerythraea* had not yet been investigated, we report as part of this study, the initial characterization of the recombinant version of *C. psychrerythraea* produced in *E. coli*.

.

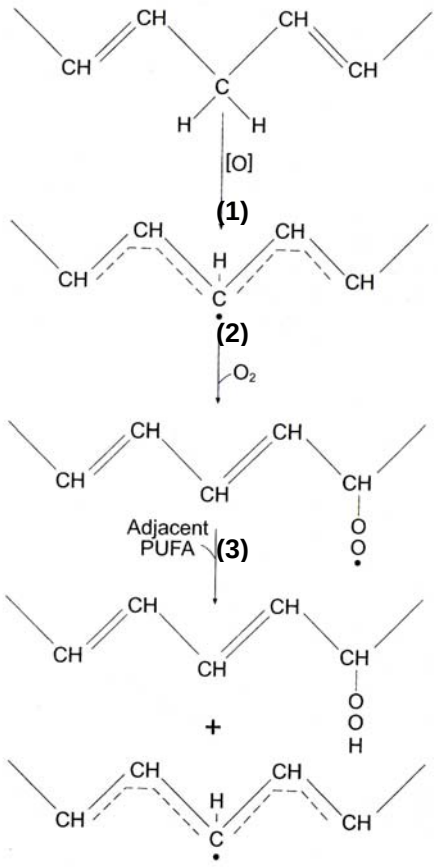

Figure 1-1. Model of lipid peroxidation. (Adapted from Imlay 2002)

(1) Initiation-The chain propagation is initiated by electron abstraction from the bis-allylic carbon atom. The oxidant [O], possibly hydroxyl radicals or iron-ligand molecular oxygen, generates the carbon-centered radicals by stabilizing their delocalization over flanking carbon atoms. (2) Propagation- Addition of oxygen maintains the conjugation, producing peroxy radicals. (3) This radical propagates the chain by oxidizing neighboring polyunsaturated fatty acids (PUFAs) producing a different fatty acid radical . This cycle continues as the new fatty acid radical reacts in the same way.

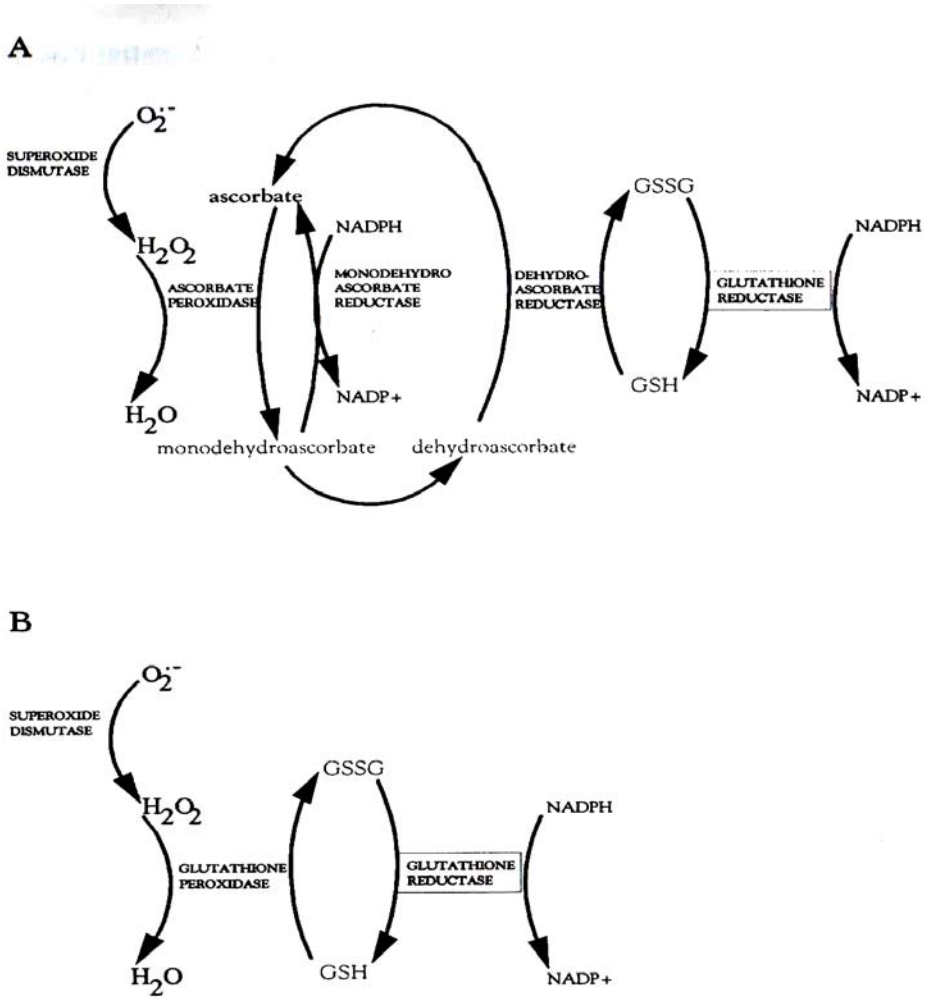

Figure 1-2a. Ascorbate-glutathione cycle in chloroplasts of higher plants. The primary oxidation products of ascorbate peroxidase catalyzed reaction, monodehydroascorbate radical and its disproportional product, dehydroascorbate, may be reduced by a NADPH dependant-monodehydroascorbate reductase and dehydroascorbate reductase in GSH-dependent reductase.

Figure 1-2b. Glutathione redox cycle in mammalian cells. Figure is adapted from Scandalios, 1997

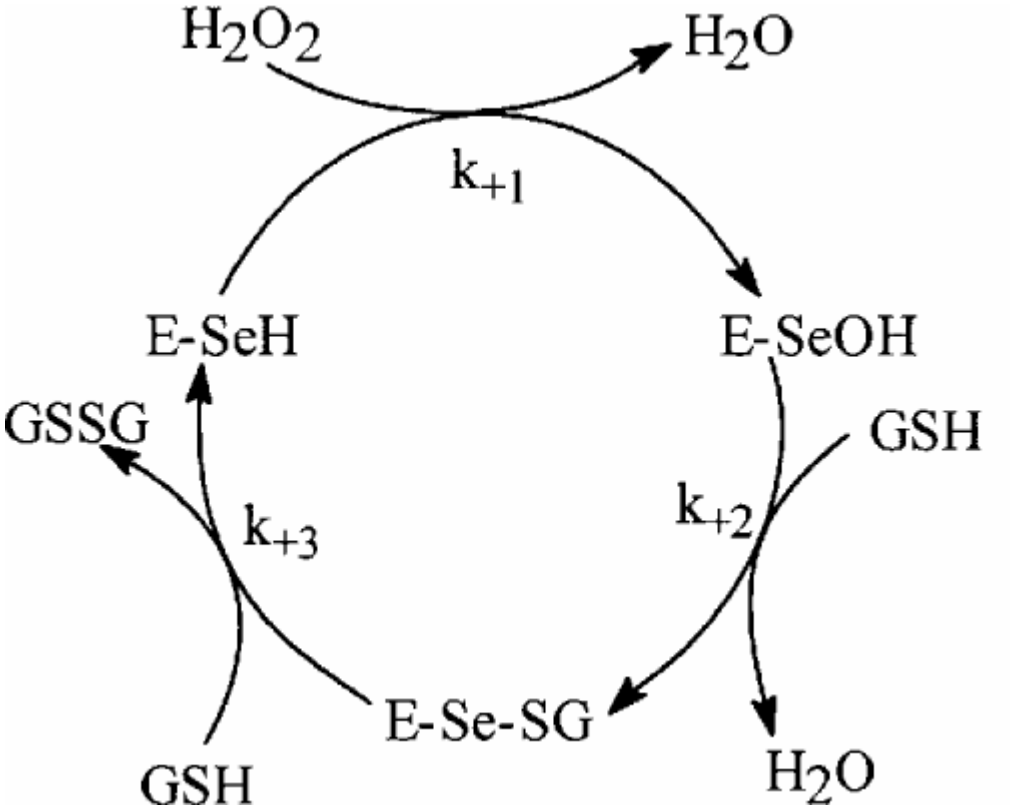

Figure 1-3. The catalytic mechanism proposed for reduction of hydroperoxides by glutathione peroxidase. The figure is modified from (33).

The enzyme catalytic site includes a selenocysteine residue in which the selenium undergoes a redox cycle involving selenol (ESeH) as the active form that reduces hydrogen peroxides and organic peroxides. The selenol is oxidized to selenenic acid (ESeOH), which reacts with reduced glutathione (GSH) to form a selenenyl sulfide adduct (ESeSG). A second glutathione then regenerates the active form of the enzyme by attacking the ESeSG to form the oxidized glutathione (GSSG). Thus, in the overall process, 2 equivalents of GSH are oxidized to the disulfide and water**.**

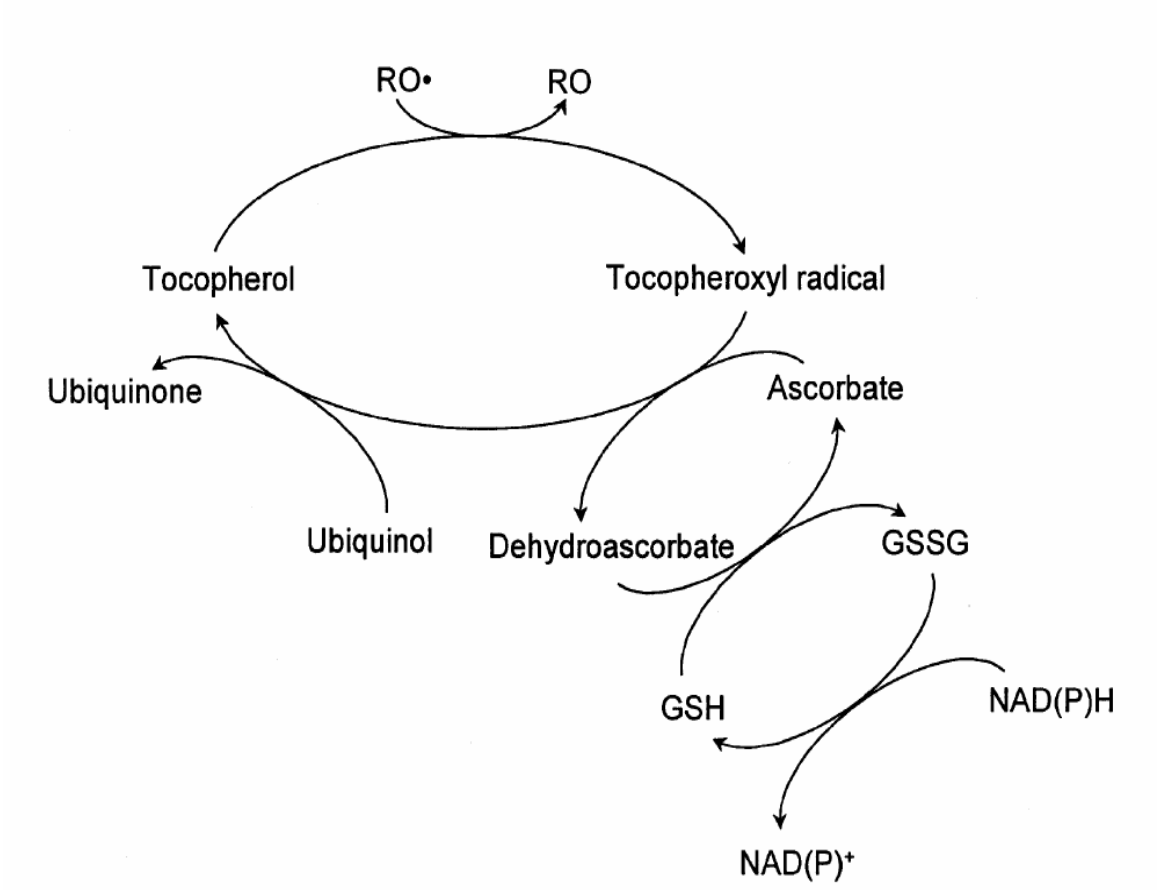

Figure 1-4. Network of low molecular mass antioxidants**.** Adapted from (103).

ROS formed in the lipophilic areas of the cell is reduced by the tocopherol located in the membranes, thus the tocopheroxyl radical is formed. This can be re-reduced directly by another liposoluble low molecular mass antioxidant, ubiquinol. However, owing to the tocopheroxyl radical charge, it can also be re-reduced by ascorbate because of a change in the localization of the membrane-cytosol boundary. The oxidized form, dehydroascorbate, can be reconverted by glutathione into its reduced, active state using the NADPH pool.

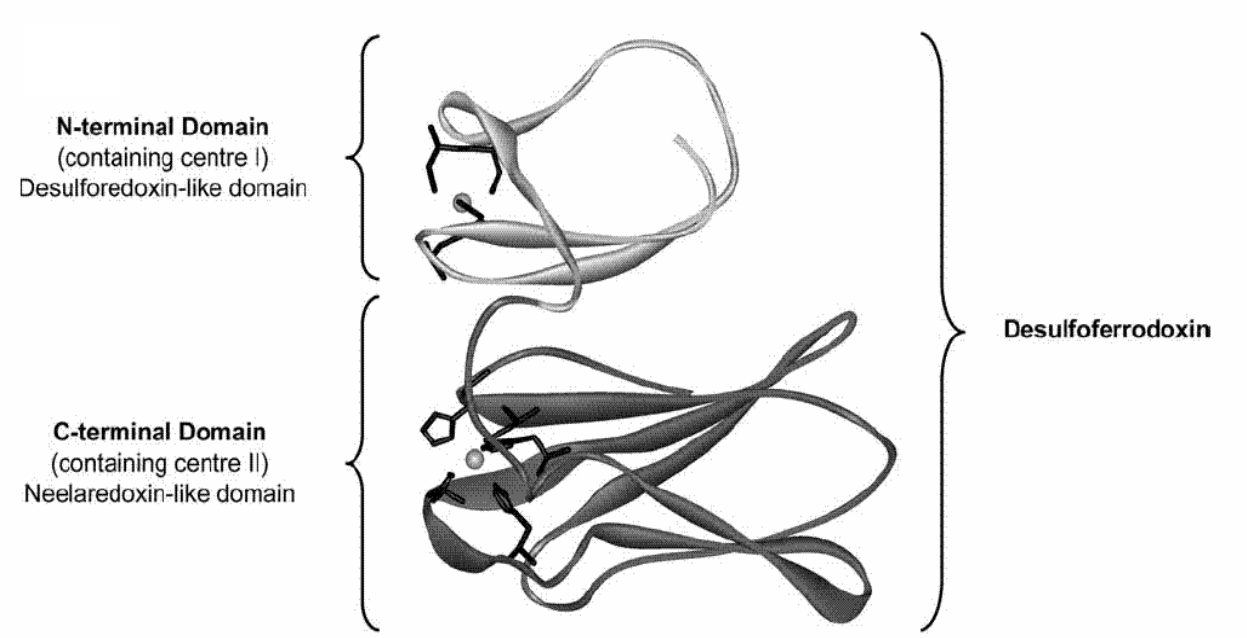

Figure 1-5. Model structure of *Desulfovibrio vulgaris* (Dv) superoxide reductase (SOR), a representative of class I SOR. The protein is shown as a backbone ribbon with the iron centers space-filled and the ligands of the iron centers as sticks. The N-terminal domain is colored light gray and the C-terminal domain dark gray. Adapted from (11).

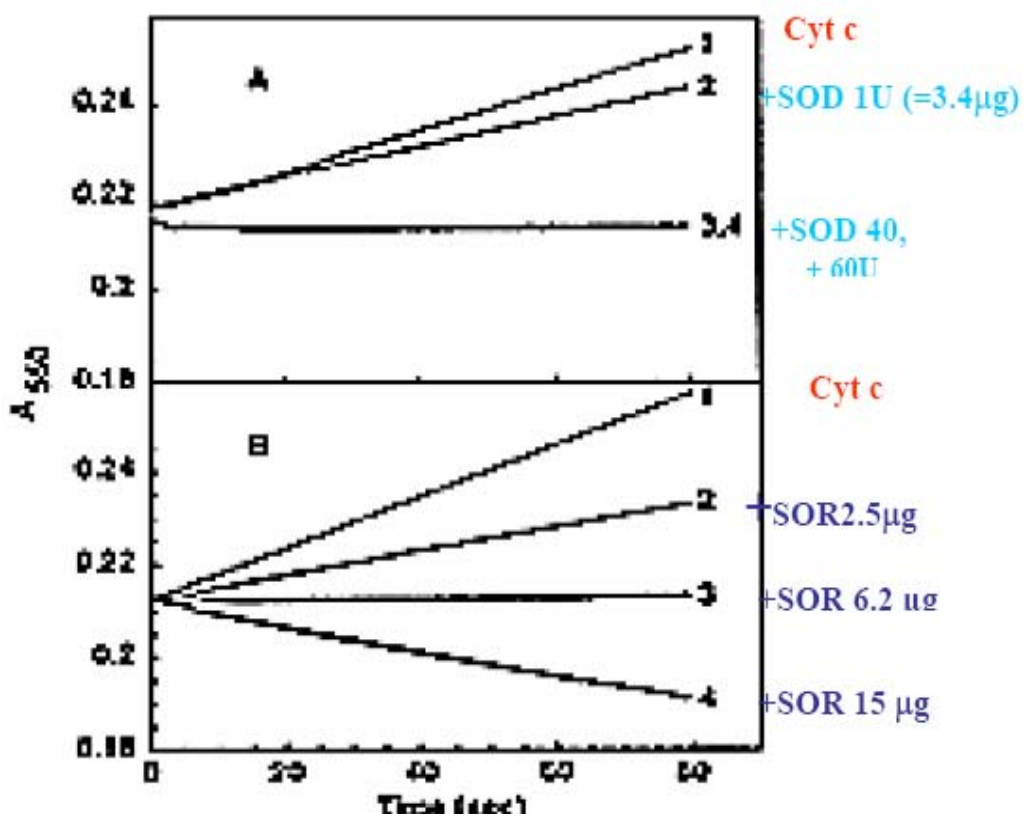

Figure 1-6. A standard SOD assay of *P. furiosus* superoxide reductase (SOR).

For this assay, superoxide is produced by xanthine/xanthine oxidase, and

O_2^- is reduced by cytochrome c. O_2^- is removed by adding SOD.

In graph A, increasing amounts of bovine SOD inhibit the cytochrome c reduction

indicating that SOD has removed the O_2^-. Adding excess bovine SOD has no

further effect. In graph B, the *P. furiosus* SOD-like enzyme was assayed. Addition of excess

SOR caused the direct oxidation of cytochrome c indicating that it functions an oxidoreductase,

not a dismutase. Graph modified from Jenney *et al* (1999)

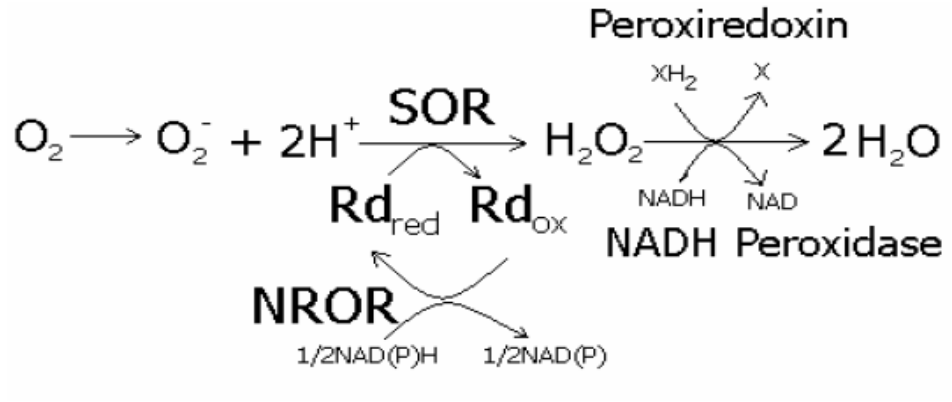

Figure 1-7. A model for the detoxification of oxygen in the hyperthemophilic, anaerobe *P. furiosus.* Figure from Jenney *et al*, (1999)

$$O_2^- + O_2^- + 2H^+ \rightarrow O_2 + H_2O_2 \qquad \text{(SOD)}$$

$$2H_2O_2 \rightarrow 2H_2O + O_2 \qquad \text{(Catalase)}$$

Figure 1-8. Common oxygen detoxification enzymes present in aerobes and the reactions they catalyze

$$O_2^- + 2H^+ + e^- \rightarrow H_2O_2 \quad \text{(SOR)}$$

$$H_2O_2 + 2H^+ \rightarrow 2H_2O \quad \text{(Rr)}$$

Figure 1-9. Oxygen detoxification enzymes in most anaerobes.

Figure 1-10. The *E. coli* FL-Rd *(norV)* and NROR *(norW)* operon contains homologs of *P. furiosus* genes that are likely involved in supporting *P. furiosus* SOR activity in *E. coli* cells . The Rd- domain of *norV* has 49% similarity to *P. furiosus* Rd (PF Rd), *NorW* has 42 % similarity to *P. furiosus* NROR. YgaA is a the regulator of the operon.

Literature cited

1. **Abreu, I. A., L. M. Saraiva, J. Carita, H. Huber, K. O. Stetter, D. Cabelli, and M. Teixeira.** 2000. Oxygen detoxification in the strict anaerobic archaeon Archaeoglobus fulgidus: superoxide scavenging by neelaredoxin. Mol Microbiol **38:**322-34.

2. **Abreu, I. A., A. V. Xavier, J. LeGall, D. E. Cabelli, and M. Teixeira.** 2002. Superoxide scavenging by neelaredoxin: dismutation and reduction activities in anaerobes. J Biol Inorg Chem **7:**668-74.

3. **Adams, M. W., J. F. Holden, A. L. Menon, G. J. Schut, A. M. Grunden, C. Hou, A. M. Hutchins, F. E. Jenney, Jr., C. Kim, K. Ma, G. Pan, R. Roy, R. Sapra, S. V. Story, and M. F. Verhagen.** 2001. Key role for sulfur in peptide metabolism and in regulation of three hydrogenases in the hyperthermophilic archaeon Pyrococcus furiosus. J Bacteriol **183:**716-24.

4. **Allen, R. D.** 1995. Dissection of Oxidative Stress Tolerance Using Transgenic Plants. Plant Physiology **107:**1049-1054.

5. **Alscher, R. G.** 1989. Biosynthesis and Antioxidant Function of Glutathione in Plants. Physiologia Plantarum **77:**457-464.

6. **Ames, B. N., M. K. Shigenaga, and T. M. Hagen.** 1995. Mitochondrial decay in aging. Biochim Biophys Acta **1271:**165-70.

7. **Ames, B. N., M. K. Shigenaga, and T. M. Hagen.** 1993. Oxidants, antioxidants, and the degenerative diseases of aging. Proc Natl Acad Sci U S A **90:**7915-22.

8. **Arora, A., R. K. Sairam, and G. C. Srivastava.** 2002. Oxidative stress and antioxidative system in plants. Current Science **82:**1227-1238.

9. **Aslund, F., M. Zheng, J. Beckwith, and G. Storz.** 1999. Regulation of the OxyR transcription factor by hydrogen peroxide and the cellular thiol-disulfide status. Proc Natl Acad Sci U S A **96:**6161-5.

10. **Atlas, R. M.** 1995. Principles of microbiology. Mosby, St. Louis.

11. **Auchere, F., S. R. Pauleta, P. Tavares, I. Moura, and J. J. Moura.** 2006. Kinetics studies of the superoxide-mediated electron transfer reactions between rubredoxin-type proteins and superoxide reductases. J Biol Inorg Chem **11:**433-44.

12. **Auchere, F., and F. Rusnak.** 2002. What is the ultimate fate of superoxide anion in vivo? J Biol Inorg Chem **7:**664-7.

13. **Auchere, F., R. Sikkink, C. Cordas, P. Raleiras, P. Tavares, I. Moura, and J. J. Moura.** 2004. Overexpression and purification of Treponema pallidum rubredoxin;

kinetic evidence for a superoxide-mediated electron transfer with the superoxide reductase neelaredoxin. J Biol Inorg Chem **9:**839-49.

14. **Bannister, J. V., W. H. Bannister, and G. Rotilio.** 1987. Aspects of the structure, function, and applications of superoxide dismutase. CRC Crit Rev Biochem **22:**111-80.

15. **Bast, A., G. R. Haenen, and C. J. Doelman.** 1991. Oxidants and antioxidants: state of the art. Am J Med **91:**2S-13S.

16. **Beyer, W. F., Jr., J. A. Reynolds, and I. Fridovich.** 1989. Differences between the manganese- and the iron-containing superoxide dismutases of Escherichia coli detected through sedimentation equilibrium, hydrodynamic, and spectroscopic studies. Biochemistry **28:**4403-9.

17. **Boehm, D. E., K. Vincent, and O. R. Brown.** 1976. Oxygen and toxicity inhibition of amino acid biosynthesis. Nature **262:**418-20.

18. **Bowler, C., M. Vanmontagu, and D. Inze.** 1992. Superoxide-Dismutase and Stress Tolerance. Annual Review of Plant Physiology and Plant Molecular Biology **43:**83-116.

19. **Bowman, J. P., J. J. Gosink, S. A. McCammon, T. E. Lewis, D. S. Nichols, P. D. Nichols, J. H. Skerratt, J. T. Staley, and T. A. McMeekin.** 1998. Colwellia demingiae sp. nov., Colwellia hornerae sp. nov., Colwellia rossensis sp. nov. and Colwellia psychrotropica sp. nov.: psychrophilic Antarctic species with the ability to synthesize docosahexaenoic acid (22 : 6 omega 3). International Journal of Systematic Bacteriology **48:**1171-1180.

20. **Buettner, G. R.** 1993. The pecking order of free radicals and antioxidants: lipid peroxidation, alpha-tocopherol, and ascorbate. Arch Biochem Biophys **300:**535-43.

21. **Carlioz, A., and D. Touati.** 1986. Isolation of superoxide dismutase mutants in Escherichia coli: is superoxide dismutase necessary for aerobic life? Embo J **5:**623-30.

22. **Chen, L., P. Sharma, J. Le Gall, A. M. Mariano, M. Teixeira, and A. V. Xavier.** 1994. A blue non-heme iron protein from Desulfovibrio gigas. Eur J Biochem **226:**613-8.

23. **Chen, L. H.** 1989. Interaction of vitamin E and ascorbic acid (review). In Vivo **3:**199-209.

24. **Christensen, J. H., G. Bauw, K. G. Welinder, M. Van Montagu, and W. Boerjan.** 1998. Purification and characterization of peroxidases correlated with lignification in poplar xylem. Plant Physiol **118:**125-35.

25. **Clay, M. D., F. E. Jenney, Jr., P. L. Hagedoorn, G. N. George, M. W. Adams, and M. K. Johnson.** 2002. Spectroscopic studies of Pyrococcus furiosus superoxide reductase:

implications for active-site structures and the catalytic mechanism. J Am Chem Soc **124:**788-805.

26. **Coelho, A. V., P. Matias, V. Fulop, A. Thompson, A. Gonzalez, and M. A. Carrondo.** 1997. Desulfoferrodoxin structure determined by MAD phasing and refinement to 1.9-angstrom resolution reveals a unique combination of a tetrahedral FeS4 centre with a square pyramidal FeSN4 centre. Journal of Biological Inorganic Chemistry **2:**680-689.

27. **Corre, E., A. L. Reysenbach, and D. Prieur.** 2001. epsilon-Proteobacterial diversity from a deep-sea hydrothermal vent on the Mid-Atlantic Ridge. Fems Microbiology Letters **205:**329-335.

28. **Coulter, E. D., and D. M. Kurtz, Jr.** 2001. A role for rubredoxin in oxidative stress protection in Desulfovibrio vulgaris: catalytic electron transfer to rubrerythrin and two-iron superoxide reductase. Arch Biochem Biophys **394:**76-86.

29. **Davies, K. J.** 1995. Oxidative stress: the paradox of aerobic life. Biochem Soc Symp **61:**1-31.

30. **De Marais, D. J.** 2000. Evolution. When did photosynthesis emerge on Earth? Science **289:**1703-5.

31. **Depege, N., J. Drevet, and N. Boyer.** 1998. Molecular cloning and characterization of tomato cDNAs encoding glutathione peroxidase-like proteins. Eur J Biochem **253:**445-51.

32. **Diesperger, H., and H. Sandermann.** 1979. Soluble and Microsomal Glutathione S-Transferase Activities in Pea-Seedlings (Pisum-Sativum-L). Planta **146:**643-648.

33. **Ding, L., Z. Liu, Z. Zhu, G. Luo, D. Zhao, and J. Ni.** 1998. Biochemical characterization of selenium-containing catalytic antibody as a cytosolic glutathione peroxidase mimic. Biochem J **332 (Pt 1):**251-5.

34. **Ernster, L., and G. Dallner.** 1995. Biochemical, physiological and medical aspects of ubiquinone function. Biochim Biophys Acta **1271:**195-204.

35. **Falkowski, P. G.** 2006. Evolution. Tracing oxygen's imprint on earth's metabolic evolution. Science **311:**1724-5.

36. **Fiala, G., and K. O. Stetter.** 1986. Pyrococcus-Furiosus Sp-Nov Represents a Novel Genus of Marine Heterotrophic Archaebacteria Growing Optimally at 100-Degrees C. Archives of Microbiology **145:**56-61.

37. **Flint, D. H., J. F. Tuminello, and M. H. Emptage.** 1993. The inactivation of Fe-S cluster containing hydro-lyases by superoxide. J Biol Chem **268:**22369-76.

38. **Forstrom, J. W., J. J. Zakowski, and A. L. Tappel.** 1978. Identification of the catalytic site of rat liver glutathione peroxidase as selenocysteine. Biochemistry **17:**2639-44.

39. **Foyer, C. H., H. LopezDelgado, J. F. Dat, and I. M. Scott.** 1997. Hydrogen peroxide- and glutathione-associated mechanisms of acclimatory stress tolerance and signalling. Physiologia Plantarum **100:**241-254.

40. **Fridovich, I.** 1998. Oxygen toxicity: a radical explanation. J Exp Biol **201:**1203-9
.

41. **Fridovich, I.** 1997. Superoxide anion radical (O2-.), superoxide dismutases, and related matters. J Biol Chem **272:**18515-7.

42. **Fridovich, I.** 1974. Superoxide dismutases. Adv Enzymol Relat Areas Mol Biol **41:**35-97.

43. **Fucci, L., C. N. Oliver, M. J. Coon, and E. R. Stadtman.** 1983. Inactivation of key metabolic enzymes by mixed-function oxidation reactions: possible implication in protein turnover and ageing. Proc Natl Acad Sci U S A **80:**1521-5.

44. **Gardner, A. M., R. A. Helmick, and P. R. Gardner.** 2002. Flavorubredoxin, an inducible catalyst for nitric oxide reduction and detoxification in Escherichia coli. J Biol Chem **277:**8172-7.

45. **Gardner, P. R., and I. Fridovich.** 1991. Superoxide sensitivity of the Escherichia coli 6-phosphogluconate dehydratase. J Biol Chem **266:**1478-83.

46. **Gardner, P. R., and I. Fridovich.** 1991. Superoxide sensitivity of the Escherichia coli aconitase. J Biol Chem **266:**19328-33.

47. **Grant, C. M., and I. W. Dawes.** 1996. Synthesis and role of glutathione in protection against oxidative stress in yeast. Redox Report **2:**223-229.

48. **Groden, D., and E. Beck.** 1979. H2o2 Destruction by Ascorbate-Dependent Systems from Chloroplasts. Biochimica Et Biophysica Acta **546:**426-435.

49. **Grunden, A. M., F. E. Jenney, Jr., K. Ma, M. Ji, M. V. Weinberg, and M. W. Adams.** 2005. In vitro reconstitution of an NADPH-dependent superoxide reduction pathway from Pyrococcus furiosus. Appl Environ Microbiol **71:**1522-30.

50. **Gutteridge, J. M.** 1982. The role of superoxide and hydroxyl radicals in phospholipid peroxidation catalysed by iron salts. FEBS Lett **150:**454-8.

51. **Gutteridge, J. M., D. A. Rowley, and B. Halliwell.** 1981. Superoxide-dependent formation of hydroxyl radicals in the presence of iron salts. Detection of 'free' iron in biological systems by using bleomycin-dependent degradation of DNA. Biochem J **199:**263-5.

52. **Halliwell, B., and S. Chirico.** 1993. Lipid peroxidation: its mechanism, measurement, and significance. Am J Clin Nutr **57:**715S-724S; discussion 724S-725S.

53. **Halliwell, B., and C. H. Foyer.** 1976. Ascorbic acid, metal ions and the superoxide radical. Biochem J **155:**697-700.

54. **Halliwell, B., and C. H. Foyer.** 1978. Properties and Physiological Function of a Glutathione Reductase Purified from Spinach Leaves by Affinity Chromatography. Planta **139:**9-17.

55. **Halliwell, B., and J. M. Gutteridge.** 1984. Oxygen toxicity, oxygen radicals, transition metals and disease. Biochem J **219:**1-14.

56. **Hassan, H. M.** 1989. Microbial superoxide dismutases. Adv Genet **26:**65-97.

57. **Hofmeister, A. E., S. P. Albracht, and W. Buckel.** 1994. Iron-sulfur cluster-containing L-serine dehydratase from Peptostreptococcus asaccharolyticus: correlation of the cluster type with enzymatic activity. FEBS Lett **351:**416-8.

58. **Holmgren, A.** 1985. Thioredoxin. Annu Rev Biochem **54:**237-71.

59. **Huber, R., P. Stoffers, J. L. Cheminee, H. H. Richnow, and K. O. Stetter.** 1990. Hyperthermophilic Archaebacteria within the Crater and Open-Sea Plume of Erupting Macdonald Seamount. Nature **345:**179-182.

60. **Hutchings, M. I., N. Mandhana, and S. Spiro.** 2002. The NorR protein of Escherichia coli activates expression of the flavorubredoxin gene norV in response to reactive nitrogen species. J Bacteriol **184:**4640-3.

61. **Imlay, J. A.** 2002. How oxygen damages microbes: oxygen tolerance and obligate anaerobiosis. Adv Microb Physiol **46:**111-53.

62. **Imlay, J. A.** 2006. Iron-sulphur clusters and the problem with oxygen. Mol Microbiol **59:**1073-82.

63. **Imlay, J. A., and S. Linn.** 1988. DNA damage and oxygen radical toxicity. Science **240:**1302-9.

64. **Imlay, K. R., and J. A. Imlay.** 1996. Cloning and analysis of sodC, encoding the copper-zinc superoxide dismutase of Escherichia coli. J Bacteriol **178:**2564-71.

65. **Jenney, F. E., Jr., M. F. Verhagen, X. Cui, and M. W. Adams.** 1999. Anaerobic microbes: oxygen detoxification without superoxide dismutase. Science **286:**306-9.

66. **Ji, M. L.** 2003, posting date. Functional evaluation of the mechanisms of reactive oxygen detoxification in the hyperthermophilic archaeon Pyrococcus furiosus using complementation studies. [Online.]

67. **Jovanovic, T., C. Ascenso, K. R. Hazlett, R. Sikkink, C. Krebs, R. Litwiller, L. M. Benson, I. Moura, J. J. Moura, J. D. Radolf, B. H. Huynh, S. Naylor, and F. Rusnak.**

2000. Neelaredoxin, an iron-binding protein from the syphilis spirochete, Treponema pallidum, is a superoxide reductase. J Biol Chem **275:**28439-48.

68. **Kelly, G. J., and E. Latzko.** 1979. Soluble Ascorbate Peroxidase - Detection in Plants and Use in Vitamin-C Estimation. Naturwissenschaften **66:**617-618.

69. **Kelly, K. A., C. M. Havrilla, T. C. Brady, K. H. Abramo, and E. D. Levin.** 1998. Oxidative stress in toxicology: established mammalian and emerging piscine model systems. Environ Health Perspect **106:**375-84.

70. **Klaunig, J. E., and L. M. Kamendulis.** 2004. The role of oxidative stress in carcinogenesis. Annu Rev Pharmacol Toxicol **44:**239-67.

71. **Liochev, S. I., and I. Fridovich.** 1992. Fumarase C, the stable fumarase of Escherichia coli, is controlled by the soxRS regulon. Proc Natl Acad Sci U S A **89:**5892-6.

72. **Liochev, S. I., and I. Fridovich.** 1997. A mechanism for complementation of the sodA sodB defect in Escherichia coli by overproduction of the rbo gene product (desulfoferrodoxin) from Desulfoarculus baarsii. J Biol Chem **272:**25573-5.

73. **Loewen, P. C.** 1984. Isolation of catalase-deficient Escherichia coli mutants and genetic mapping of katE, a locus that affects catalase activity. J Bacteriol **157:**622-6.

74. **Loewen, P. C., and J. Switala.** 1987. Multiple catalases in Bacillus subtilis. J Bacteriol **169:**3601-7.

75. **Lombard, M., M. Fontecave, D. Touati, and V. Niviere.** 2000. Reaction of the desulfoferrodoxin from Desulfoarculus baarsii with superoxide anion. Evidence for a superoxide reductase activity. J Biol Chem **275:**115-21.

76. **Lombard, M., D. Touati, M. Fontecave, and V. Niviere.** 2000. Superoxide reductase as a unique defense system against superoxide stress in the microaerophile Treponema pallidum. J Biol Chem **275:**27021-6.

77. **Lopez-Huertas, E., W. L. Charlton, B. Johnson, I. A. Graham, and A. Baker.** 2000. Stress induces peroxisome biogenesis genes. Embo J **19:**6770-7.

78. **Lushchak, V. I.** 2001. Oxidative stress and mechanisms of protection against it in bacteria. Biochemistry (Mosc) **66:**476-89.

79. **Ma, K., and M. W. Adams.** 1999. A hyperactive NAD(P)H:Rubredoxin oxidoreductase from the hyperthermophilic archaeon Pyrococcus furiosus. J Bacteriol **181:**5530-3.

80. **Massey, V.** 1994. Activation of molecular oxygen by flavins and flavoproteins. J Biol Chem **269:**22459-62.

81. **Massey, V., S. Strickland, S. G. Mayhew, L. G. Howell, P. C. Engel, R. G. Matthews, M. Schuman, and P. A. Sullivan.** 1969. The production of superoxide anion radicals in the reaction of reduced flavins and flavoproteins with molecular oxygen. Biochem Biophys Res Commun **36:**891-7.

82. **McCord, J. M., and I. Fridovich.** 1969. Superoxide dismutase. An enzymic function for erythrocuprein (hemocuprein). J Biol Chem **244:**6049-55.

83. **McCord, J. M., B. B. Keele, Jr., and I. Fridovich.** 1971. An enzyme-based theory of obligate anaerobiosis: the physiological function of superoxide dismutase. Proc Natl Acad Sci U S A **68:**1024-7.

84. **McKersie, B. D., J. Murnaghan, K. S. Jones, and S. R. Bowley.** 2000. Iron-superoxide dismutase expression in transgenic alfalfa increases winter survival without a detectable increase in photosynthetic oxidative stress tolerance. Plant Physiology **122:**1427-1437.

85. **Meister, A.** 1994. Glutathione-ascorbic acid antioxidant system in animals. J Biol Chem **269:**9397-400.

86. **Methe, B. A., K. E. Nelson, J. W. Deming, B. Momen, E. Melamud, X. Zhang, J. Moult, R. Madupu, W. C. Nelson, R. J. Dodson, L. M. Brinkac, S. C. Daugherty, A. S. Durkin, R. T. DeBoy, J. F. Kolonay, S. A. Sullivan, L. Zhou, T. M. Davidsen, M. Wu, A. L. Huston, M. Lewis, B. Weaver, J. F. Weidman, H. Khouri, T. R. Utterback, T. V. Feldblyum, and C. M. Fraser.** 2005. The psychrophilic lifestyle as revealed by the genome sequence of Colwellia psychrerythraea 34H through genomic and proteomic analyses. Proc Natl Acad Sci U S A **102:**10913-8.

87. **Mittler, R.** 2002. Oxidative stress, antioxidants and stress tolerance. Trends Plant Sci **7:**405-10.

88. **Mittler, R.** 2002. Oxidative stress, antioxidants and stress tolerance. Trends in Plant Science **7:**405-410.

89. **Mock, T., and D. N. Thomas.** 2005. Recent advances in sea-ice microbiology. Environmental Microbiology **7:**605-619.

90. **Moore, T. D., and P. F. Sparling.** 1996. Interruption of the gpxA gene increases the sensitivity of Neisseria meningitidis to paraquat. J Bacteriol **178:**4301-5.

91. **Moore, T. D., and P. F. Sparling.** 1995. Isolation and identification of a glutathione peroxidase homolog gene, gpxA, present in Neisseria meningitidis but absent in Neisseria gonorrhoeae. Infect Immun **63:**1603-7.

92. **Moura, I., P. Tavares, J. J. Moura, N. Ravi, B. H. Huynh, M. Y. Liu, and J. LeGall.** 1990. Purification and characterization of desulfoferrodoxin. A novel protein from Desulfovibrio desulfuricans (ATCC 27774) and from Desulfovibrio vulgaris (strain

Hildenborough) that contains a distorted rubredoxin center and a mononuclear ferrous center. J Biol Chem **265:**21596-602.

93. **Neftel, A., P. Jacob, and D. Klockow.** 1984. Measurements of Hydrogen-Peroxide in Polar Ice Samples. Nature **311:**43-45.

94. **Nisbet, E. G., and N. H. Sleep.** 2001. The habitat and nature of early life. Nature **409:**1083-91.

95. **Noctor, G., A. C. M. Arisi, L. Jouanin, K. J. Kunert, H. Rennenberg, and C. H. Foyer.** 1998. Glutathione: biosynthesis, metabolism and relationship to stress tolerance explored in transformed plants. Journal of Experimental Botany **49:**623-647.

96. **Noctor, G., and C. H. Foyer.** 1998. ASCORBATE AND GLUTATHIONE: Keeping Active Oxygen Under Control. Annu Rev Plant Physiol Plant Mol Biol **49:**249-279.

97. **Nordberg, J., and E. S. Arner.** 2001. Reactive oxygen species, antioxidants, and the mammalian thioredoxin system. Free Radic Biol Med **31:**1287-312.

98. **Oleinick, N. L., S. M. Chiu, L. R. Friedman, L. Y. Xue, and N. Ramakrishnan.** 1986. DNA-protein cross-links: new insights into their formation and repair in irradiated mammalian cells. Basic Life Sci **38:**181-92.

99. **Packer, L., E. H. Witt, and H. J. Tritschler.** 1995. alpha-Lipoic acid as a biological antioxidant. Free Radic Biol Med **19:**227-50.

100. **Pai, E. F., and G. E. Schulz.** 1983. The catalytic mechanism of glutathione reductase as derived from x-ray diffraction analyses of reaction intermediates. J Biol Chem **258:**1752-7.

101. **Panchuk, II, R. A. Volkov, and F. Schoffl.** 2002. Heat stress- and heat shock transcription factor-dependent expression and activity of ascorbate peroxidase in Arabidopsis. Plant Physiology **129:**838-853.

102. **Pianzzola, M. J., M. Soubes, and D. Touati.** 1996. Overproduction of the rbo gene product from Desulfovibrio species suppresses all deleterious effects of lack of superoxide dismutase in Escherichia coli. J Bacteriol **178:**6736-42.

103. **Podda, M., and M. Grundmann-Kollmann.** 2001. Low molecular weight antioxidants and their role in skin ageing. Clin Exp Dermatol **26:**578-82.

104. **Radi, R., K. M. Bush, T. P. Cosgrove, and B. A. Freeman.** 1991. Reaction of xanthine oxidase-derived oxidants with lipid and protein of human plasma. Arch Biochem Biophys **286:**117-25.

105. **Raymond, J., and D. Segre.** 2006. The effect of oxygen on biochemical networks and the evolution of complex life. Science **311:**1764-7.

106. **Rivett, A. J., J. E. Roseman, C. N. Oliver, R. L. Levine, and E. R. Stadtman.** 1985. Covalent modification of proteins by mixed-function oxidation: recognition by intracellular proteases. Prog Clin Biol Res **180:**317-28.

107. **Rodrigues, J. V., I. A. Abreu, L. M. Saraiva, and M. Teixeira.** 2005. Rubredoxin acts as an electron donor for neelaredoxin in Archaeoglobus fulgidus. Biochem Biophys Res Commun **329:**1300-5.

108. **Rusnak, F., C. Ascenso, I. Moura, and J. J. Moura.** 2002. Superoxide reductase activities of neelaredoxin and desulfoferrodoxin metalloproteins. Methods Enzymol **349:**243-58.

109. **Sammartano, L. J., R. W. Tuveson, and R. Davenport.** 1986. Control of sensitivity to inactivation by H2O2 and broad-spectrum near-UV radiation by the Escherichia coli katF locus. J Bacteriol **168:**13-21.

110. **Scandalios, J. G.** 1997. Oxidative stress and the molecular biology of antioxidant defenses. Cold Spring Harbor Laboratory Press, Plainview, N.Y.

111. **Schut, G. J., S. D. Brehm, S. Datta, and M. W. Adams.** 2003. Whole-genome DNA microarray analysis of a hyperthermophile and an archaeon: Pyrococcus furiosus grown on carbohydrates or peptides. J Bacteriol **185:**3935-47.

112. **Shacter, E.** 2000. Quantification and significance of protein oxidation in biological samples. Drug Metab Rev **32:**307-26.

113. **Silva, G., J. LeGall, A. V. Xavier, M. Teixeira, and C. Rodrigues-Pousada.** 2001. Molecular characterization of Desulfovibrio gigas neelaredoxin, a protein involved in oxygen detoxification in anaerobes. J Bacteriol **183:**4413-20.

114. **Stadtman, E. R.** 1990. Metal ion-catalyzed oxidation of proteins: biochemical mechanism and biological consequences. Free Radic Biol Med **9:**315-25.

115. **Stadtman, E. R.** 1992. Protein oxidation and aging. Science **257:**1220-4.

116. **Stadtman, E. R., and R. L. Levine.** 2003. Free radical-mediated oxidation of free amino acids and amino acid residues in proteins. Amino Acids **25:**207-18.

117. **Stadtman, E. R., and R. L. Levine.** 2000. Protein oxidation. Ann N Y Acad Sci **899:**191-208.

118. **Stadtman, E. R., J. Moskovitz, B. S. Berlett, and R. L. Levine.** 2002. Cyclic oxidation and reduction of protein methionine residues is an important antioxidant mechanism. Mol Cell Biochem **234-235:**3-9.

119. **Stetter, K. O.** 1996. Hyperthermophiles in the history of life. Ciba Found Symp **202:**1-10; discussion 11-8.

120. **Stoyanovsky, D. A., D. Wu, and A. I. Cederbaum.** 1998. Interaction of 1-hydroxyethyl radical with glutathione, ascorbic acid and alpha-tocopherol. Free Radic Biol Med **24:**132-8.

121. **Thomas, M. J., K. S. Mehl, and W. A. Pryor.** 1982. The role of superoxide in xanthine oxidase-induced autooxidation of linoleic acid. J Biol Chem **257:**8343-7.

122. **Ursini, F., M. Maiorino, R. Brigelius-Flohe, K. D. Aumann, A. Roveri, D. Schomburg, and L. Flohe.** 1995. Diversity of glutathione peroxidases. Methods Enzymol **252:**38-53.

123. **Valasek, M. A., and J. J. Repa.** 2005. The power of real-time PCR. Adv Physiol Educ **29:**151-9.

124. **Van Dover, C. L., C. R. German, K. G. Speer, L. M. Parson, and R. C. Vrijenhoek.** 2002. Evolution and biogeography of deep-sea vent and seep invertebrates. Science **295:**1253-7.

125. **VanCamp, W., K. Capiau, M. VanMontagu, D. Inze, and L. Slooten.** 1996. Enhancement of oxidative stress tolerance in transgenic tobacco plants overproducing Fe-superoxide dismutase in chloroplasts. Plant Physiology **112:**1703-1714.

126. **Vogt, W.** 1995. Oxidation of methionyl residues in proteins: tools, targets, and reversal. Free Radic Biol Med **18:**93-105.

127. **Weinberg, M. V., F. E. Jenney, Jr., X. Cui, and M. W. Adams.** 2004. Rubrerythrin from the hyperthermophilic archaeon Pyrococcus furiosus is a rubredoxin-dependent, iron-containing peroxidase. J Bacteriol **186:**7888-95.

128. **Weisiger, R. A., and I. Fridovich.** 1973. Mitochondrial superoxide simutase. Site of synthesis and intramitochondrial localization. J Biol Chem **248:**4793-6.

129. **Williams, E., T. M. Lowe, J. Savas, and J. Diruggiero.** 2007. Microarray analysis of the hyperthermophilic archaeon Pyrococcus furiosus exposed to gamma irradiation. Extremophiles **11:**19-29.

130. **Woese, C. R., O. Kandler, and M. L. Wheelis.** 1990. Towards a natural system of organisms: proposal for the domains Archaea, Bacteria, and Eucarya. Proc Natl Acad Sci U S A **87:**4576-9.

131. **Xia, L., M. Bjornstedt, T. Nordman, L. C. Eriksson, and J. M. Olsson.** 2001. Reduction of ubiquinone by lipoamide dehydrogenase. An antioxidant regenerating pathway. Eur J Biochem **268:**1486-90.

132. **Yeh, A. P., Y. Hu, F. E. Jenney, Jr., M. W. Adams, and D. C. Rees.** 2000. Structures of the superoxide reductase from Pyrococcus furiosus in the oxidized and reduced states. Biochemistry **39:**2499-508.

133. **Yonei, S., R. Yokota, and Y. Sato.** 1987. The distinct role of catalase and DNA repair systems in protection against hydrogen peroxide in Escherichia coli. Biochem Biophys Res Commun **143:**638-44.

134. **Yost, F. J., Jr., and I. Fridovich.** 1973. An iron-containing superoxide dismutase from Escherichia coli. J Biol Chem **248:**4905-8.

CHAPTER 2

In vitro reconstitution and in vivo complementation studies of the *P. furiosus* superoxide detoxification system

Abstract

A scheme for the detoxification of superoxide in *Pyrococcus furiosus* has been previously proposed in which superoxide reductase (SOR) reduces (rather than dismutates) superoxide to hydrogen peroxide by using electrons from reduced rubredoxin (Rd). Rd is reduced with electrons from NAD(P)H by the enzyme NAD(P)H: rubredoxin oxidoreductase (NROR). The present work allowed the complete pathway from NAD(P)H to the reduction of SOR via NROR and Rd to be reconstituted in vitro using recombinant proteins both at high (80°C) and low (23°C) temperatures, consistent with its proposed role in the superoxide reduction pathway. Additionally, an *in vivo* study was conducted in which superoxide detoxification deficient *E. coli* strains were complemented with genes from the *P. furiosus* superoxide reduction pathway. It was observed that *P. furiosus* SOR can complement for the superoxide scavenging activity of superoxide dismutase, demonstrating its function *in vivo*.

2.1 Introduction

Pyrococcus furiosus is a strict anaerobic hyperthermophilic archeaon that lives in both shallow and deep sea hydrothermal vents (5). The vent fluids contain microbes that oxidize the gases, especially hydrogen sulfide and use it as their energy source (9, 15). It is known that *P. furiosus* can periodically be exposed to oxygen in their environments, and therefore, having some mechanism to detoxify reactive oxygen species would be highly advantageous for their survival. It was proposed by Jenny *et al* that *P. furiosus* has an oxygen detoxification system that does not use the traditional oxygen-detoxification enzymes superoxide dismutase (SOD) and catalase. Instead, it employs a novel enzyme system centered on superoxide reductase (SOR), which functions to reduce superoxide to hydrogen peroxide, using rubredoxin (Rd) as an electron donor, while Rd receives electrons from NROR (10). The reduction of superoxide by SOR produces hydrogen peroxide but no oxygen, which can be advantageous to anaerobic organism. For the superoxide reduction process, it has been shown that rubredoxin, a small (6 kDa) iron-containing protein, serves as the electron donor for SOR (1, 10) and that rubredoxin is reduced by NAD(P)H:rubredoxin oxidoreductase (12).

There has been accumulating evidence that a SOR catalyzed detoxification mechanism is valid *in vitro*. However, it had not been demonstrated that NAD(P)H can serve as an initial electron source for the superoxide reduction pathway in which Rd receives electrons from NAD(P)H via the enzyme NAD(P)H:Rd oxidoreductase. Recombinant forms of *P. furiosus* SOR (4) and Rd (1) were available, and a recombinant form of NROR was obtained and characterized by Grunden (7). This study has shown that the complete pathway from NAD(P)H to reduction of SOR via NROR and Rd can be reconstituted *in vitro* using available recombinant forms of enzymes at 23^{o}C as well as 80^{o}C, and that FAD is an essential cofactor in NROR required for

reduction of Rd. Additionally, direct measurement of hydrogen peroxide production was monitored in the *in vitro* SOR pathway reconstitution enzyme assays supporting the fact that *P. furiosus* SOR reduces the superoxide to hydrogen peroxide and does not dismutate it as does the classic superoxide dismutase enzyme.

In our previous *in vivo* complementation studies (11), *E. coli* mutant strains, which are deficient in homologs of *P. furiosus* genes involved in its oxygen detoxification mechanism, were employed to verify the SOR pathway due to the fact that *P. furiosus* is not very amenable to genetic manipulation. The study showed that *P. furiosus* SOR was able to restore growth of an *E. coli sodA, sodB* mutant when it was cultured under aerobic conditions in M63 minimal media without amino acids, indicating that SOR has the capability of complementing for the SOD activity in the cells. Since the *E. coli sodA, sodB* mutant lacks protection from superoxide, its iron-sulfur cluster containing-enzymes are easily susceptible to oxidative damage from superoxide molecules. One of the important iron-sulfur cluster enzymes in *E. coli* is dihydroxyacid dehydratase, which is the key enzyme for the synthesis of branched amino acids (2). The *E. coli* mutant strain deficient in SodA and SodB was not able to restore its growth when it was grown in minimal media without supplying amino acids, while the *sodA, sodB* mutant strain expressing SOR was able to grow in the minimal media without amino acid supplementation. Another observation from the previous study was that *P. furiosus* SOR showed only partial complementation to a *sodA, sodB* and *norV E. coli* mutant. It was thought that *norV* (flavorubredoxin) in *E. coli* (6) could be serving as the primary electron donor for *P. furiosus* SOR in the *in vivo* complementation studies. This conjecture concerning NorV was made based on the finding that NorV is the only protein in *E. coli* containing a rubredoxin-like domain (49% similarity between *P. furiosus* rubredoxin and the rubredoxin-like domain of *E. coli* NorV)

(Grunden unpublished data) and that rubredoxin is known as the physiological electron donor to *P. furiosus* SOR from *in vitro* assays (12). Therefore, it was thought that the observed limited growth of the *E. coli sodA, sodB, norV* mutant strain expressing *P. furiosus* SOR might be due to the fact that SOR receives the electrons inefficiently in the cells that do not produce NorV.

Our previous *in vivo* SOR pathway complementation studies also provided preliminary evidence that rubredoxin can be the physiological electron donor to SOR (11). However, it was necessary to co-express the *P. furiosus* Rd and SOR in the *E. coli sodA, sodB* and *norV* mutant strain and show the full growth restoration to test the feasibility of the SOR pathway *in vivo*. It was also important to demonstrate the role of the *P. furiosus* NROR in the oxygen detoxification system *in vivo* by expressing *P. furiosus* SOR and NROR in a *sodA, sodB*, and *norW E. coli* mutant strain. *E. coli* has a homolog of *P. furiosus* NROR (encoded as *norW)* that is located adjacent to flavorubredoxin gene (*norV*), and NorW is known as electron donor to the rubredoxin-like domain of NorV using NADPH as an electron donor (6). It was considered valuable to understand the complete SOR mediated oxygen detoxification system of *P. furiosus* by evaluating its function both in *in vitro* assay systems and in *in vivo* complementation studies.

In this current study, it is demonstrated that the complete SOR pathway is involved in superoxide detoxification using an *in vitro* assay wherein superoxide is reduced to hydrogen peroxide by SOR. In the *in vitro* assays it was also shown that NAD(P)H can serve as the electron source for rubredoxin and that this electron transfer is mediated by NROR. The reduced Rd was then shown to support the reduction of superoxide to hydrogen peroxide via superoxide reductase. To validate the *P. furiosus* SOR activity in our previous *in vivo* complementation study, enzyme assays were performed on extracts from the strains that were included in this

study. Additionally, the co-expression of SOR and Rd in the *E. coli* SodA, SodB and NorV mutant strain was further examined.

Cloning, protein expression and purification of the recombinant form of *P. furiosus* NROR was performed by A. Grunden (7). The experimental procedures performed in this current study are described below.

2.2 Materials and methods

2.2.1 Construction of the rNROR expression vector for the *in vitro* reconstitution experiments.

All standard molecular biology techniques were performed essentially as described previously (16). The gene encoding *P. furiosus* NROR (PF1197) was PCR amplified using boiled genomic DNA as the template. The forward and reverse primers were 5'-CACGGTGAT**CATATG**AAGGTAGTTATTGTTGGA-3' (spanning –12 to +21 on the coding strand) and 5'-ATAATATAC**GCAGGAAGAGC**CGGAGTA GAAATCTAAGAT-3' (corresponding to +1,058 to +1,096 on the noncoding strand), respectively (Stratagene, La Jolla, Calif.). The sequences in boldface mark recognition sites for *Nde*I and *Sap*I. Amplification was performed using *P. furiosus* DNA polymerase (Stratagene) and a Robocycler-40 thermocycler (Stratagene) with the following parameters: one cycle of denaturation at 95°C for 5 min, annealing at 50°C for 1.5 min, and extension at 72°C for 2 min. This was followed by 39 cycles with a 1-min denaturation at 95°C, 1.5-min annealing at 50°C, and 2-min extension at 72°C. The amplified 1.14-kb NROR gene was gel purified and isolated using the Gene Clean III kit (Qbiogene, Carlsbad, Calif.). Initial attempts to clone PF1197 employed the T7 expression vector pET-21b system (Novagen, Milwaukee, Wis.), but the resulting constructs proved toxic to *E. coli* and could not be maintained. As a result, an intein-based fusion system was constructed by digesting the NROR gene with *Nde*I and *Sap*I and ligating it into the intein-chitin binding domain (CBD) fusion vector pCYB1 (New England Biolabs, Beverly, Mass.), which was similarly digested, yielding plasmid pBVII-2. Because expression of the NROR-intein-CBD fusion is driven by the moderate-strength *tac* promoter in plasmid pBVII-2, it was thought that greater

expression could be achieved if the NROR-intein-CBD fusion was transferred to an expression vector containing the stronger T7 promoter. As a result, the 3,427-bp NROR-intein-CBD fragment was removed from plasmid pBVII-2 using the restriction enzyme *Nde*I and the blunt-end cutter *Dra*I. The NROR-intein-CBD fragment was then ligated into the T7 promoter-containing plasmid pET-21b (Novagen), restricted with *Nde*I and *BamH*I. The *BamH*I site was modified using the Klenow fragment of DNA polymerase (Stratagene) to give a blunt end compatible with the *Dra*I end on the insert. The resulting plasmid pBVII-3 was then used to obtain recombinant NROR. Prior to recombinant NROR expression, the gene sequence of NROR in the pBVII-3 construct was determined in its entirety by the Molecular Genetics Instrumentation Facility (MGIF) of the University of Georgia. DNA sequences were analyzed using the computer software package MacVector (Accelrys, Burlington, Mass.).

2.2.2 Expression and purification of recombinant NROR.

For expression of the recombinant NROR gene in *E. coli*, plasmid pBVII-3 was transformed into strain BL21(DE3), which has isopropyl-ß-D-thiogalactopyranoside (IPTG)-induced expression of T7 RNA polymerase. The recombinant strain was grown in a 100-liter fermentor at 37°C using Luria-Bertani (LB) as the growth medium, supplemented with ampicillin (100 µg/ml) (University of Georgia BioXpress fermentation facility, Department of Biochemistry). Expression of the plasmid-borne NROR-intein-CBD fusion was induced by the addition of IPTG (0.4 mM) once the culture had reached an optical density at 600nm (OD_{600}) of 0.8. To purify rNROR, all steps were performed under anaerobic conditions using degassed buffers. rNROR was isolated from 50 g of frozen *E. coli* cell paste suspended in 150 ml of buffer A (20 mM Tris-HCl [pH 8.0], 500 mM NaCl, 0.1 mM EDTA, 0.1% Triton X-100), and the cells

were lysed by freeze-thaw and sonication. A cell extract was obtained by centrifugation at 100,000 x *g* for 60 min, and this was applied at a flow rate of 0.5 ml/min to a chitin-agarose bead column (2.5 by 10 cm; New England Biolabs) equilibrated with column buffer A. The loaded column was subsequently washed with 3 column volumes of buffer A to remove any loosely bound protein. At this point, cleavage buffer (20 mM Tris-HCl [pH 8.0], 50 mM NaCl, 0.1 mM EDTA, 0.1 mM FAD, 30 mM dithiothreitol [DTT]) was applied to the column at a flow rate of 4 ml/min until the entire column bed was equilibrated with cleavage buffer. The column was then incubated at 4°C for 24 h to allow for intein-mediated cleavage of the NROR-intein-CBD fusion and release of rNROR. Recombinant NROR protein was eluted from the column as the elution buffer (20 mM Tris-HCl, [pH 8.0], 50 mM NaCl, 0.1 mM EDTA) was applied to the column at a flow rate of 2 ml/min. Fractions containing pure rNROR as judged by sodium dodecyl sulfate-polyacrylamide gel electrophoresis (SDS-PAGE) were concentrated, and the buffer was exchanged with storage buffer (50 mM Tris-HCl [pH 8.0], 2 mM dithiothreitol, 2 mM sodium dithionite, 10% glycerol) using YM-10 Centricon concentrators (Millipore, Bedford, Mass.). In an effort to show that NROR is only catalytically active when FAD is bound, rNROR was also purified as indicated above, except that FAD was not applied to the chitin-agarose column in the cleavage buffer. The absence of FAD in this rNROR preparation was confirmed by UV-visible analysis.

2.2.3 Enzyme assays.

rNROR reconstituted with FAD was prepared anaerobically as follows. rNROR that had been purified without FAD addition was mixed with a 10-fold molar excess of either FAD or flavin mononucleotide (FMN) and was incubated at 85°C for 15 min. Unbound cofactor was

removed by gel filtration. rNROR assays were performed at 80°C using reaction mixtures (2 ml) containing 50 mM CAPS [3-(cyclohexamino)-1-propanesulfonic acid] buffer (pH 10.2), 0.3 mM NADH, and 1 mM BV. The assay was initiated by the addition of rNROR, and a molar absorbance of 7,800 M^{-1} cm^{-1} at 598 nm was used to calculate the rate of BV reduction (12). One unit of activity is equivalent to 1 μmol of BV reduced/min. Coupled reduction of SOR and rNROR via rubredoxin was assayed using the following conditions. Recombinant *P. furiosus* SOR (29 μM) was placed in a sealed, anaerobic cuvette at time 0 containing degassed, 100 mM EPPS buffer (pH 8.0, 23°C) and 300 μM NADPH. Recombinant *P. furiosus* NROR (2.2 nM) and rubredoxin (5 μM) were then added, and the resultant reduction of SOR was monitored by the decrease in absorbance at 658 nm (extinction coefficient for SOR at 658 nm is 2,778 M^{-1} cm^{-1}).

For the hydrogen peroxide assays, a standard SOD reaction mixture (2 ml) was prepared which contained 50 mM potassium phosphate buffer, pH 7.8; 0.2 mM xanthine; 3.4 μg xanthine oxidase; and 20 μM horse heart cytochrome *c* (10). Production of superoxide in the reaction was initiated with the addition of xanthine oxidase, and the reaction mixtures were incubated for 1 min at 23°C before further additions. Positive controls contained either 30 U of bovine liver SOD or 170 nM dithionite-reduced SOR. For the experimental samples, 170 nM each of recombinant *P. furiosus* SOR (4), Rd (1), and NROR that had been preincubated together anaerobically at 23°C for 2 min in 100 mM EPPS buffer (pH 8.0), 0.3 mM NADPH was added after the initial 1-min period for superoxide generation. Negative control reaction mixtures lacked SOR, NROR, or Rd. After 3 min of incubation at 23°C, the amount of hydrogen peroxide was determined using a colorimetric method (14). For this method, 1 ml of the reaction mixture was added to 1 ml of the phenol red solution. This contained 10 mM potassium phosphate buffer, pH 7.0; 140 mM NaCl; 5.5 mM dextrose; 0.28 nM phenol red; and 8.5 U of horseradish peroxidase/ml. The resulting

mixture was incubated at 23°C for 5 min. Ten microliters of 1 N NaOH was then added to increase the pH to 12.5, and the absorbance of the samples was determined at 610 nm. To quantify only the amount of hydrogen peroxide generated by enzymatic scavenging and not that produced as a result of spontaneous dismutation, control samples were prepared that contained all of the assay components but without the addition of SOD or SOR. The amount of hydrogen peroxide present in the samples was calculated using a standard curve.

2.2.4 Bacterial strains and plasmids for the *in vivo* complementation study

The bacterial stains and plasmids used in this study are listed in Table 2-1.

2.2.5 Construction of compatible recombinant *P. furiosus* SOR and Rd expression plasmids for use in the *in vivo* study

In order to produce a plasmid for use in *E. coli* that could support co-expression of *P. furiosus* Rd and SOR, a strategy to clone *P. furiosus* Rd in a plasmid that is compatible with the existing SOR plasmid was developed. A few trials were attempted to obtain the co-expression of Rd and SOR in our previous study (11), but recombinant expression of SOR and Rd was not observed. In this current study, we attempted to clone Rd into a low-copy number cloning vector, pACYC184, which is compatible with the existing pMJ1 (*P. furiosus* SOR in pTrc99A) vector. To do this, the existing plasmid pMJ2 (*P. furiosus* Rd in pTrc99A) was cut with the restriction enzyme *Sph*I to release a DNA fragment that contained the Rd gene and *Trc* promoter. This sticky end DNA piece was polished by using a PCR Polishing Kit (Stratagene) to obtain the blunt ends according to the manufacturer's instruction. The treated DNA fragments were precipitated with ethanol and ligated to the *Dra*I site of the modified pACYC184 vector (see below). Since pACYC184 has two *Dra*I sites located in the chloramphenicol resistance gene, the two sites were cut with *Dra*I and the large pACYC184 fragment was gel purified, religated, and

transformed into Top 10 cells. The newly made vector (pMJ200) has one *Dra*I site disrupting the chloramphenicol resistance gene of pACYC184. pMJ200 was cut with *Dra*I and ligated with the polished DAN fragments that contained the *P. furiosus* Rd gene and its promoter site. The ligation mix was transformed into *E. coli* Top 10 chemically competent cells (Invitrogen). Colony PCR was performed to screen for cells containing plasmids with insert. One clone out of 76 colonies showed the presence of the Rd insert. The positive clone was further analyzed by restriction enzyme digestion and PCR amplification to verify the presence of the insert in the clone.

2.2.6 Expression of recombinant *P. furiosus* SOR and Rd proteins in *E. coli* strain JM105.

Plasmids containing the *P. furiosus* Rd (pMJ200) and SOR (pMJ1) were co-transformed into the *E. coli* JM105 for recombinant protein expression using the conventional $CaCl_2$ method. Both genes are inducible with isopropyl-β-D thiogalactopyranoside (IPTG), a non-degradable analog of allolactose. 30 ml cultures of JM105/pTrc99A, JM105/pMJ1 (SOR in pTrc99A), JM105/pMJ2 (Rd in pTrc99A), and pMJ200 (Rd in modified pACYC184) were grown in LB with appropriate antibiotics at 37^{o}C with shaking. 1 mM of IPTG was added to the cultures once they reached an $O.D._{600}$ of ~1.0 to induce the expression of recombinant *P. furiosus* genes. The cultures were incubated 3 more hours before harvesting. The pellets from the 30 ml cultures were resuspended in lysozyme buffer (0.03mg/ml lysozyme in 50mM Tris, pH 8.0) and sonicated on ice for bursts of 1 min. three times. The cell extracts were centrifuged at 10,000 g for 30 min. The supernatants were collected and heat-treated for 20 min. at 80^{o}C followed by centrifugation at 10,000g for 20 min to remove the denatured *E. coli* proteins. Protein concentrations of the samples were determined by the Bradford method (3). 2X protein denaturing dye (0.125M tris-HCl, 4% SDS, 20% v/v glycerol, 0.2M DTT, 0.02% bromophenol blue, pH 6.8) was added to the

samples, and boiled at 100°C for 5 min. Samples (5~10 μg each) were loaded onto 12.5% polyacrylamide SDS gels. The proteins were visualized by staining the gels with Coomassie-Blue.

2.2.7 Cloning and Expression of recombinant *P. furiosus* NROR proteins in *E. coli* strain JM105.

Construction of a non- tagged *P. furiosus* NROR expression plasmid was completed in this study. The primers used for PCR amplification of *P. furiosus* NROR were the following: Forward primer containing a *Sac*I site 5'-**GAGCTC**CAAGGAGATGAAATGAAGGTAGTT-3 and Reverse primer containing a *Bam*HI site 5'-GTTGGGACTTCACAT**GGATCCT**AGTGGAGA-3' The following PCR amplification parameters were used: one cycle of denaturation at 95°C for 4 min., 30 cycles of 30 sec. denaturation at 95°C, 1min. annealing at 56°C, and extension for 2 min. at 72°C. The amplified PCR product was purified and digested with *Sac*I and *BamH*I and ligated to corresponding restriction sites of the cut pTrc99A vector. The resulting plasmid was named pMJ4 and was transformed into XL1-Blue using the $CaCl_2$ method. The plasmid was analyzed by restriction site digestion and PCR amplification. The confirmed plasmid was transformed into JM105 for protein over-expression. The same methods as indicated above for Rd and SOR over-expression were used for *P. furiosus* NROR protein over-expression.

2.2.8 The use of the *P. furiosus* SOR enzyme assay to verify the SOR activity of the complemented strains.

Our previous *in vivo* study showed that *P. furiosus* SOR complemented the *sodA, sodB* mutations in *E. coli* strain NC906 and the *sodA, sodB*, and *norV* mutations in *E. coli* strain

MJ100 by restoring their growth in an M63 minimal media that lacks amino acid supplementation. Cultures of the strains in the complementation growth studies were prepared for use in the *P. furiosus* SOR enzyme activity assays. 30 ml aliquots of M63 minimal media lacking amino acids, but containing glycerol as the carbon source and the appropriate antibiotics were prepared. Prior to inoculation, 0.1 mM of IPTG was added to each culture. For each culture, the appropriate volumes of inocula were added to give a starting OD_{600} of 0.06. MJ002 (*P. furiosus* SOR expression in *sodA*, *sodB* deficient strain) and MJ102 (*P. furiosus* SOR expression in sodA, *sodB, norV* deficient strain) were incubated along with the controls (MJ01, and MJ001, and MJ101) at 37^{o}C aerobically. Growth of the cultures was monitored by measuring the OD_{600} at 3, 5, 7, 9, and 11h after inoculation. At the 11h time point, cultures were harvested and washed with wing buffer (50 mM potassium phosphate buffer, pH 7.8, 0.1mM EDTA) and frozen until used. Cell pellets were resuspended with wing buffer and sonicated on ice for 1 min. for 3 times and centrifuged with Beckman Avanti at 20,000g for 30 min. The cell free extracts were collected, and protein concentrations were determined based on the Bradford method (3). SOR activity was detected through competition with cytochrome c using a Shimadzu UV-2401 PC spectrophotometer. The standard assay was performed in 3mL of 50mM potassium phosphate buffer, pH 7.8, 0.1 mM EDTA at 25°C. The reaction mixture contained 10μM of horse heart ferricytochrome c (Sigma), 50 μM xanthine (Sigma) and sufficient xanthine oxidase to produce a rate of reduction of ferricytochrome c at 550 nm of 0.025 absorbance per minute. Under this standard condition, 1 unit of SOR activity is defined as the amount of enzyme that inhibits the rate of cytochrome c reduction by 50% (13).

2.2.9 *In vivo P. furiosus* SOR-Rd complementation studies using the *E. coli sodA, sodB, norV* deficient strains.

In order to test the ability of the *P. furiosus* SOR- Rd co-expression to complement an *E. coli* strain deficient in the *sodA, sodB*, and *norV* genes, co-transformation of the plasmids, pMJ1 (*P. furiosus* SOR in pTrc99A) and pMJ20 (*P. furiosus* Rd in the modified pACYC184 plasmid) were transformed in to the wild type *E. coli* strain NC905 and the *sodA, sodB,* and *norV* mutant *E. coli* strain MJ100 giving the strains MJ003 and MJ103, respectively. Overnight cultures were prepared in M63 minimal media containing glucose as the carbon source with amino acid supplementation. The same methods as indicated above were used for these culture preparations and growth studies.

2.3 Results

2.3.1 Expression and purification of recombinant NROR for the *in vitro* reconstitution experiments

The *P. furiosus* NROR was cloned into the intein-CBD-fusion expression plasmid pCYB1 (New England Biolab) by A. Grunden, and recombinant NROR-intein-CBD fusion protein was produced using this expression system (~91kDa) (Figure 2-1, lane 2). Untagged rNROR was isolated by binding the rNROR-intein-CBD fusion protein onto a chitin sepharose column, eluting off contaminating *E. coli* proteins and by cleaving the intein–CBD fusion in the presence of reducing agent and 0.1mM FAD. Fractions contained rNROR were pooled and concentrated.

2.3.2 Catalytic properties of recombinant NROR

Reconstitution experiments of aopoemzyme-rNROR were performed to examine the catalytic efficiency with and without bound FAD in order to investigate the role of FAD as cofactor. Apo-rNROR was prepared by omitting FAD from the cleavage buffer. Since thermophilic enzymes have rigid structures that prevent full activity at low temperature heat treatment of the samples at 85^{o}C for 15 min. was performed to increase the activity. When NROR assays were performed using NADH as the electron donor and benzyl viologen as the electron acceptor, it was determined that there was 3.5 unit of activity with apoenzyme (Table 2-2). However, when the NROR preparation was reconstituted with 10-fold molar excess of FAD, the activity increased 15 times compared to rNROR without FAD. Reconstitution of rNROR with 10 fold FMN yielded inactive enzyme, indicating that catalytic activity of *P. furiosus* NROR requires the cofactor FAD, not FMN.

2.3.3 Reconstitution of a recombinant NADPH-dependent, superoxide reduction pathway.

There has been accumulated evidence that *P. furiosus* SOR reduces superoxide to hydrogen peroxide (10). It has previously been shown that the native form of *P. furiosus* NROR catalyzed the NADPH-dependant reduction of rubredoxin (12) and that SOR was able to catalyze the reduction of superoxide using reduced rubredoxin as an electron carrier (10). However, the NADPH-dependent coupled enzyme system had not been experimentally demonstrated. Utilizing the recombinant forms of *P. furiosus* SOR, Rd, and NROR, the NADPH-dependent SOR reduction pathway was investigated to test the feasibility of the reaction pathway *in vitro*. When SOR (29 μM) was incubated at 23°C with 300 μM NADPH, no direct reduction of SOR was observed, as illustrated in Figure 2-2. When recombinant *P. furiosus* NROR (2.2 nM) was then added, there was still no reduction of SOR, indicating that NROR cannot directly reduce this enzyme. However, upon addition of recombinant rubredoxin (5 μM), SOR is rapidly reduced, as shown by the steep decrease in absorbance at 658 nm. The rate of SOR reduction was calculated to be 42.5 μmol/min/mg of NROR at 23°C.

2.3.4 Analyzing the *in vitro* reconstitution of the SOR pathway by measuring hydrogen peroxide production.

The *in vitro* reconstitution of an NADPH-dependent pathway for superoxide reduction was directly evaluated by analyzing for hydrogen peroxide production, the hypothesized end product of SOR catalyzed reduction of superoxide (10). As controls, superoxide was generated from xanthine/xanthine oxidase and subsequently converted to hydrogen peroxide with either bovine liver SOD or dithionite-reduced SOR. The amount of superoxide converted to hydrogen peroxide was comparable in both these samples (Table 2-3). When SOR that had been pre-incubated anaerobically with NROR and Rd (170 nM each) in the presence of 0.3 mM NADPH

was added to the assay mixture, the amount of hydrogen peroxide increased about two-fold, which would be expected given that the SOR-catalyzed reduction of superoxide provides two equivalents of hydrogen peroxide compared to the SOD-catalyzed dismutation reaction. However, if SOR, Rd, or NROR was omitted, negligible amounts of hydrogen peroxide were detectable. Thus, these results directly demonstrate that SOR mediates reduction of superoxide to hydrogen peroxide in an NADPH-dependent manner via a coupled reaction between NROR, Rd, and SOR. Furthermore, it is important to note that unlike many reactions involving enzymes from hyperthermophilic sources, this coupled reaction proceeds rapidly at mesophilic temperatures. This is consistent with its proposed involvement in oxygen detoxification in *P. furiosus* during exposure to oxygen at low temperatures (10)

2.3.5 Construction of compatible recombinant *P. furiosus* SOR and Rd plasmids and their co-expression in *E. coli*

To achieve the co-expression of *P. furiosus* Rd and SOR, a compatible and low-copy number expression vector was constructed. This construct used the Rd gene and its promoter region portion of the existing pMJ2 plasmid (Rd-pTrc99A). The Rd gene insert was polished and ligated in to the *Dra*I site of pMJ200 (modified pACYC184 plasmid). Low transformation efficiency resulted from transformation of the ligation mix into *E. coli* XL1 Blue cells, and only one clone was obtained. This plasmid was analyzed by restriction site digestion and PCR verification (Figure 3). When it was digested using *Bam*HI and *Sal*I, the Rd DNA fragment showed the expected size (165 bp) and the Rd gene was also amplified in PCR reactions using Rd specific primers and the plasmid DNA as the template. The pMJ1 and pMJ20 plasmids were co-transformed and *P. furiosus* SOR and Rd proteins were over-expressed in JM105 prior to heat treatment for 20 min. at 80^{o}C. Supernatants were collected and mixed with 2X protein loading

dye. Samples were loaded in 12.5% SDS protein gels and visualized with Coomassie Blue (Figure2-4). A distinct band corresponding to the expected size (~14.5 kDa) of the *P. furiosus* SOR was observed along with a less dense band in the same lane (lane 5), which corresponds the expected size of *P. furiosus* Rd (~less than 6kDa). Considering that *P. furiosus* Rd is cloned in a low copy number vector (p15A origin) while *P. furiosus* SOR is in a medium copy number vector, the thickness of the bands is consistent with the anticipated protein expression levels.

2.3.6 *P. furiosus* SOR showed high activity in the *sodA, sodB* deficient strain and *sodA, sodB,* and *norV* mutant strain. The previous *P. furiosus* SOR complementation studies, demonstrated that *P. furiosus* SOR can function *in vivo* in *E. coli* to complement defects in *sodA* and *sodB* by supporting aerobic growth of the *sod* mutant strain in amino acid deficient minimal media (11). For this study, we are extending those findings by verifying the activity of *P. furiosus* SOR in the extracts of the cultures from the complementation studies. 30ml cultures of MJ002 (SOR/NC906) and MJ102 (SOR/MJ100) along with controls, MJ01 (pTrc99A/NC905), MJ001 (pTrc99A/NC906) and MJ101 (pTrc99A/MJ100) were grown aerobically at 37°C in M63 minimal media containing glycerol but lacking amino acid supplementation to test the activity of SOR in the complementation growth studies. All cultures were grown for 11 hours after inoculation. At each time point, OD_{600} was measured for each culture to observe the growth restoration (Figure 2-4). After 11 hours of growth, the cultures were harvested and the cell free extracts were used in enzyme assays. The growth patterns were similar to the previous study. The SodA, SodB mutant strain expressing *P. furiosus* SOR (MJ002) showed a high degree of restored growth (~75% of the O.D. of the wild type strain) and MJ102 had 35% of the growth of the wild type strain indicating that activity of *P. furiosus* SOR contributes to the viability of *sod*

deficient *E. coli* under aerobic growth conditions, presumably by scavenging superoxide radicals before they damage cell constituents.

To test the contribution of SOR activity to the growth restoration, cytochrome c-based enzyme assays were performed to measure the specific activity of each strain (Table 2-4). The reduction rate of cytochrome c by superoxide radicals was monitored at 550 nm utilizing the xanthine-xanthine oxidase system as a source for superoxide. SOR will compete for superoxide and inhibit the reduction rate of cytochome c. From the table, *P. furiosus* SOR complemented strains (MJ002 and MJ102) showed significant activity levels supporting the idea that *P. furiosus* SOR contributes to restoring growth in the *sod* mutant strains which have impaired amino acids synthesis due to loss of key amino acid biosynthesis enzymes which have iron-sulfur clusters sensitive to destruction by superoxide. The two SOR expression strains had approximately 3 times higher SOD/SOR activity compared to the wild type strain indicating that *P. furiosus* SOR is highly active in the *E. coli* complementation system. Note, however, that the NC906 strain still showed small amount of activity probably due to the presence of the third dismutase, SodC of *E. coli*. The partially complemented strain, MJ102 (SOR/MJ102), showed high SOR activity along with the MJ002 (SOR/NC906) strain, suggesting that *P. furiosus* SOR is able to receive electrons in the *E. coli* extract from donor(s) other than the *norV* rubredoxin-like donor. From these results, it was considered worthwhile to test whether the combination of *P. furiosus* SOR and Rd can complement the growth of the *sodA, sodB*, and *norV* mutant strain better than the expression of just SOR alone. Also from these studies, it is interesting to note that *P. furiosus* SOR showed significant levels of activity when expressed in *E. coli* cells grown under mesophilic aerobic conditions despite the fact that these enzymes come from an obligate hyperthermophilic anaerobic source. These findings lend further credence to the idea that the

function of the SOR pathway enzymes is to provide protection to *P. furiosus* under the conditions when it would most likely be exposed to oxygen in its environment, which is in cold and oxygen-saturated sea water rather than within the oxygen-depleted hydrothermal vent systems (10).

2.3.7. Co-expression of *P. furiosus* SOR and Rd in *E. coli* wild type strain NC 905 limits its growth in M63 minimal media lacking amino acid supplementation.

To further investigate the *P. furiosus* SOR and Rd functions in the detoxification mechanism *in vivo*, it was necessary to co-express the two genes in mutant strains in which the corresponding homologous genes are disrupted, and observe the growth in M63 minimal media without supplementation of amino acids. However, our experimental plans were stymied by the findings that the co-expression of *P. furiosus* SOR and Rd in both the wild type *E. coli* and *sodA*, *sodB* mutant strains prevented the growth of the cells in M63 minimal media containing glycerol but lacking amino acid supplementation. In order to investigate the toxicity of the co-expression of the proteins, plasmids containing the two genes were transformed in to the wild type *E. coli* NC905 strain, and growth of the transformants in M63-glycerol minimal media lacking amino acid supplementation was monitored (Table 2-5). The MJ03 (co-expression of SOR in pTrc99A and Rd in pACYC194 in NC905 strain) culture had no growth 18 hours after the inoculation while other controls, MJ01 (NC905-pTrc99A), MJ02 (NC905-Rd in pTrc99A), and MJ04 (NC 905-Rd in pACYC184), had shown significant growth indicating that co-expression of SOR and Rd caused toxicity in *E. coli*. It is assumed that more than two foreign proteins are a burden for the *E. coli* cell to carry. It is possible that expression of *P. furiosus* SOR and Rd genes can disrupt the NAD(P)H pool of *E. coli* cells, which can limit the growth. In order to confirm the toxicity of the expression, the co-expression strain along with control strains were grown in LB

media and the growth observed (Table 2-6). From the table, MJ105 (NC905- Rd-SOR in pTrc99A), a strain containing the Rd and SOR in a single transcript showed significant growth inhibition in LB media, and MJ103 (NC905-SOR in pTrc99A and Rd in modified pACYC184), the strain that has the SOR and Rd expressed from different vectors exhibited inhibition of growth rate, while the controls showed no inhibition. Due to the fact that co-expression of *P. furiosus* proteins retards the growth of *E. coli*, further investigation regarding the co-expressing the *P. furiosus* SOR and NROR in the *E. coli* sodA, sodB, and norW mutant (MJ200) were unable to be performed, despite achieving the protein expression of *P. furiosus* NROR-pTrc99A vector in the JM105 strain (Figure 2-6).

CONCLUSION

Previous studies have shown that *P. furiosus* can reduce superoxide, and that rubredoxin is reduced by NAD(P)H via NAD(P)H: rubredoxin oxidoreductase (NROR) (10). Based on these facts a model was proposed in which *P. furiosus* SOR catalyzed the reduction of superoxide to hydrogen peroxide and used electrons from reduced rubredoxin to perform the reduction of superoxide (7, 10) (Figure 2-7). However, at the time this superoxide detoxification pathway was first proposed, the coupled reduction of Rd by NAD(P)H via NROR and the subsequent reduction of superoxide to hydrogen peroxide by SOR had not been experimentally demonstrated. Here in this study, the complete superoxide detoxification pathway has been shown using an *in vitro* assay to proceed as predicted by the model. The *in vitro* reconstitution assays which included recombinant *P. furiosus* SOR, Rd and NROR demonstrated that SOR-mediated reduction of superoxide to hydrogen peroxide can occur at high efficiency both at 80^{o}C as well as at 25^{o}C, supporting the notion of their roles in oxygen protection, as *P. furiosus* can be exposed to significant levels of oxygen at low temperature (8). Additionally, direct measurement of hydrogen peroxide levels in the reconstitution enzyme assay samples confirmed that the SOR converts superoxide to hydrogen peroxide by pure reduction mechanisms and not by a dismutation.

Even though the detoxification mechanisms of reactive oxygen species in *P. furiosus* has been demonstrated using *in vitro* assay systems, an *in vivo* study had not previously been attempted. Due to the fact that a *P. furiosus* genetic system has not been developed, *E. coli*, which is very amenable to genetic manipulation, was used to investigate whether the *P. furiosus* SOR superoxide detoxification system functions *in vivo* as predicted by the pathway model. From the *in vivo* growth study, *P. furiosus* SOR was shown to restore aerobic growth of an *E.*

coli sodA, sodB mutant strain and a *sodA, sodB*, and *norV* mutant strain in amino acid deficient M63-glycerol minimal media, indicating that *P. furiosus* SOR can complement for the superoxide scavenging activity of superoxide dismutase. The SOR enzyme assays from extracts prepared from the complementation study samples further demonstrated that the recombinant *P. furiosus* SOR had significant SOR/SOD activity *in vivo*. Even though a full evaluation of the complete SOR detoxification pathway using the *E. coli* complementation system was prevented by the loss of viability in *E. coli* cells that co-expressed SOR and Rd, the *in vivo* studies did demonstrate that *P. furiosus* SOR can provide protection against the superoxide toxicity in foreign host cells. As a basis of future studies, this achievement can be applied to other foreign host cells, such as plant, fungi, and animal cells in an effort to provide improved protection against superoxide-mediated cellular damage.

Table 2-1. Bacterial strains and plasmids used in this study

Strains	Genotype	Source
XL1-Blue	*recA1 endA1 gyrA96 thi-1 hsdR17 supE44 relA lac [F' proAB lacIqZΔM15Tn10(Tet')]*	Invitrogen
JM105	F' *traD36 proA+ proB+ lacIq delta(lacZ)M15 delta(pro-lac) hsdR4 sbcB15 rpsL thi endA1* lambda	Lab collection
NC905	F- lambda- *ilvG- rfb*-50 *rph*-1	H. Hassan
NC906	NC905 *sodA, sodB*::Kan^r	H. Hassan
MJ01	pTrc99A/NC905	Previous study
MJ02	pMJ2/NC905	In this study
MJ03	pMJ1, pMJ20/NC905	In this study
MJ04	pMJ20/NC905	In this study
MJ105	pMJ5/NC905	
MJ001	pTrc99A/NC906	Previous study
MJ002	pMJ1/NC906	Previous study
MJ003	pMJ20/NC906	In this study
MJ100	NC906*norV*::Cm^r	Previous study
MJ101	pTrc99A/NC906 *norV*::Cm^r	Previous study
MJ102	pMJ1/NC906 *norV*::Cm^r	Previous study
MJ103	pMJ1, pMJ20/NC906 *norV*::Cm^r	In this study
MJ200	NC906*norW*::Cm^r	Previous study
Plasmids	**Genotype**	**Source**
pTrc99A	Trc promoter, Amp^r, ColE1 ori	Amersham Pharmacia
pMJ1	pTrc99A *P. furiosus* SOR	Previous study
pMJ2	pTrc99A *P. furiosus* Rd	Previous study
pMJ4	pTrc99A *P. furiosus* NROR	In this study
pMJ5	pTrc99A *P. furiosus* Rd-SOR	In this study
pACYC184	Cloning vector, p15A ori, Cm^r, Tet^r	New England BioLab
pMJ200	Cloning vector, p15A ori, Tet^r	New England BioLab
pMJ20	Trc promoter, p15A, Tet^r *P. furiosus* Rd	In this study

Table 2-2. Reconstitution of recombinant *P. furiosus* NROR

Sample	Specific Activity (U/mg)
As purified apoenzyme	3.5
Heat treated, without FAD	21.9
Heat treated, with FAD	352
Heat treated, with FMN	<0.1

For purification of rNROR for the reconstitution experiment, 0.1mM FAD was omitted from the cleavage buffer. The enzyme assays were performed at 80^{o}C. Samples were heat treated at 85^{o}C for 15 Min.

Table 2-3. *In vitro* reconstitution of *P. furiosus* NAD(P)H- dependant superoxide reduction pathway as monitored by hydrogen peroxide production.

Addition to reaction mixture	Amount of hydrogen peroxide (μmole)
SOD	0.36
Dithionite-reduced SOR	0.48
SOR, NROR, Rd, NADPH	0.81
SOR, NROR, NADPH	0.09
SOR, Rd, NADPH	0.16
NROR, Rd, NADPH	0.09

All assays were performed at 23°C. The reaction contained a superoxide generation system (xanthine oxidase, xanthine, and horse heart cytochrome c). Bovine SOD (30U), NADPH (0.3 mM), SOR, NROR, and Rd (each 170 nM) were added.

Table 2-4. SOR specific activities for various *E. coli* strains grown in M63 without amino acid supplementation.

Strains	Specific activity (U/mg)
MJ01 (pTrc99A-NC905)	17.9
MJ001 (pTrc99A-NC906)	1.20
MJ002 (SOR-NC906)	52.9
MJ101 (pTrc99A-MJ100)	0.98
MJ102 (SOR-MJ100)	54.8

Table 2-5. Relative growth level of various *E. coli* strains in amino acid deficient M63-glycerol minimal media.

Strains	**O.D.$_{600}$ (t=0)**	**O.D.$_{600}$ (t=18 h)**
MJ01 (NC905-pTrc99A)	0.057	2.275
MJ02 (NC905-Rd in pTrc99A)	0.059	0.935
MJ03 (NC905-SOR in pTrc99A, Rd in Modified pARCY184)	0.06	0.011
MJ04 (NC 905-Rd in modified pACYC184)	0.061	0.983

The experimental cultures were inoculated with enough inoculum to give a starting O.D. of 0.06.

Table 2-6. Relative growth level of various *E. coli* strains in LB media

Strains	**O.D.$_{600}$ (t=0)**	**O.D.$_{600}$ (t=6 h)**
MJ01 (NC905-pTrc99A)	0.059	1.42
MJ02 (NC905-Rd in pTrc99A)	0.058	1.25
MJ03 (NC905-SOR in pTrc99A, Rd in Modified pARCY184)	0.059	0.73
MJ04 (NC905-Rd in modified pACYC184)	0.061	1.39
MJ05 (NC905- Rd and SOR in pTrc99A as an single transcript)	0.060	0.12

The experimental cultures were inoculated with enough inoculum to give a starting O.D. of 0.06.

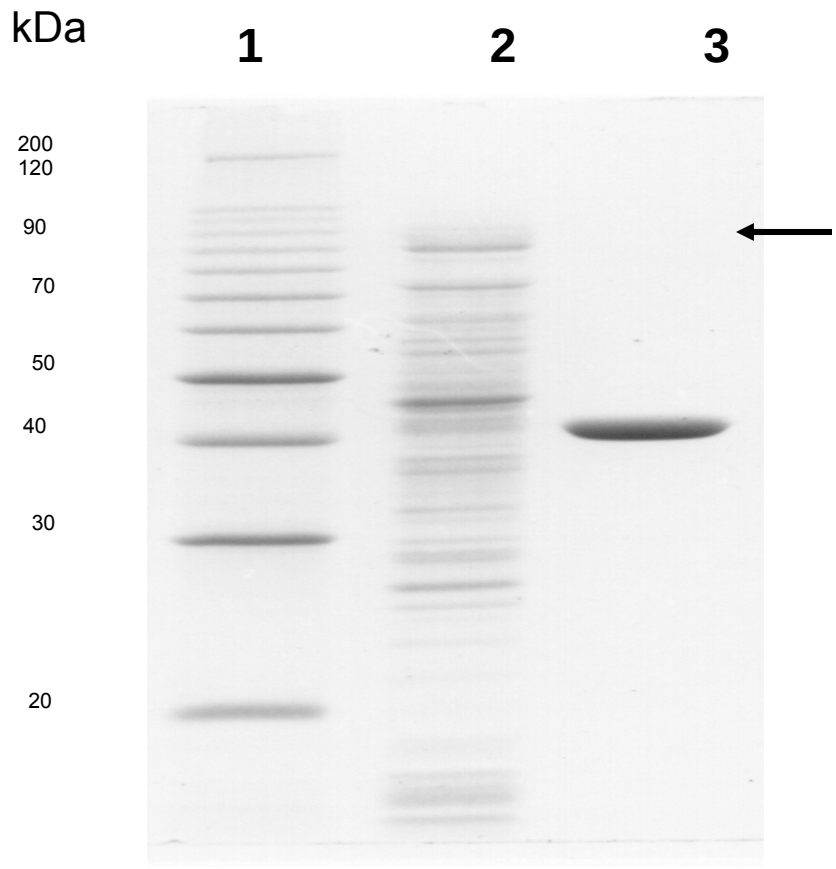

Figure 2-1. SDS-12% polyacrylamide gel electrophoresis of purified *P. furiosus* rNROR

Lane 1: Molecular Marker

Lane 2: Cell free extract

Lane 3: rNROR

The arrow marks the location of NROR-intein-CBD fusion (~91kDa) in lane 2

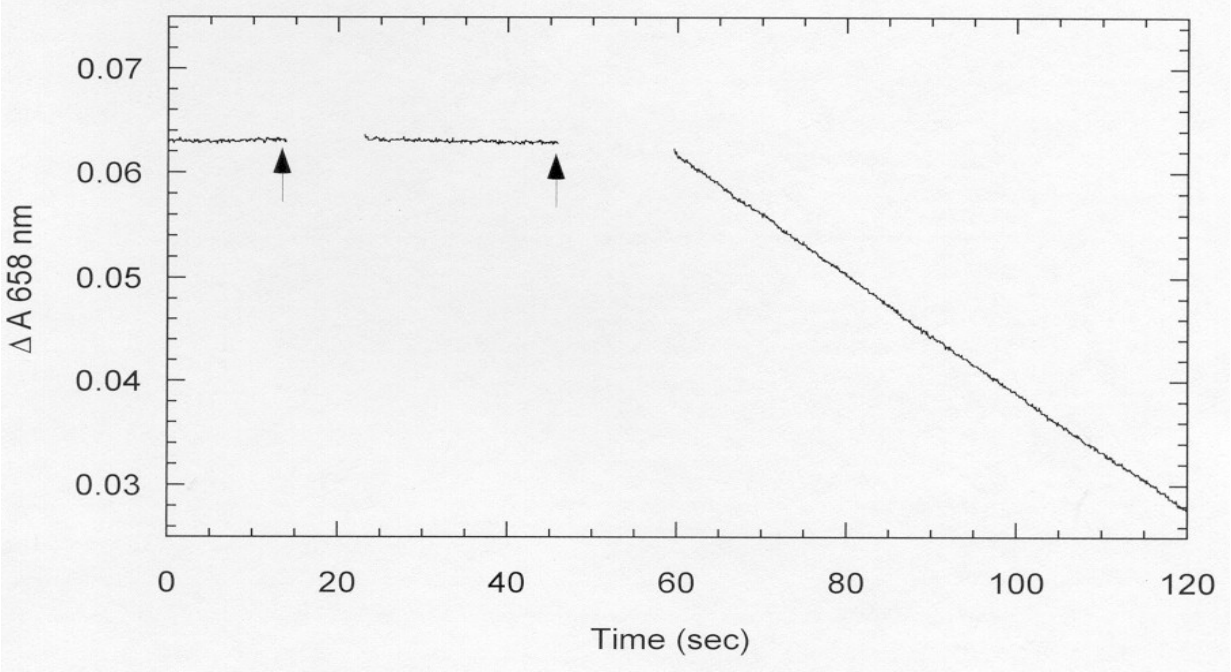

Figure 2-2. Reduction of *P. furiosus* superoxide reductase by recombinant NROR via rubredoxin. Recombinant *P. furiosus* SOR (29 μM) was placed in a sealed, anaerobic cuvette at time 0 containing degassed, 100mMEPPS buffer (pH 8.0, 23°C) and 300 μM NADPH. The first arrow indicates addition of recombinant NROR (2.2 nM) to the assay. Recombinant *P. furiosus* rubredoxin (5 μM) was then added as shown by the second arrow. Empty spaces in the trace represent times when the cuvette was removed from the spectrophotometer for additions and/or mixing. The reduction of SOR was monitored by the decrease in absorbance at 658 nm.

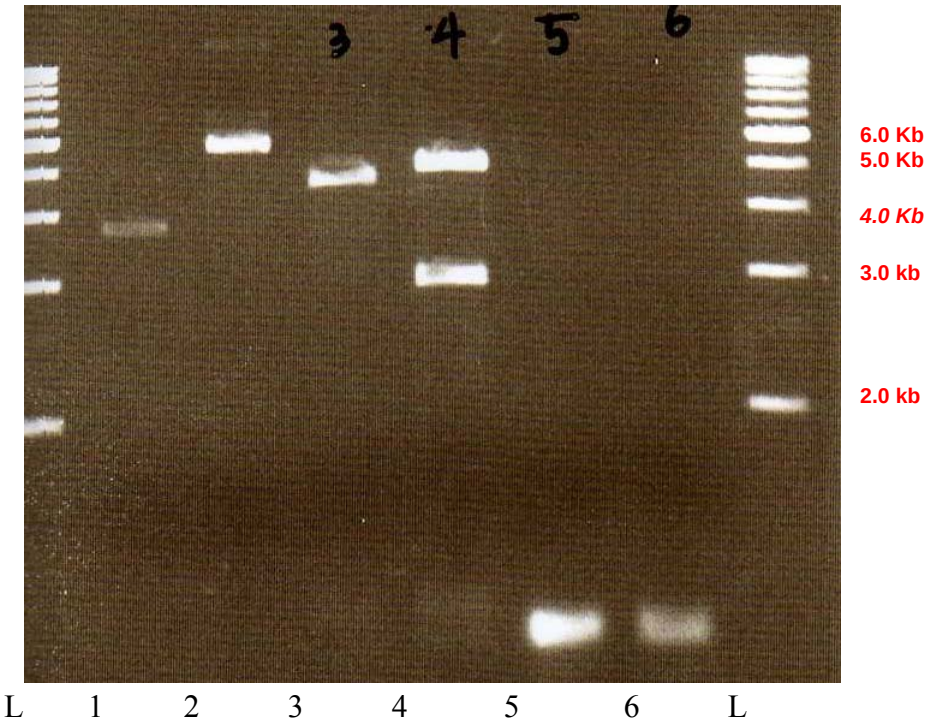

Figure 2-3. Restriction site analysis and PCR verification for the cloned *P. furiosus* Rd

L: Molecular marker, Lane 1: pMJ200 (modified pACYC184, supercoiled), Lane 2: clone #35 (supercoiled), Lane 3: pMJ200 digested by *Sal*I/ *Bam*HI, Land 4: clone #35 digested by *Sal*I/ *BamHI*, Lane 5: Rd specific PCR products using clone #35 as template, Lane 6: Rd specific PCR products using *P. furiosus* genomic DNA as template

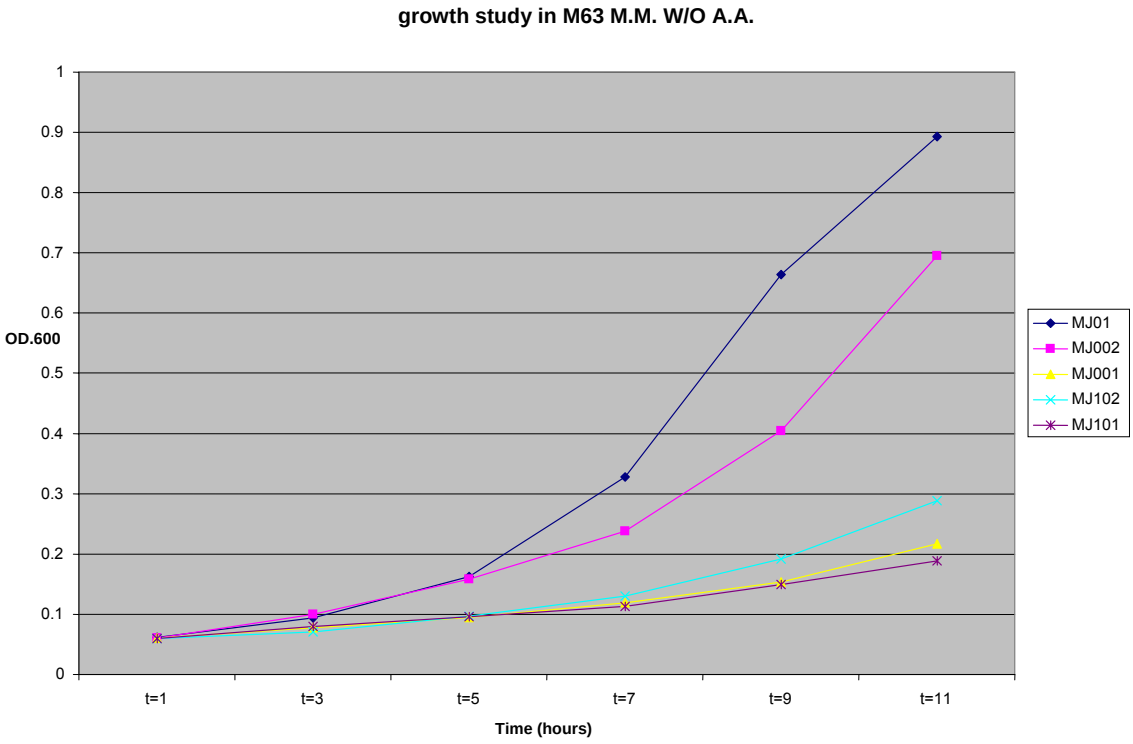

Figure 2-4. Complementation study of the ability of *P. furiosus* SOR to restore growth of an *E. coli sodA, sodB, norV* mutant in M63 glycerol minimal medium without amino acid supplementation. The experimental cultures were inoculated with enough inoculum to give a starting O.D. of 0.06. MJ01: pTrc99A in *E. coli* wild type, MJ002: *P. furiosus* SOR in *E. coli sodA, sodB* mutant, MJ001: *pTrc99A* in *E. coli sodA, sodB* mutant, MJ102: *P. furiosus* SOR in *E. coli sodA, sodB, norV* mutant, MJ101: pTrc99A in *E. coli sodA, sodB, norV* mutant.

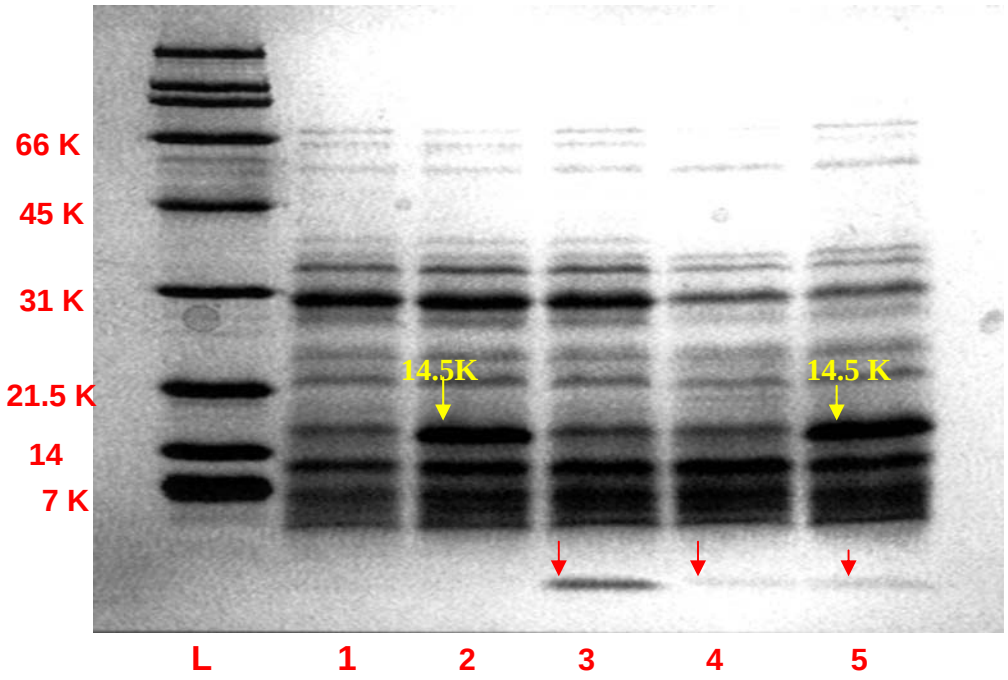

Figure 2-5. *P. furiosus* SOR in pTrc99A and Rd in modified pACYC184 co-expression in *E. coli* JM105. L. Molecular marker, Lane 1: Control: pTrc99A, Lane 2: pMJ1: *P. furiosus* SOR in pTrc99A, Lane 3: pMJ2: *P. furiosus* Rd in pTrc99A, Lane 4: pMJ20: *P. furiosus* Rd in pMJ200, Lane 5: pMJ1+ pMJ20:co-expression of *P. furiosus* SOR- pTrc99A and Rd-pMJ200

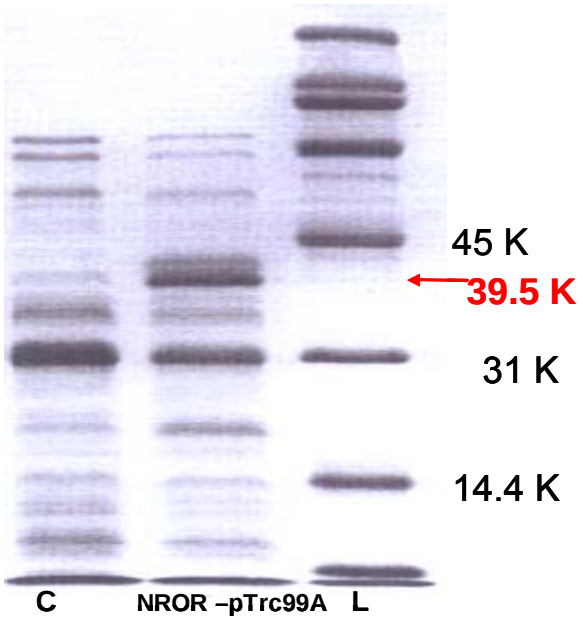

Figure 2-6. *P. furiosus* NROR protein expression in JM105

C: pTrc99A, NROR-pTrc99a: *P. furiosus* NROR in pTrc99A, L: M.W. standard

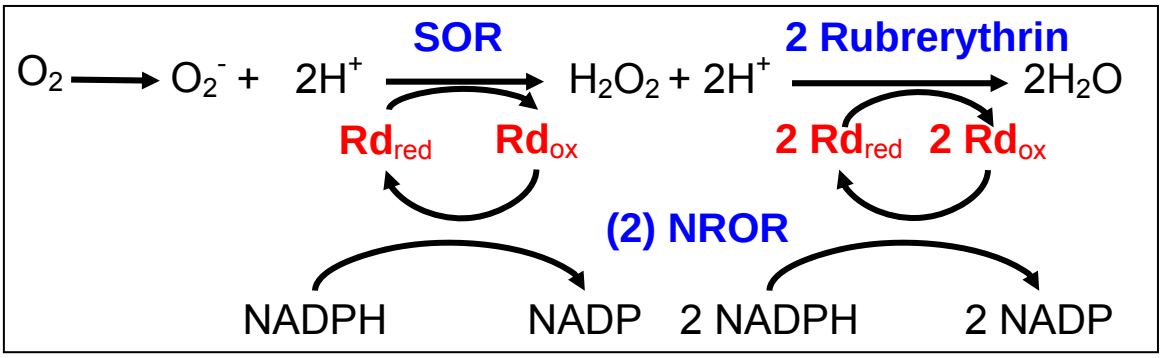

Figure 2-7 . Model of the pathway for detoxification of reactive oxygen species in *P. furiosus* (modified from Grunden, 2005).

Literature cited

1. **Adams, M. W., J. F. Holden, A. L. Menon, G. J. Schut, A. M. Grunden, C. Hou, A. M. Hutchins, F. E. Jenney, Jr., C. Kim, K. Ma, G. Pan, R. Roy, R. Sapra, S. V. Story, and M. F. Verhagen.** 2001**.** Key role for sulfur in peptide metabolism and in regulation of three hydrogenases in the hyperthermophilic archaeon Pyrococcus furiosus. J Bacteriol **183:**716-24.

2. **Boehm, D. E., K. Vincent, and O. R. Brown.** 1976. Oxygen and toxicity inhibition of amino acid biosynthesis. Nature **262:**418-20**.**

3. **Bradford, M. M.** 1976. A rapid and sensitive method for the quantitation of microgram quantities of protein utilizing the principle of protein-dye binding. Anal Biochem **72:**248-54.

4. **Clay, M. D., F. E. Jenney, Jr., P. L. Hagedoorn, G. N. George, M. W. Adams, and M. K. Johnson.** 2002. Spectroscopic studies of Pyrococcus furiosus superoxide reductase: implications for active-site structures and the catalytic mechanism. J Am Chem Soc **124**:788-805.

5. **Fiala, G., and K. O. Stetter.** 1986. Pyrococcus-Furiosus Sp-Nov Represents a Novel Genus of Marine Heterotrophic Archaebacteria Growing Optimally at 100-Degrees C. Archives of Microbiology **145**:56-61.

6. **Gardner, A. M., R. A. Helmick, and P. R. Gardner. 2002.** Flavorubredoxin, an inducible catalyst for nitric oxide reduction and detoxification in Escherichia coli. J Biol Chem **277:**8172-7.

7. **Grunden, A. M., F. E. Jenney, Jr., K. Ma, M. Ji, M. V. Weinberg, and M. W. Adams.** 2005. In vitro reconstitution of an NADPH-dependent superoxide reduction pathway from Pyrococcus furiosus. Appl Environ Microbio**l 71**:1522-30.

8. **Huber, R., P. Stoffers, J. L. Cheminee, H. H. Richnow, and K. O. Stetter.** 1990. Hyperthermophilic Archaebacteria within the Crater and Open-Sea Plume of Erupting Macdonald Seamount. Nature **345**:179-182.

9. Jannasch, H. W., C. O. Wirsen, S. J. Molyneaux, and T. A. Langworthy. 1992. Comparative Physiological Studies on Hyperthermophilic Archaea Isolated from Deep-Sea Hot Vents with Emphasis on Pyrococcus Strain GB-D. Appl Environ Microbiol **58:**3472-3481.

10. **Jenney, F. E., Jr., M. F. Verhagen, X. Cui, and M. W. Adams. 1999.** Anaerobic microbes: oxygen detoxification without superoxide dismutase. Science **286:**306-9**.**

11. **Ji, M. L. 2003,** posting date. Functional evaluation of the mechanisms of reactive oxygen detoxification in the hyperthermophilic archaeon Pyrococcus furiosus using complementation studies. Master's thesis

12. **Ma, K., and M. W. Adams.** 1999. A hyperactive NAD(P)H:Rubredoxin oxidoreductase from the hyperthermophilic archaeon Pyrococcus furiosus. J Bacteriol **181:**5530-3.

13. **McCord, J. M., and I. Fridovich.** 1969. Superoxide dismutase. An enzymic function for erythrocuprein (hemocuprein). J Biol Chem **244:**6049-55.

14. **Pick, E., and Y. Keisari.** 1980. A simple colorimetric method for the measurement of hydrogen peroxide produced by cells in culture. J Immunol Methods **38**:161-70.

15. **Stetter, K. O.** 1996. Hyperthermophiles in the history of life. Ciba Found Symp 202:1-10; discussion 11-8.

16. **Sambrook, J., and D. W. Russell** (2001). Molecular cloning: a laboratory manual. Cold Spring Harbor Laboratory Press, Cold Spring Harbor, N. Y**.**

CHAPTER 3

Transcriptional regulation of genes in the *P. furiosus* superoxide detoxification pathway

Abstract

The transcriptional expression levels of genes that are involved in the SOR-centered superoxide reduction pathway in *P. furiosus* were investigated in order to determine how these genes are expressed and regulated in response to various oxidative stresses. In this study, quantitative real time PCR trials indicated that superoxide reductase (SOR), rubredoxin (Rd), and rubrerythrin reductase (Rr), which are known to be the enzymes that provide a protective mechanism against oxidative stress in their environment, were constitutively expressed when cells are exposed to various oxidative stresses. However, the expression of the *P. furiosus* superoxide reduction pathway genes increased dramatically during oxidative stress conditions when cells are also experiencing cold temperatures (4°C) , which is consistent with the observation of the long-term survival of *Pyrococcus furiosus* during exposure to cold, oxygen-saturated seawater after its ejection in vent fluids from hydrothermal chimneys in its natural habitat.

3.1 Introduction

Pyrococcus furiosus is a strict anaerobic hyperthermophilic archeaon which lives in hydrothermal vents in the deep sea (6). Some microbes in the vents, including *P. furiosus,* grow heterotrophically on sugars and peptides and reduce sulfur to hydrogen sulfide (9, 18). When microbes in the vents have contact with cold, oxygen-containing seawater, as would occur when they are released in the vent fluid into the seawater, it has been found that they showed long-term survival at low temperature during this period of dissemination into the seawater (8). Based on these findings, it was expected that there must be a protective mechanism that operates in *P. furiosus* that enables it to survive exposure to oxygen in the cold seawater.

In 1999, Jenny *et al* (10) proposed a superoxide detoxification mechanism that functions in anaerobes in which superoxide is reduced to hydrogen peroxide by superoxide reductase (SOR), which receives the electrons from rubredoxin (Rd). The electrons shuttled to Rd come from NADPH through the action of NAD(P)H dependent rubredoxin oxidoreductase (NROR) (10, 13). The further conversion of hydrogen peroxide to water molecules was thought to occur by the action of peroxidases, and several potential candidate peroxidase genes had been identified in the *P. furiosus* genome (10) (Figure 3-1).

Further investigation of the proposed model for the superoxide detoxification mechanism in *P. furiosus* had been performed to test the feasibility. An *in vitro* reconstitution study demonstrated that superoxide had been enzymatically reduced to hydrogen peroxide in the presence of NAD(P)H when the proteins SOR, Rd, and NROR were supplied in the reaction mix (7). In addition, *P. furiosus* SOR was shown to complement an *E. coli* SodA, SodB deficient strain, grown at 37°C, demonstrating its function *in vivo* (11). Recently, the reduction of hydrogen peroxide to water molecules has been shown to occur by an enzyme called rubrerythrin

reductase (Rb) (21). Thus, these studies have confirmed the proposed superoxide detoxification model and provided impetus for further investigation of the oxidative stress mechanism of hyperthermophilic anaerobic organisms.

In *P. furious,* there are advantages to utilizing the SOR centered superoxide reduction system when it is exposed to oxidative stress. Unlike superoxide dismutase and catalase, it does not generate oxygen that can further propagate the generation of reactive oxygen species, an obvious advantage to anaerobes. Another feature of the system is that the enzymes involved in the pathway are known to be functional at room temperature which is far below the optimal growth temperature of *P. furiosus* (10). These findings can explain the long-term of survival of hyperthermophilic anaerobes upon exposure to cold, oxygen-saturated seawater when they are ejected into the seawater during the eruption of the submarine volcanoes (8). It is an interesting fact that the essential genes (SOR, Rd, and NROR) of the SOR centered reduction system are active at the low temperature, and that the SOR, Rd, and Rr genes are organized in the *P. furiosus* genomes in an operon (Figure 3-2). Because the superoxide detoxification genes exist in an operon, it is reasonable to expect that they will be regulated as a transcriptional unit; however, that needs to be experimentally verified. Also, since the genes of the superoxide detoxification pathway are ideally expressed to provide protection to the cell prior to the cell's exposure to oxidative stress, there is question as to whether the SOR pathway genes are constitutively expressed at some level or are directly expressed in response to an oxidative stress event. There have been several studies focused on gene expression in *P. furious*. Even though a few studies mentioned transcriptional expression of genes from the *P. furiosus* SOR reduction system (17, 21, 22) , no clear quantitative transcriptional analysis of oxidative stress conditions has been conducted yet for *P. furiosus*. Quantitative real-time PCR is a technique used to analyze mRNA

expression levels, which allows the quantification of rare transcripts and small changes in gene expression (19). In this study, the four key genes (SOR, Rd, NROR, Rb) involved in the *P. furiosus* superoxide reduction system were chosen for expression analysis under various oxidative stress conditions using quantitative real time PCR methods, and the *P. furiosus* glyceraldhyde-3-phosphate ferredoxin oxidoreductase (GAPOR) gene was used as a control reference. GAPOR in *P. furious* is the corresponding enzyme of GAPDH (glyceraldehyde-3-phosphate dehydrogenase) in Bacteria and Eukarya, which catalyzes the conversion of GAP (glyceraldehyde-3- phosphate) to 3-phosphoglycerate (20). The RNA encoding GAPDH is a ubiquitously expressed, moderately abundant message. It is frequently used as an endogenous control for quantitative RT-PCR analysis because its expression is constant at different times and after experimental manipulation (4, 5, 23). Air exposure under both growth temperature (90°C) and cold temperature (4°C) conditions, and chloramphenicol exposure were used as the experimental oxidative stress conditions to evaluate the SOR pathway gene expression. Previous studies have shown that part of the antibacterial action of chloramphenicol is that it produces superoxide radicals in microbes that are exposed to it (2). Therefore, the aim of this investigation was to study the transcriptional expression levels of genes that are involved in the SOR-centered superoxide reduction pathway in *P. furiosus* in order to determine how these genes are expressed and regulated in response to various oxidative stresses.

3.2 Materials and Methods

3.2. 1 Growth conditions, treatment of cells and RNA extraction for QRT-PCR

P. furious was grown with maltose as the primary carbon source in 100 ml serum bottles at 90^{o}C under anaerobic conditions in the absence of sulfur. The medium was prepared the same way as the previously reported (1). Cultures grown to approximately 1 x 10^{7} cells/ml were

subsequently treated with five different conditions as described in Table 1. After the treatments, all the cultures were placed back in the 90°C oven for an hour. Two culture bottles were prepared for each condition (total of 100 ml culture), and after the treatments, the cells were harvested in an anaerobic chamber (Plas-Labs, Michigan). The cells were harvested and cooled rapidly using a glass cooling coil packed with ice and an Econo Pump (BioRad, California). The cells were then pelleted by centrifugation under anaerobic conditions and were either stored at -80°C or used immediately for RNA isolation. RNAeasy mini kits (Qiagen, California) were used to extract the total RNA and an extra step of DNAse treatment was added to the protocol (Qiagen, California). RNA integrity was electrophoretically verified by ethidium bromide staining the RNA gels and by spectrophotometric determinations (OD_{260}/OD_{280} nm absorption ratio > 1.95). The isolated RNA was stored at -80^{o}C until used.

In order to investigate the impact of the various oxidative stress conditions on growth rates of the *P. furiosus* cultures, identical culture conditions were used to generate growth curves for each growth condition. For the cultures evaluated for their growth parameters following the oxidative stresses, the treated cultures were incubated for 1 hour following the treatment described in Table 3-1. These treated cultures were subsequently used as inoculums (1 %) for the growth study cultures. Cell growth was evaluated using a Petroff-Hauser counter for microscopic cell counts, and the generation time was calculated for each culture.

3.2.2 Primer design and optimization of RT-PCR

Four target genes, SOR, Rd, Rr, and NROR and GAPOR, a reference gene, were studied for transcriptional expression of the *P. furious* superoxide reduction system. Gene specific primers were designed as described in Table 3-2 and generated by MWG Biotech (High Point, NC). Gradient PCR samples were prepared using the RT primers and Taq DNA polymerase in

order to determine the optimum experimental annealing temperature to use for the RT experiments (iCycler, BioRad Laboratories, Hercules, CA). These reactions indicated that an annealing temperature of 58°C was ideal for the primer sets used. For the quantitative reverse transcriptase reactions, a total of 2ng of each RNA sample was used in each 25 µl qRT-PCR reaction. In addition each reaction contained 12.5 µl of iScript One-step RT-PCR mix with SYBR Green (Bio-Rad) and 0.5 µl of reverse transcriptase and 0.5 µl of 2 µM gene specific primers. The reactions were performed at least twice in duplicate for each condition for each primer set to obtain the data. The RT reactions were completed using an iCycler real time detection system (Bio-Rad Laboratories, Hercules, CA) programmed with the following protocol: incubation at 50^{o}C for 30 min for the reverse transcription step, heating at 95^{o}C for 4 min to activate Taq polymerase and inactivate the reverse transcriptase, amplification step consisting of 35 cycles (95^{o}C for 30 sec of denaturing, 58^{o}C for 30 sec of annealing, 72^{o}C for 30 sec of extension), melting step of 60-90^{o}C with heating rate of 1^{o}C per 10 sec and finally a cooling step of 4^{o}C.

3.2.3 Standard curves and quantification of real time PCR

In order to generate the DNA standard curves, each gene was amplified with its own gene specific primers using *P. furiosus* genomic DNA as template. The resulting PCR products were cleaned and quantified for serial dilution. The DNA standard curve was generated using known amounts of purified Rr PCR product as the template. Standard curve reactions were placed in each experimental PCR plate to ensure that reproducible standard curves were generated for each RT experiment. Five different standard curves for each gene (linear vs. log plot of Ct values/crossing points of gene specific DNA dilutions against the amount of the gene specific DNA) were run in a different plate using the purified PCR product of each gene as template. The

reaction conditions were the same as described above except that they contained 5 pmole of the primers and did not have the reverse transcriptase added. The abundance of unknown amounts of the sample RNA was calculated from their respective gene-specific standard curve using the derived Ct values.

3.3 Results and Discussion

3.3.1 Generation of gene-specific standard curves

Since space on the RT plates is limited to 96 reactions, two PCR plates were run for each experiment, one which contained the Rr DNA standards and the experimental reactions, and the second which contained the reactions to generate the standard curves for SOR, Rd, Rr, NROR, and GAPOR genes. Using this setup, a validated reliable standard curve of Rr DNA was run together with the plate containing all the experimental RNA samples (internal assay) that could be compared to the standard curve of Rr run alongside the other gene standard controls. Both of the Rr DNA standards showed similar linear functions (less than 0.1 difference in their slopes) and generated reproducible results, validating the other genes' standard curves. The resulting standard curves and their equations are shown in Figure 3-3, and they generated highly reproducible curves for each target gene due to the stability of DNA (16). It was found that reactions for each gene generated a standard curve with a different slope. These differences in slope are presumably due to different priming sites or different rates of priming efficiency (4).

3.3.2 Relative quantification of expression of the superoxide detoxification pathway genes

Since the standard curves for the five target genes are different from each other, copy numbers of mRNA for each gene were calculated according to Ct values and averaged. The copy numbers of mRNA for the *P. furiosus* GAPOR gene under the various stress conditions remained constant for each test condition, and therefore, it served as an ideal reference gene transcript. The

averaged copy numbers of expressed mRNA for the target genes were normalized against that of the reference gene (GAPOR). These normalized values of the target genes for the oxidative stress treatment conditions were shown relative to the expression levels for the genes from the un-treated (anaerobically grown) control culture.

3.3.3 Expression levels of the superoxide detoxification pathway genes as determined by quantitative reverse transcriptase PCR

Even though there were a few studies mentioning the transcriptional expression of the *P. furiosus* superoxide reduction system in relation to oxidative stress, no study was performed to investigate the expression of the superoxide reduction pathway genes under low temperature conditions, where the organisms face the oxidative stress in their natural habitat. This study included the cold temperature condition, which can be a critical factor for expressing the superoxide reduction system. From the results of this study, the relative fold change of mRNA quantity for the genes involved in the SOR reduction system was obtained in response to the various stress conditions (Figure 3-4). In the *P. furiosus* genome, Rr, Rd, and SOR are organized as a single transcriptional unit (Figure 3-2). These genes, which are known to express proteins that provide a protective mechanism against oxidative stress in their environment (7, 10, 13), are constitutively expressed when cells are exposed to various oxidative stresses when cells are at their growth temperature, suggesting that a basal level of superoxide reduction activity is present normally in the *P. furiosus* cells (21). However, one interesting feature of the results presented here is that superoxide reduction pathway genes are highly induced (approximately 3~4 times) only when the cells were exposed to air followed by being cooled down to 4^{o}C. This indicates that expression of the *P. furiosus* superoxide reduction pathway genes increases dramatically during oxidative stress conditions under cold conditions, which fits well with the idea that *P.*

furiosus would normally only experience oxidative stress when it is in cold seawater. These expression findings are also consistent with the observation of the long-term survival of *Pyrococcus* during exposure to cold, oxygen-saturated seawater (10) after its ejection in vent fluids from hydrothermal chimneys (8). There was another observation that superoxide reductase (SOR), rubredoxin (Rd) and rubrerythrin (Rr) were among the most highly expressed genes when *P. furiosus* was exposed to gamma irradiation followed by being cooled down to 4^{o}C (22), providing further evidence that these genes function to limit oxidative stress damage at low temperature.

Another interesting finding from the results presented in Figure 4 is the expression levels of the NROR gene, which is present in a different location of the genome in *P. furiosus* and is not part of the SOR operon (Figure 3-2). It is likely that NROR is induced differently from the other three genes. Its expression pattern did not follow the high level of gene induction that was observed for SOR, Rd, and Rr in response to the oxygen exposure at 4°C (only a 2-fold increase), while it showed high expression (8-fold) in the case of exposure to highly concentrated chloramphenicol treatment (500 μg/ml). There is a relationship between antibiotic susceptibility and production of oxidative stress with an increase of superoxide anion production in microorganisms (3). *Staphylococcus aureus* and *Escherichia coli* sensitive to chloramphenicol incubated with this antibiotic suffered oxidative stress (2). NROR might be involved not only in the SOR-mediated superoxide reduction system, but also in other redox reactions to protect the cells from oxidative damage or to maintain redox homeostasis, and therefore, it is desirable that its expression be regulated separately from the SOR operon . In summary, SOR, Rd, and Rr genes that are localized to a single operon, were highly expressed when the *P. furiosus* cells were exposed to air at 4°C, a finding that fits well with the idea that *P. furiosus* lives in an

environment transiently exposed to cold, oxygen-containing seawater, and must be able to survive this exposure using the SOR pathway since they lack SOD and/or catalase enzymes in their genomes.

3.3.4 Effects of oxidative stress on the growth of *P. furiosus*

In order to investigate the influence of various oxidative stresses on the growth of *P. furiosus*, stress-treated cultures were used as inoculum for fresh cultures. These cultures inoculated with the treated cells were monitored for their growth rates (Figure 3-5). The culture that was inoculated with the chilled, air exposed cells (oxygen & cold stress), which mimics the natural environment during dissemination of cells from the vents, showed the fastest growth of all of the treated cultures (Table 3-3). When *P. furiosus* cells are injected into cold, oxygen-containing seawater from a hot vent, they experience a rapid drop in temperature and oxygen exposure as they disperse throughout the seawater. If the cells are reintroduced into the vent system, they presumably will recover their growth and begin multiplying again. This growth data is supported by the SOR operon expression data from Figure 4 that the transcriptional expression of the *P. furiosus* SOR reduction system is effectively induced when the cultures were exposed to oxygen at 4°C. The lowest growth rate was observed for the cultures in which the starting inoculum was from the high concentration chloramphenicol treatment (500 μg/ml).

Chloramphenicol is known as an inhibitor of ribosomal activity and protein synthesis by preventing the binding of amino acyl-tRNA to the A site on the 50S subunit (15). It is stable and functional at high temperature; however, *P. furiosus* has not been reported to being sensitive to the protein synthesis inhibiting properties of chloramphenicol (12, 14). It is presumed that high amounts of chloramphenicol used in the *P. furiosus* cultures did compromise metabolism in the cells and that the cells could not be fully protected by the superoxide reduction system.

Table 3-1. Growth conditions used for oxidative stress treatments of *P. furiosus*

Stress condition	Description of treatment
Oxygen stress	Culture bottles were opened in the air for 2 min. with 2 times of stirring while the culture was hot (90°C).
Cold stress	Incubated for 1 hour at 4°C anaerobically
Oxygen & cold stress	Incubated for 30 min at 4°C, and cultures were opened in air for 2 min. with 2 times of stirring while cold Degassed and sparged with argon gas
CAM 150 stress	Injected chloramphenicol (150 μg/ml) while culture was hot
CAM 500 stress	Injected chloramphenicol (500 μg/ml) while culture was hot

Table 3-2. Primers used for qRT quantification experiments evaluating expression of the superoxide detoxification genes

Target genes	Primers	PCR product size
SOR	Forward: 5'-GAGCACCCATCAGATACATAGAA-3'	125 bp
	Reverse: 5'-ACATCACTCGTGTTTGGGC-3'	
Rd	Forward:5'ATGCGGATACATATATGATGAAGATGC-3'	95 bp
	Reverse: 5'-GGCAAACCCAATCATCTGGTAGC-3'	
Rub	Forward:5'ACCCACTATGCTTTAGAGGCGG-3'	130 bp
	Reverse: 5'-CAGCGGTGTATCCACAGATTGG-3'	
NROR	Forward:5'-GGATTTATTCACAGGAACAGGC-3'	97 bp
	Reverse: 5'-CAATGAGCGTGGCTTCTTCTGC-3'	
GAPOR	Forward:5'-AAAGAACTGGACTACCTGTGGCG-3'	104 bp
	Reverse: 5'-TGAGAGGACCGTTTGCTTCG-3'	

Table 3-3. Generation times of *P. furiosus* cultures in response to various stress conditions

Growth condition	Generation time
Anaerobically grown	39.5 min.
Oxidative stress	43 min.
Cold stress	44 min.
Cold & oxidative stress	41 min.
chloramphenicol (150 μg/ml)	54 min.
Chloramphenicol (500 μg/ml)	67 min.

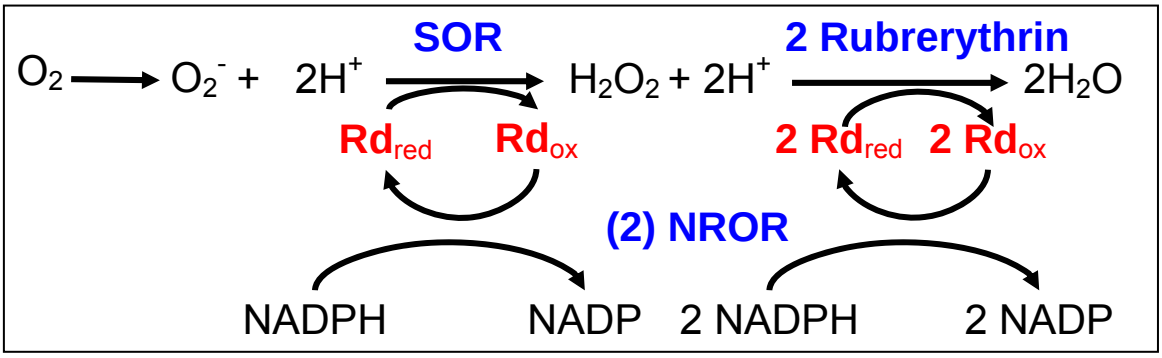

Figure 3-1. Model of the pathway for detoxification of reactive oxygen species in *P. furiosus* (modified from Grunden, 2005).

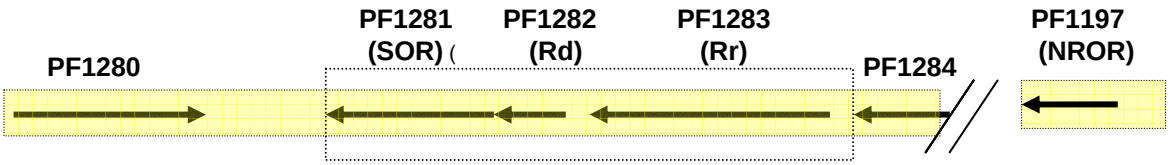

Figure 3-2. Organization of genes involved in *P. furiosus* SOR reduction system

PF1280: hypothetical protein, PF1281: SOR, PF1282:Rd, PF1283: Rr, PF1284: hypothetical protein, PF1197: NROR

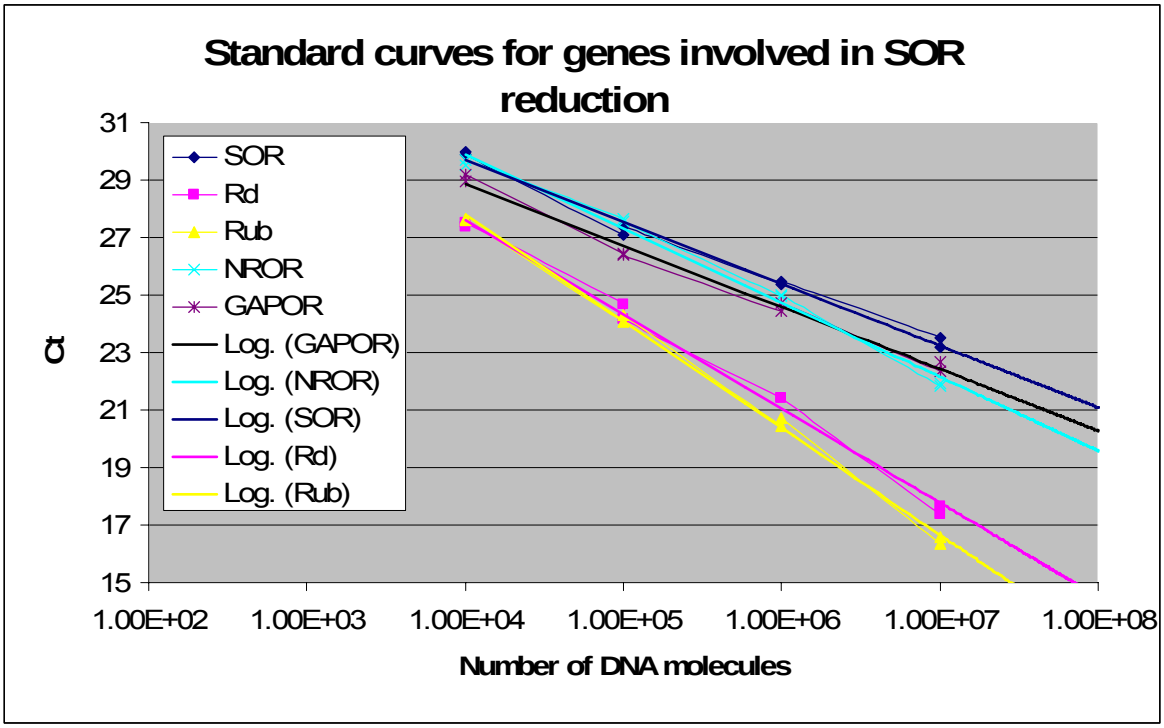

Genes	Trendline	R square
SOR	y = -0.9521Ln(x) + 38.54	$R^2 = 0.9924$
Rd	y = -1.4243Ln(x) + 40.734	$R^2 = 0.9938$
Rub	y = -1.6088Ln(x) + 42.594	$R^2 = 0.9975$
NROR	y = -1.1185Ln(x) + 40.184	$R^2 = 0.9904$
GAPOR	y = -0.9342Ln(x) + 37.483	$R^2 = 0.9914$

Figure 3-3. Standard curves for the genes involved in the superoxide reduction pathway and their equations. Purified PCR products specific for the genes were used for the serial dilutions.

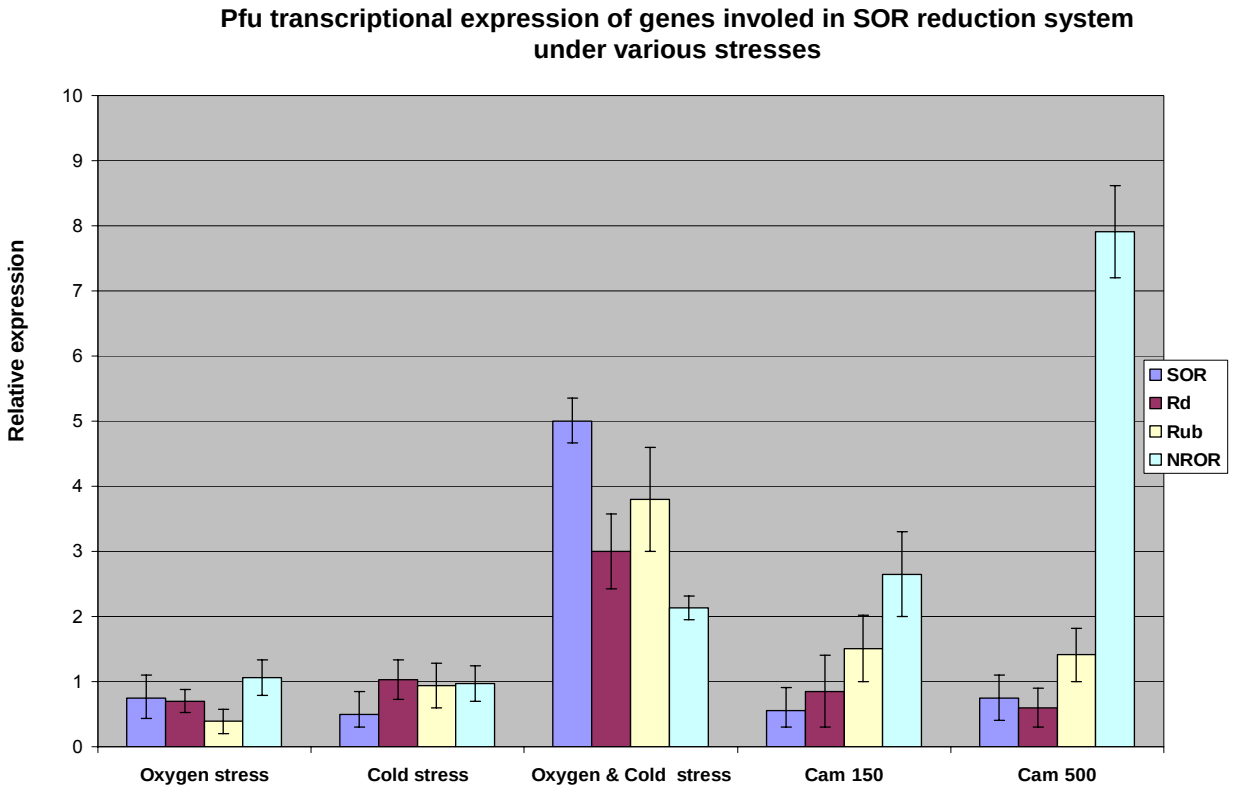

Figure 3-4. Relative expression of genes involved in the *P. furiosus* superoxide reduction pathway under various oxidative-stress conditions. Growth and stress conditions are described in table (3-1). X axis represents the various stress condition, and Y axis stands for the relative fold change of quantity in mRNA.

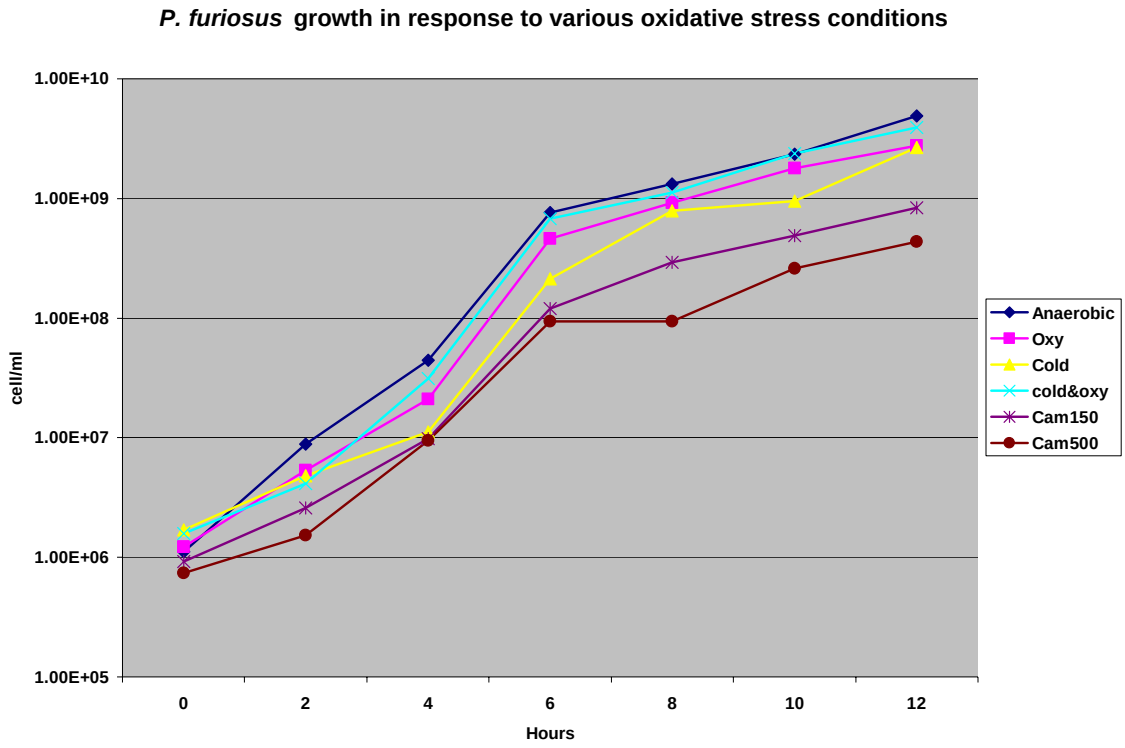

Figure 3-5. Growth of *P. furiosus* cultures exposed to various oxidative stresses. All the cultures were grown anaerobically at 90°C. Various stress-treated inocula were used to observe the influence on the growth the cultures. Anaerobic: inoculum used cells grown anaerobically without stress, Oxy: treated with air exposure while cells were hot, cold: inoculum used cells treated with cold temperature anaerobically, Cold & Oxy: inoculum used cells treated with cold temperature followed by air exposure, Cam150: inoculum used cells treated with chloramphenicol (150 µg/ml) while hot, Cam500: inoculum used cells treated with chloramphenicol (500 µg/ml) while hot. Generation time for each condition is indicated in Table 3-3.

Literature cited

1. **Adams, M. W., J. F. Holden, A. L. Menon, G. J. Schut, A. M. Grunden, C. Hou, A. M. Hutchins, F. E. Jenney, Jr., C. Kim, K. Ma, G. Pan, R. Roy, R. Sapra, S. V. Story, and M. F. Verhagen.** 2001. Key role for sulfur in peptide metabolism and in regulation of three hydrogenases in the hyperthermophilic archaeon Pyrococcus furiosus. J Bacteriol **183:**716-24.

2. **Albesa, I., M. C. Becerra, P. C. Battan, and P. L. Paez.** 2004. Oxidative stress involved in the antibacterial action of different antibiotics. Biochem Biophys Res Commun **317:**605-9.

3. **Becerra, M. C., and I. Albesa.** 2002. Oxidative stress induced by ciprofloxacin in Staphylococcus aureus. Biochem Biophys Res Commun **297:**1003-7.

4. **Bustin, S. A.** 2000. Absolute quantification of mRNA using real-time reverse transcription polymerase chain reaction assays. J Mol Endocrinol **25:**169-93.

5. **Edwards, D. R., and D. T. Denhardt.** 1985. A study of mitochondrial and nuclear transcription with cloned cDNA probes. Changes in the relative abundance of mitochondrial transcripts after stimulation of quiescent mouse fibroblasts. Exp Cell Res **157:**127-43.

6. **Fiala, G., and K. O. Stetter.** 1986. Pyrococcus-Furiosus Sp-Nov Represents a Novel Genus of Marine Heterotrophic Archaebacteria Growing Optimally at 100-Degrees C. Archives of Microbiology **145:**56-61.

7. **Grunden, A. M., F. E. Jenney, Jr., K. Ma, M. Ji, M. V. Weinberg, and M. W. Adams.** 2005. In vitro reconstitution of an NADPH-dependent superoxide reduction pathway from Pyrococcus furiosus. Appl Environ Microbiol **71:**1522-30.

8. **Huber, R., P. Stoffers, J. L. Cheminee, H. H. Richnow, and K. O. Stetter.** 1990. Hyperthermophilic Archaebacteria within the Crater and Open-Sea Plume of Erupting Macdonald Seamount. Nature **345:**179-182.

9. **Jannasch, H. W., C. O. Wirsen, S. J. Molyneaux, and T. A. Langworthy.** 1992. Comparative Physiological Studies on Hyperthermophilic Archaea Isolated from Deep-Sea Hot Vents with Emphasis on Pyrococcus Strain GB-D. Appl Environ Microbiol **58:**3472-3481.

10. **Jenney, F. E., Jr., M. F. Verhagen, X. Cui, and M. W. Adams.** 1999. Anaerobic microbes: oxygen detoxification without superoxide dismutase. Science **286:**306-9.

11. **Ji, M. L.** 2003, posting date. Functional evaluation of the mechanisms of reactive oxygen detoxification in the hyperthermophilic archaeon Pyrococcus furiosus using complementation studies. [Online.]

12. **Londei, P., S. Altamura, R. Huber, K. O. Stetter, and P. Cammarano.** 1988. Ribosomes of the extremely thermophilic eubacterium Thermotoga maritima are uniquely insensitive to the miscoding-inducing action of aminoglycoside antibiotics. J Bacteriol **170:**4353-60.

13. **Ma, K., and M. W. Adams.** 1999. A hyperactive NAD(P)H:Rubredoxin oxidoreductase from the hyperthermophilic archaeon Pyrococcus furiosus. J Bacteriol **181:**5530-3.

14. **Noll, K. M., and M. Vargas.** 1997. Recent advances in genetic analyses of hyperthermophilic archaea and bacteria. Arch Microbiol **168:**73-80.

15. **Pestka, S.** 1971. Inhibitors of ribosome functions. Annu Rev Microbiol **25:**487-562.

16. **Pfaffl, M. W., and M. Hageleit.** 2001. Validities of mRNA quantification using recombinant RNA and recombinant DNA external calibration curves in real-time RT-PCR. Biotechnology Letters **23:**275-282.

17. **Schut, G. J., S. D. Brehm, S. Datta, and M. W. Adams.** 2003. Whole-genome DNA microarray analysis of a hyperthermophile and an archaeon: Pyrococcus furiosus grown on carbohydrates or peptides. J Bacteriol **185:**3935-47.

18. **Stetter, K. O.** 1996. Hyperthermophiles in the history of life. Ciba Found Symp **202:**1-10; discussion 11-8.

19. **Valasek, M. A., and J. J. Repa.** 2005. The power of real-time PCR. Adv Physiol Educ **29:**151-9.

20. **van der Oost, J., G. Schut, S. W. Kengen, W. R. Hagen, M. Thomm, and W. M. de Vos.** 1998. The ferredoxin-dependent conversion of glyceraldehyde-3-phosphate in the hyperthermophilic archaeon Pyrococcus furiosus represents a novel site of glycolytic regulation. J Biol Chem **273:**28149-54.

21. **Weinberg, M. V., F. E. Jenney, Jr., X. Cui, and M. W. Adams.** 2004. Rubrerythrin from the hyperthermophilic archaeon Pyrococcus furiosus is a rubredoxin-dependent, iron-containing peroxidase. J Bacteriol **186:**7888-95.

22. **Williams, E., T. M. Lowe, J. Savas, and J. Diruggiero.** 2007. Microarray analysis of the hyperthermophilic archaeon Pyrococcus furiosus exposed to gamma irradiation. Extremophiles **11:**19-29.

23. **Winer, J., C. K. Jung, I. Shackel, and P. M. Williams.** 1999. Development and validation of real-time quantitative reverse transcriptase-polymerase chain reaction for monitoring gene expression in cardiac myocytes in vitro. Anal Biochem **270:**41-9.

CHAPTER 4

Production of a thermostable archaeal superoxide reductase in plant cells

Abstract

Pyrococcus furiosus superoxide reductase (SOR) is a thermostable archaeal enzyme that reduces superoxide without producing oxygen. The recombinant SOR enzyme retains its function and heat stability when assayed *in vitro.* Importantly, expressing SOR in plant cells (NT-1 tobacco cell culture and in Arabidopsis plants) enhances their survival at high temperature and from drought (when expressed in Arabidopsis plants) indicating that it functions *in vivo*. The archaeal SOR provides a novel mechanism to reduce superoxide and demonstrates the potential for using archaeal genes to alter eukaryotic metabolism

4.1. Introduction

There are many sources of reactive oxygen species (ROS) in plants. It can be produced endogenously resulting from such processes as photosynthesis and cellular respiration (26). The other sources for oxidative stress can come from environmental stress, such as drought, chilling, heavy metal exposure, ultraviolet light, air pollution, and pathogen attack (26). The enhanced production of ROS during stress can pose a threat to cells resulting in damage to lipid membranes, proteins, DNA, and RNA. The major ROI-scavenging mechanisms of plants include superoxide dismutase (SOD), ascorbic peroxidase (APX), and catalase (CAT) (21). SOD removes superoxide and decreases the risk of hydroxyl radical formation from superoxide via the metal-catalyzed Haber–Weiss-type reaction (14). Three isozymes of SOD, Mn-SOD, Cu/Zn-SOD, and Fe-SOD have been identified in various plants. Mn-SOD is predominantly found in mitochondria and peroxisomes. Cu/Zn-SOD is located mainly in the cytosolic fraction as well as chloroplastic and mitochondria fractions. Fe-SOD is predominantly detected in chloroplasts (3). H_2O_2 is eliminated from plant cells by the action of catalases and peroxidases. Ascorbate peroxidase (APX) is one of the most important antioxidant enzymes of plants that detoxify hydrogen peroxide using ascorbate for reduction (12). The ascorbate peroxidase (APX) family of isoenzymes is crucial in maintaining H_2O_2 content at nontoxic concentrations in many of the compartments of the cell. Catalase is largely restricted to the peroxisomes, but it is necessary during stress when high levels of ROS are produced (21).

Ascorbic acid and glutathione have been shown to act as antioxidants in the detoxification of ROS. These are found at high concentrations (5-20 mM ascorbic acid and 1-5 mM glutathione) in chloroplasts and other cellular compartments (24). Their roles as antioxidants are non-enzymatic; they directly quench ROS. A major function of glutathione is

the re-reduction of ascorbate in the ascorbate-glutathione cycle (11, 12). Efficient recycling of glutathione and ascorbic acid is ensured by glutathione reductase (GR) and monodehydroascorbate reductase (MDAR) and dehydroascorbate reductase (DHAR) using NADPH as reducing power (4, 22).

There is increasing evidence for considerable interlinking between the responses to heat stress and oxidative stress in plants (28). Drought and low temperature can cause significant ROS production (8). Over-expression of radical scavenging enzymes, such as SOD and GR, have resulted in an increased resistance to drought, ozone, low temperature, and heat stress (8, 23, 27). These experiments indicate that modification of ROI scavenging systems can lead to significant changes in oxidative stress tolerance and provide some indication that these approaches can be used to improve plant performance (1).

The archaeal hyperthermophile *P. furiosus* detoxifies ROS through the SOR pathway (18) shown in Figure 4-1. SOR reduces superoxide to peroxide, which is then reduced to water by the enzyme rubrerythrin reductase (Rr) (29). Earlier chapters of this thesis (Chapter 2) have provided experimental proof that *P. furiosus* SOR receives electrons from rubredoxin (Rd) which is reduced via NAD(P)H:rubredoxin oxidoreductase (NROR) by NADPH (15). *In vivo* growth studies demonstrated that the recombinant form of *P. furiosus* SOR gene can complement an *E. coli* strain deficient in *sodA, sodB* (19). *E. coli* does not produce either Rd or NROR, and therefore, the *in vivo* complementation study also indicated that there were functional electron donors other than Rd in *E . coli* that could provide electrons to the recombinant form of *P. furiosus* SOR.

There are several advantages of *P. furiosus* SOR compared to mesophilic SODs: 1) unlike SOD, it reduces superoxide without producing an oxygen molecule as a by-product which

can potentially generate further ROS; 2) it has a wide functional temperature range that supports activity (from 4^{o}C to 100^{o}C); and 3) it is known to be functional when it is over-expressed in foreign cells, such as in *E. coli* (19). Given the apparent advantages that SOR has over SOD, there was interest in determining whether these advantages could provide improved ROS detoxification in plants if *P. furiosus* SOR were functionally expressed in plant tissues.

In this study, for the first time an archaeal gene, *P. furiosus* SOR, was introduced into plant cells, in this case, into tobacco cell NT-1 cultures. The SOR transgenic NT-1 cells were evaluated for the functional expression of the archaeal SOR gene and were studied to determine whether the *P. furiosus* SOR enhanced survival of the transgenic plant cells after short term, high temperature exposure by alleviating the toxicity of reactive oxygen. Furthermore, the *P. furiosus* SOR gene was cloned into a plant expression plasmid, which was then transformed into Arabidopsis. The expression of *P. furiosus* SOR in the plants was verified by RT-PCR and Western blot analysis. SOR enzyme assays were performed to demonstrate the functional activity of the recombinant protein, and higher SOR activity was detected in the SOR transgenic plant extracts compared to wild type.

The work from this study was performed in collaboration with Dr. Wendy Boss's laboratory in the Department of Plant Biology at North Carolina State University. Most of the experiments involving the transgenic plants, such as cloning, growing, heat and drought stress experiments, RT PCR, and some of the Western blots were done by Dr. Yangju Im from Dr. Boss's lab. I provided the recombinant form of the *P. furiosus* SOR gene, conducted the SOR enzyme assays, and expressed and purified the *P. furiosus* SOR and Rd proteins for antibody production.

4.2. Materials and Methods

4.2.1 Vector construction

The gene encoding *P. furiosus* SOR was PCR amplified using pfu DNA polymerase and the indicated primers (forward primer; 50-CAC CAT GAT TAG TGA AAC CAT AAG-30 and reverse primer; 50-TCA CTC TAA AGT GAC TTC GTT TTC-30) to amplify the coding region of SOR. The resulting PCR product was subcloned into the pENTR/SD/D-TOPO destination vectors (Invitrogen, Carlsbad, CA) and then into pK7WGF2 (Functional Genomics Division of the Department of Plant Systems Biology, Gent, Belgium) using LR recombination reactions according to the manufacture's instructions (Invitrogen). The resulting construct enabled production of green fluorescence protein (GFP)-fusion-SOR proteins under the control of a cauliflower mosaic virus (CaMV) 35S promoter in plants.

4.2.2 Transformation into *Nicotiana tabacum*1

Recombinant plasmids were transformed into *Agrobacterium tumefaciens* EHA105 using the freeze-thaw method (10). *Nicotiana tabacum*1 (NT1) cells were transformed via *A. tumefaciens* mediated gene transfer using the following protocol: A single-transformant *A. tumefaciens* colony containing each plasmid was cultured in 5 ml of yeast extract broth media (0.5% [w/v] beef extract, 0.5% [w/v] peptone, 0.5% [w/v] sucrose, 0.1% [w/v] yeast extract, and 2.5 mm MgCl2) supplemented with 20 mg/L rifampicin and 300 mg/L spectinomycin, at 28^{o}C, with shaking at 250 rpm for 2 d. Wild-type NT1 cells were cultured for 4 d in 25 ml of NT1 culture medium, at 27^{o}C, with shaking at 120 rpm. Four milliliters of this culture were gently mixed with 200 µl of 2-d-old *A. tumefaciens* cultures transformed with either pK7WGF2- 35S-GFP–SOR or vector control pK7WGF2-35S-GFP. The NT1 cell and *A. tumefaciens* mix was incubated for 48 h at 27^{o}C and suspended in an equal volume of NT1 culture medium.

Approximately 0.5 ml of the resulting cell suspension was plated onto solid NT1 culture medium containing 0.8% (w/v) phytagar (Gibco BRL), 50 mg/L kanamycin, and 200 mg/L timetin, and excess liquid was allowed to dry before incubation. Plates were incubated for 4 weeks at 27^{o}C. For each transformation, 4 independent microcalli were selected, suspended in 1 ml of NT1 medium containing 50 mg/L kanamycin and 200 mg/L timetin, and incubated for 7 d at 27^{o}C, at 120 rpm, in darkness. Suspension cultures were retained and transferred to 25 ml of NT1 medium containing 50 mg/L kanamycin, and incubated 7 d as described above. To maintain the lines, cells were subcultured weekly, as described above, in 25 ml of NT1 medium containing 50 mg/L kanamycin.

4.2.3. Determination of gene expression in *Nicotiana tabacum*1

To verify transformation and determine if the transgene was expressed, independently transformed NT1 cell lines were harvested after 4 d of growth. RNA was isolated using the RNAeasy kit (Qiagen), with an additional DNase treatment to remove contaminating genomic DNA. Reverse transcription (RT) was carried out to generate cDNA using 1 µg of total RNA, 0.5 µg oligo dT15 (Promega), 0.5 mM of each dNTP, 10U RNase inhibitor and 4U of Omniscript reverse transcriptase enzyme (Qiagen) and RNase free water in a volume of 20 µl. Reactions were incubated at 37^{o}C for 1 h. GFP-fused-SOR transcripts were detected by PCR using 2.5 µl of each RT reaction and internal GFP (forward primer; 50-TGA CCC TGA AGT TCA TCT GCA CCA-30 and reverse primer 50-TGT GGC GGA TCT TGA AGT TCA CCT-30) or gene specific primers (SOR and actin specific primer) as indicated above. PCRs contained 2.5 µl 10X PCR buffer, 2.5 mM MgCl2, 0.2 mM of each dNTP, 0.4 µM of each primer and 1.25U HotStar Taq DNA Polymerase (Qiagen) in a volume of 25 µl. PCR conditions were 95°C for 15 min followed by 25 cycles of 94^{o}C for 30 s, 55^{o}C for 30 s and 72^{o}C for 30 s for 25 cycles for GFP

and Actin, or followed by 25 cycles of 94°C for 30 s, 49°C for 30 s and 72°C for 30 s for SOR or followed by 25 cycles of 94°C for 30 s, 50°C for 30 s and 72°C for 45 s for GFP-fused-SOR. PCR products were analyzed by gel electrophoresis in 2% agarose gels.

4.2.4 Immunoblotting

Total protein was extracted from cells, boiled in SDS–PAGE sample buffer for 5 min, briefly centrifuged at 13000 X g, and separated by SDS–PAGE on 10% (w/v) polyacrylamide gels. Each lane was loaded with 30 µg of protein as quantified by the Bradford protein assay (8). Proteins were transferred to PVDF membrane by electroblotting in 1X CAPS buffer containing 10% (w/v) MeOH for 1 h at 50 V. The membrane was blocked with 5% (w/v) milk in Tris-buffered saline buffer followed by three washes in Tris-buffered saline with 0.2% (v/v) Tween (TBST). The primary antibody used was anti-mouse GFP monoclonal (BD Biosciences) at a dilution of 5000 for 1 h followed by three washes in TBST. Horseradish peroxidase-conjugated anti-mouse was used as the secondary antibody at a dilution of 20,000-fold for 1 h followed by three washes in TBST. Immunoreactivity was visualized by incubating the blot in SuperSignal West Pico Chemiluminescence substrate (Pierce, Rockford, IL) and exposure to X-ray film. Total protein was visualized by staining the blots with Amido black (Sigma, St. Louis).

4.2.5 SOR assays in NT1 cell culture

The wild-type, GFP-, and SOR-expressing NT1 cell lines were grown aerobically for 6 d in a 27°C incubator with shaking (120 rpm). Cells were then harvested by passing the cultures through Whatman filter paper. The resulting cell paste was lysed using liquid nitrogen and grinding with mortar and pestle. Broken cells were resuspended in sterile phosphate buffer (50 mM potassium phosphate, pH 7.8, 0.1 mM EDTA) and centrifuged in a Beckman Avanti 30

centrifuge for 30 min at 40,000 g, 4°C to remove cellular debris. Cell extracts were dialyzed using a low molecular weight cutoff membrane

(3500 Da MWCO Pierce Slide-a-lyzer cassettes) in 2 L of phosphate buffer overnight at 4 ^{o}C to remove any contaminating manganese or iron but retain reductant in the cell extract required for SOR activity (two buffer changes were made during the dialysis). After overnight dialysis, each cell extract was divided into an untreated sample (1.8 ml) and a sample to be heat-treated (2–4 ml). The heat-treated cell extracts used to generate the data reported in Table 1 were incubated at 85^{o}C for 15 min. Heat-denatured protein was removed by centrifugation in a Beckman Avanti 30 centrifuge for 30 min at 40,000 X g at 4^{o} C. The supernatant from this step as well as the untreated cell extract were subsequently used for the SOR assays. The Bradford method was used to determine the protein content of both the untreated and heat-treated cell extracts (9). SOR activity was detected through competition with cytochrome c for superoxide using a Shimadzu UV-2401 PC spectrophotometer. The standard assay was performed in 3 ml of 0.05M of potassium phosphate buffer, pH 7.8, 0.1 mM EDTA at 25^{o}C. The reaction mixture contained 10 µM of horse heart ferricytochrome cytochrome c (Sigma), 50 µM xanthine (Sigma) and sufficient xanthine oxidase (Sigma) to produce a rate of reduction of ferricytochrome c at 550 nm of 0.025 absorbance per minute. Note that the reductant necessary for SOR activity was supplied by the NT1 cell extracts added to the assay mixtures. Under this standard condition, 1 unit of SOR activity is defined as the amount of enzyme that inhibits the rate of reduction of cytochrome c by 50% (20). To unequivocally demonstrate that active, heat-stable SOR was expressed in the transgenic NT1-SOR cell lines, a second set of SOR activity assays was done using a longer, higher temperature heat treatment step (20 min at 90^{o}C). The reductant that is required for SOR activity but was degraded during this heat-treatment step was reconstituted by

the addition of NADPH and purified recombinant *P. furiosus* Rd and NROR to the assay mixture. For the SOR activity, a standard reaction mixture (2 ml) was prepared which contained 50 mM potassium phosphate buffer, pH 7.8; 0.2 mM xanthine, 3.4 μg xanthine oxidase, and 20 μM horse heart cytochrome c. For the reconstituted samples, 0.45 mM NADPH and 170 nM each of recombinant *P. furiosus* Rd and NROR that had been pre-incubated together anaerobically at 23^{o}C for 2 min in 100 mM EPPS [N-(2-hydroxyethyl)-piperazine- N0-(3-propanesulfonic acid)] buffer, pH 8.0, was added to the heat treated NT1 extracts and incubated anaerobically for an additional min. This reconstitution mixture was then added directly to the SOR activity assay mix and the resulting activity monitored using the spectrophotometer.

4.2.6 Temperature challenge experiments of the wild type and transgenic tobacco cell culture

Four-day-old suspension cultured cells that had been incubated at 27^{o}C were collected and resuspended in a final concentration of 0.05 g ml^{-1} in NT1 medium prior to heat stress. For the heat stress, cells were incubated on a rotary shaker at 40^{o}C and 120 rpm. To quantify dead cells, heat-treated cells were incubated with a final concentration of 0.05% aqueous Evans blue for 10 min, and washed with deionized water until no blue dye eluted from the cells (5). Dye that bound dead cells was solubilized in 1 ml of 50% methanol that contained 0.5% SDS for 30 min at 50^{o}C. Dye extracted solution was quantified by monitoring the absorbance at 600 nm. Direct counting of dead cells was performed microscopically after staining with using more than 100 cells for each experiment.

4.2.7 Production of monoclonal antibodies specific for *P. furiosus* SOR and Rd

4.2.7.1 Construction of *P. furiosus* SOR and Rd expression plasmids

P. furiosus SOR and Rd genes were PCR amplified using boiled genomic DNA as the template. The primers used for PCR amplification of the *P. furiosus* SOR and Rd were the following: 5'-GAGGTGCTCGAGATGATTAGTGAA-3' (SOR forward containing a *Xho*I site), 5'-GGGAATTCAAACCGTCACTCTAAA-3' (SOR reverse containing a *Eco*RI site), 5'-ATCTGGATGGTGAGCTCATGGCAAA-3' (Rd forward containing a *Sac*I site), 5'-CATCTGCAGCACCTCAATCTTCTAAC-3' (Rd reverse containing a *Pst*I site).
The following programs was used for amplification: 30 cycles consisting of denaturation at 95°C for 1 min, annealing at 56°C for 1 min, and extension at 72°C for 1 min. using *Pfu* polymerase for amplification. The PCR products were digested with *Xho*I and *Eco*RI for the *P. furiosus* SOR construct or *Sac*I and *Pst*I for the *P. furiosus* Rd construct. These enzyme restricted PCR products were purified by gel extraction (Qiagen) and ligated into the *Xho*I-*Eco*RI sites (SOR expression plasmid) or the *Sac*I-*Pst*I sites (Rd expression plasmid) of plasmid pBADHisA (Invitrogen). The *P. furiosus* SOR and Rd genes were cloned into the pBAD/HisA vectors to generate recombinant protein fused with N-terminal His_6 tags. The resulting plasmid constructs were transformed into *E. coli* XL1-Blue chemically competent cells (Invitrogen). Plasmid DNA was isolated from the transformants using the Qiagen Miniprep system and was screened by visualization on DNA agarose gels. The expression constructs were verified by sequencing (MWG Biotech).

4.2.7.2 Overexpression and purification of recombinant *P. furiosus* SOR and Rd.

The recombinant forms of His_6- SOR and His_6-Rd were over-expressed in *E. coli* Top 10 cells following induction with 0.02% of arabinose. Cell-free extracts from 30 ml cultures were

prepared using sonication and cellular proteins were visualized on 12.5% polyacrylamide gels to determine whether SOR and Rd proteins were successfully expressed. For large-scale over-expressions for protein purification, 2L cultures of the SOR and Rd expressing cells were induced by adding 0.02 % arabinose when an $O.D_{.600}$ reached about 1. The induced cultures were incubated at room temperature for 4h prior to harvesting the cells for protein purification. Cell pellets were suspended in 20 mM sodium phosphate, pH 8 containing 1mM benzamidine. 2L of over-expressed cell suspension was passed through a French press cell (20000 lb/in^2) twice. The lysed cell suspensions were centrifuged using a Sorval ss-34 rotor at 18,000 rpm for 30 min. to remove cell debris. The collected supernatant was sparged with argon and heat treated at 80^oC for 30 min. The denatured protein was removed by centrifugation at 3,000 g for 30 min. The heat treated cell extract was applied to a 5 ml Ni-chelating affinity column (HiTrap Chelating HP by GE Healthcare) using Buffer A (20 mM sodium phosphate, 50mM NaCl, pH 7.4) as a binding buffer and Buffer B (20mM of sodium phosphate, 500mM NaCl, 500mM imidazole pH 7.4) as the elution buffer. Fractions containing SOR and Rd proteins were collected and applied to the Ni chelating affinity column again. Purified fractions were collected and concentrated using Centriplus YM3 (Amico) concentrators. The concentrated protein was then dialyzed overnight at 4°C in 50mM Tris, pH at 8.

4.2.8 Generation of Arabidopsis plants expressing *P. furiosus* SOR

4.2.8.1 Transformation of the *P. furiosus* SOR-expression plasmid into Arabidopsis.

The SOR expression plasmid used previously to transform the NT1 tobacco cells was also used to transform Arabidopsis. In this case, the SOR-expression plasmid was transformed into TOP10 chemically competent cells and selected on LB media containing spectinomycin. Before the recombination step, clones were verified by PCR using an M13 forward primer and

SOR reverse primer. Recombinant plasmids were transformed into Arabidopsis plants via *Agrobacterium tumefaciens* EHA105 by the freeze-thaw method.

4.2.8.2 Reverse-Transcriptase PCR.

Arabidopsis plants were lysed using liquid nitrogen and grinding with mortar and pestle. Qiagen kits were used to isolate RNA and make cDNA. Primers specific for GFP, GFP/ SOR, and actin mRNA along with Taq polymerase were used in the RT-PCR to demonstrate that mRNA encoding the GFP-SOR fusion protein is present in the transformed plants.

4.2.8.3 Immunoblot analysis.

Wild type and transgenic seedlings were homogenized and total protein was separated by gel electrophoresis and electroblotted onto a PVDF membrane. The membrane was blocked overnight with milk. Proteins were visualized after treating the blot with recombinant SOR (Cocalico Biologicals) monoclonal antibody (primary antibody) and anti-rabbit as the secondary antibody. Detection was through chemiluminescent methods.

4.2.8.4 SOR enzyme activity assays.

Two-week or twp-month old wild type and transgenic seedlings were harvested and ground with liquid nitrogen. The ground samples were then resuspended in phosphate buffer (50 mM potassium phosphate, pH 7.8, 0.1 mM EDTA) and heat-treated at 85˚C for 15 min and centrifuged at 15,300 rpm for another 15 min in order to reduce plant SOD background activity. The specific activity of SOR was measured by detection of the inhibition rate of cytochrome C reduction with a Shimadzu UV-2401 PC spectrophotometer.

4.2.8.5 Heat Stress Experiments.

For one of the heat stress experiments, a heat-stress of 45°C was applied to wild type and SOR-expressing transgenic Arabidopsis seeds for 5 hrs while control groups are incubated at

22°C. Following heat-stress, the experimental group was returned to the 22°C incubator and all plates were left at 22°C for 1 week. Germination rate was monitored after 2 days.

In a second heat-stress experiment, three groups of seeds were monitored for survival rate after heat stress. In the beginning, all seeds were left to germinate in a 22°C incubator for 10 days. Group 1 (control) remained in the 22°C incubator. Group 2 seedlings were exposed to a temperature acclimation consisting of incubation at 38°C for 1.5 hours and then additional 2-hour incubation at 45°C. Group 3 seedlings were brought from the 22°C incubator and were directly exposed to 45°C for 2 hours. Following heat-stress, the experimental group was returned to the 22°C incubator and all plates were left at 22°C for 1 week. The number of seedlings that survived was counted after 7 days.

4.2.8.6 Drought Stress Experiments.

Triplicates of both wild type and SOR transgenic plants were grown in a 22°C incubator with 8/16 h (day/night) cycle for 2 months in the phytotron. This 2 month-old plants were incubated at room temperature (30% humidity) and were not watered for 11 days under continuous light to test the drought resistance. The biological experiments were performed three times.

4.2.8.7 SOR activity gel

Nondenaturing PAGE gels were used according to (30), using riboflavin in both the resolving and concentrating gels. SOD activity was detected as in (6); the gels were first soaked in 2.45 mm nitroblue tetrazolium for 20 min, then in a10-fold diluted solution containing 28 mm tetramethylenediamine, 2.8 mm riboflavin and 36 mm potassium phosphate, pH 7.8 for 15 min. The gel was then rinsed with distilled water and illuminated for 10 min.

4.3 Results and Discussion

4.3.1 *Pyrococcus furiosus* SOR is expressed as a fusion with GFP in tobacco cell culture

In order to monitor SOR gene expression in a eukaryotic system, SOR-NT1 cells were grown in suspension culture and generated SOR as a fusion protein with *Aquaria victoria* GFP (16). The NT1 cells were transformed with a construct driven by the CaMV 35S promoter, which was designed so that GFP would be fused to the N-terminus of the protein as shown in Figure. 4-2. Four independent, kanamycin resistant transgenic lines transformed with SOR (SOR1, SOR2, SOR3, and SOR4) and one control line containing GFP vector (NT1-GFP) were obtained.

Figure 4-3 shows transgene expression in recombinant tobacco cell lines as detected by RT-PCR. An approximately 0.45 kb transcript indicative of transgene expression was detected only in the cell lines transformed with GFP-fused-SOR when probed with SOR-specific primers. No transcript was detected in wild-type and vector control cell lines. A ~0.3 kb transcript, indicative of GFP expression, was detected in the cell lines transformed either with the GFP-fused-SOR constructs or the vector control when probed with internal GFP-specific primers. No transcript was detected in the wild-type cell line when probed with GFP-specific primers. An actin primer was used as a control to indicate that an equal amount of each template was used for all RT-PCR samples.

In order to verify the gene product, Western blot analysis was performed. GFP-fused-SOR could be detected in lines transformed with the GFP-fused-SOR gene and the GFP gene, but not in wild-type cells. A Western blot of protein extracts prepared from 4-day tobacco cell cultures, incubated with antiserum recognizing the GFP tag (BD Bioscience) is presented in Figure. 4-4. The antiserum reacted with a polypeptide of 42 kDa, present in the GFP-fused-SOR cell lines, with a 27 kDa polypeptide in the GFP vector control cell line, but did not react with

protein in the wild-type tobacco cell line. The size of the protein (approximately 42 kDa, where the GFP protein is 27 kDa plus 15 kDa for SOR) detected in NT1 cells indicates that the GFP–SOR fusion is correctly translated in the tobacco cells.

4.3.2 SOR expressed in transgenic tobacco cells has heat-stable activity

To determine whether the recombinant protein was functional, SOR activity was compared in the four transgenic and vector control lines using the soluble fraction of whole cell extracts. SOR activity was determined using a standard SOD/SOR assay (20) and the results are presented in Table 4-1. The activity data listed in Table 1 is the average of 9 values (3 replicates from 3 separate experiments). The average deviation for each sample's activity is indicated. Note that the assay that was used to determine the SOR activity also detects endogenous SOD activity (18). Therefore, in order to ascertain the activity attributable primarily to SOR, a heat-treatment of the Tobacco cell extract (incubation at 85^{o}C for 15 min) was performed prior to the assay. This heat-treatment was designed to take advantage of the fact that the transgenic tobacco cells expressing *P. furiosus* SOR should retain its heat-stability and remain catalytically active even after incubation at 85^{o}C, whereas the plant SOD is only partially heat-stable (17). As shown in Table 1, after incubating at 85^{o}C for 15 min only 39% or 38% of the SOD activity is retained in the heat treated wild-type and GFP-expressing NT1 cells, respectively. We consistently observed lower SOD activity in the GFP expressing lines and almost total loss of activity upon heat treatment (1.4 ± 0.7 U/mg heat-stable activity). The finding that endogenous SOD levels are consistently and significantly lower in the transgenic GFP-expressing NT1 cell line compared to the wild-type cell has important potential ramifications for transgenic crop design. Because field-grown plants are constantly exposed to environmental stresses, the reduction of endogenous SOD activity in response to producing a cytosolic recombinant protein poses a possible

challenge for developing healthy and productive transgenic crops. Importantly, the GFP–SOR cells had 14–30-fold increased heat-stable SOR activity compared to the NT1-GFP transgenic cell line and a 2.8–6.1-fold increase compared to the non-transformed wild type cells. In 2 cell lines (NT1-SOR3 and NT1-SOR4), 100% of the activity was heat stable. Because there was endogenous SOD activity in the wild-type NT1 cell extracts after the 85^{o}C treatment, to completely eliminate residual endogenous SOD activity and to unequivocally establish that the SOR activity reported for the transgenic tobacco cell lines in Table 4-1 is as heat-stable as the native *P. furiosus* protein activity, a second set of SOR assays was conducted. For these experiments a longer, higher temperature heat-treatment step was used followed by the addition of recombinant proteins to deliver the reductant required for the SOR assay. In this case, the NT1-GFP and NT1-SOR3 cell line extracts were exposed to a 20 min heat treatment at 90^{o}C. As shown in Table 4-2, the extended heat-treatment not only effectively abolished the endogenous SOD activity in the NT1 cell extracts but also removed available reductant for the SOR in the extract. Addition of exogenous reductant (recombinant *P. furiosus* electron transfer proteins Rd and NROR [170 nM each] and the reductant NADPH [0.45 mM]), successfully reconstituted SOR activity in the heat-treated NT1-SOR3 extract. There was no significant activity in the NT1-GFP heat-treated extract. These data demonstrate that the SOR protein produced in the transgenic tobacco cells was extremely heat stable and even though the archaeal enzyme could catalyze the reduction of superoxide using reductants available from the tobacco cells, it functioned even more effectively with the *P. furiosus* electron transfer partners Rd and NROR.

4.3.3 Recombinant SOR protects transgenic tobacco cells from heat stress

The recombinant *P. furiosus* SOR not only had heat stable activity in vitro, but also functioned *in vivo* as evidenced by enhanced survival of the transgenic tobacco cells after

exposure to heat stress. The NT1 cells are normally grown at 27^{o}C. As shown in Figure 4-5, when the temperature was raised to 40^{o}C, within 4 h, 23% of the wild-type cells and 17% of the NT1-GFP cells were dead based on Evans Blue staining; however, only 8% of the transgenic tobacco cells expressing *P. furiosus* SOR were dead. The NT1-SOR1 and NT1-SOR4 cell lines were chosen in particular for the heat stress experiments since the activity data indicated that the NT1-SOR1 cell line produced a lower level of SOR activity and the NT1-SOR4 cell line the highest heat-stable SOR activity (Table 4-1). As seen in Figure 5B, both the NT1-SOR1 and NT1-SOR4 cell lines, provided a 3-fold or 2.1-fold increase in viability after the 4 h heat treatment compared to the NT1 wild-type or NT1-GFP cell lines, respectively.

Although ROS signaling is a complex process, and as others have noted, expressing one redox regulatory gene alone will likely not be the ultimate answer to dampening ROS and increasing plant viability (2, 13), the *P. furiosus* SOR pathway genes are relatively small and in theory additional components of the pathway, e.g., rubrerythrin reductase, could be expressed, and would dampen ROS signals by reducing superoxide and peroxide without producing oxygen. Ultimately, this work validates the concept of using genes from the domain Archaea to produce functional recombinant proteins in plants and demonstrates the potential for using archaeal genes to alter plant signaling pathways to analyze down stream ROS-mediated events and to potentially enhance plant survival in extreme environments.

4.3.4 Cloning, protein over-expression and purification of recombinant *P. furiosus* SOR and Rd for antibody production

In order to confirm the presence of correct inserts, the plasmids were digested with appropriate restriction enzymes and DNA gels were used to determine if the expected restriction sizes resulted. The expected sizes of DNA fragments (401 bp and 195 bp respectively) were

obtained for both *P. furiosus* SOR and Rd genes (Figure 4-6, Figure 4-7). The positive clones of SOR and Rd genes were sent for sequencing (MWG Biotech).

The *P. furiosus* SOR and Rd constructs were transformed into the Top10 (Invitrogen) *E. coli* strain for the protein expression. 2 liters of cell cultures were broken and the resulting cell extracts were heat-treated for 30 min. at 80^{o}C anaerobically. Purified recombinant *P. furiosus* SOR and Rd proteins were obtained by applying the his-tagged fusion proteins to Ni chelating affinity columns. Only partial purification was obtained when the protein extracts were applied to a single Ni chelating affinity column; however, >95% purity was obtained when the SOR or Rd enriched fractions were reapplied to a second Ni chelating affinity column. The expected sizes of *P. furiosus* SOR and Rd (~17 kDa and ~8 kDa) were observed when the purified proteins were electrophoresed through12.5% polyacrylamide SDS gels (Figure 4-8, Figure 4-9). The concentrated proteins (1.2mg/ml on SOR, 0.9 mg/ml on Rd) were dialyzed in 50mM Tris pH at 8 and sent to Cocalico Biologicals for antibody production.

4.3.5 *P. furiosus* SOR is expressed as a fusion with GFP in Arabidopsis.

4.3.5.1 Detection of SOR expressed in Arabidopsis through visualization of GFP fluorescence.

Arabidopsis plants containing recombinant *P. furiosus* SOR recombined in their genomes were selected using kanamycin resistance. The expression of the GFP-SOR in the transgenic Arabidopsis was visualized using fluorescence microscopy. As indicated in Figure 4-10, the GFP-fused SOR is expressed throughout the transgenic plants including the leaves and roots.

4.3.5.2 *P. furiosus* SOR is successfully produced and functional in Arabidopsis as demonstrated by RT-PCR, immunoblot assay, enzyme assay and heat stress experiments.

RT-PCR analysis shows that SOR mRNA is produced in the transgenic Arabidopsis. Figure 4-11 shows transgene expression in Arabidopsis as detected by RT-PCR. Specific primer pairs were used to identify *P. furiosus* SOR, GFP, and actin (a loading control).

A Western blot of heat-treated (at 80^{o}C for 15 min.) cell free extracts was prepared from 2 month old Arabidopsis plants, and was incubated with antiserum recognizing recombinant *P. furiosus* SOR (Cocalico Biologicals). In Figure 4-12, samples of protein extracts from *P. furiosus* SOR transgenic Arabidopsis plants contained bands detected by the SOR antibody (Lane 3 and 4) that appeared to be approximately 15 kDa, while the sample of the wild type Arabidopsis plants contains no reacting protein bands (Lane 2). In the lane 6, the detected band of purified *P. furiosus* SOR has a His_6 tag fusion, and therefore, is expected to have a slightly higher molecular weight (~17 kDa) than the untagged SOR protein (~14 kDa). As another positive control, the cell extract of *P. furiosus* SOR in expressed in NC906 (*E. coli* sodA, SodB mutant) showed the same molecular weight of the detected SOR band for the SOR expressed in the Arabidopsis (Lane 1). Since the native *P. furiosus* SOR proteins are tetramers, it is believed that the extra higher bands in the samples are dimerized or tetramerized molecules of the protein that have not been completely denatured. Detection of multimeric hyperthermophile proteins on denaturing gels is common due to the extreme stability of these proteins.

In order to determine whether the recombinant protein was functional, SOR activity was compared in the two transgenic and wild type lines using the soluble fraction of whole cell extract samples used in the Western blot analysis discussed above. SOR activity was determined using a standard SOD/SOR assay (20) and the results are presented in Table 4-3. In the non heated samples, there was no difference in enzyme activities between the wild type and

transgenic lines, and significant activity was present in the *P. furiosus* SOR complemented *E. coli* mutant strain. In order to remove the endogenous SOD activity of the plant cells, cell extracts were heat-treated at 80^{o}C for 15 min. For the heat-treated samples, the *P. furiosus* SOR transgenic lines showed significant activities compared to wild type indicating that heat stable *P. furiosus* SOR is still active while only a portion of the endogenous SOD activities in Arabidopsis plants was retained after the heat-treatment. In order to confirm the *P. furiosus* SOR activities in the transgenic lines, activity gels were prepared using both the wild type and transgenic Arabidopsis plant extracts and extracts of the *P. furiosus* SOR complemented *E. coli* SodA, SodB mutant. No activity was observed in these gels for any of the samples. However, recombinant *P. furiosus* SOR activity was detected in activity gels containing samples of the fungi, *Neurospora crassa,* transformed with SOR (Figure 4-13). The *N. crassa* samples were heat-treated at 80^{o}C for 15 min. and showed activity in the gel. It is presumed that fairly high protein concentrations are needed to support the *P. furiosus* SOR activity in the gel. Since the samples from the *N. crassa* were prepared by drying, the protein concentration of the *N. crassa* cell extracts was around 5~6 mg/ml for non heat-treated samples, and ~1mg/mL for heat treated samples. It was generally not possible to obtain such high protein concentrations the plant cell extracts due to limited plants material.

Wild type and transgenic Arabidopsis seeds and seedlings were exposed to heat stresses to determine whether *P. furiosus* SOR conferred protection to the transgenic lines compared to the wild type lines. As indicated in Figure 4-14, the germination rate of the seeds of SOR transgenic lines was significantly higher than wild type seeds after they were exposed to a heat stress of 45 °C for 5 hours. In the heat stress experiment involving the seedlings, it was observed that no wild type seedling survived after direct heat exposure at 45^{o}C for 2 hour while

SOR transgenic lines showed survival rates of at least 50% (Figure 4-15). These results indicate that there are significant differences between the wild type and SOR transgenic lines in terms of dealing with heat stress. It is thought that *P. furiosus* SOR expressed in the seeds and seedlings of the transgenic Arabidopsis might dampen the reactive oxygen toxicity produced by abiotic environmental stresses, increasing their resistance to heat exposure.

4.3.5.3 SOR transgenic plants exhibited drought tolerance.

The two-month old plants that were grown at 22^{o}C in the phytotron were incubated at room temperature. A drought stress was imposed by not watering the plants for 11 days. The SOR transgenic plants showed normal growth under optimal growth conditions. However, 11 days after water was withheld, there were significant differences between the wild type and GFP control lines and SOR transgenic lines. While wild type and GPF vector control plants exhibited withered/dried, purple pigmented leaves, SOR transgenic plants showed less pigmentation and higher leaf mass (Figure 4-16). The observed red pigmentation in the leaves is called anthocyanins, which have been shown to act as a "sunscreen", protecting cells from photo-damage by absorbing UV and blue-green light, thereby protecting the tissues from photo inhibition. Photo inhibition over a long time may cause the formation of highly reactive free oxygen radicals (29, 27). One possible explanation for continued biomass production under drought stress of the SOR transgenic plants would be that SOR reduces the O_2 levels of the leaves, thus reducing the propensity for photo inhibition during stress. Since SOR reaction results in a net loss of O_2, there would be a decreased availability of O_2 for free radical production during stress.

It is known that in plants pathogen exposure or environmental conditions such as extreme temperature, drought and water stress especially in combination with high light intensities can

cause oxidative stress damage by overproduction of reactive oxygen species (8, 27). There have been studies which show that over-expression of the ROS detoxification enzymes, such as SOD, provide tolerance to oxidative stress in plants (7, 25, 27). It is thought that expression of SOR in transgenic plants could also detoxify superoxide radicals improving the plants resistance to heat, drought and even pathogen exposure (data is not shown). One can expect that hydrogen peroxide generated by SOR reduction of superoxide can affect the tolerance of transgenic plants to oxidative stress. However, there was a report that over-expression of chloroplast-localized Cu/Zn SOD in transgenic tobacco can lead to alterations in the expression of another protective enzyme, namely APX (27), one of the most important antioxidant enzymes of plants that detoxifies hydrogen peroxide using ascorbate for reduction (12). The ascorbate peroxidase (APX) is crucial in maintaining H_2O_2 content at nontoxic concentrations in many of the compartments of the cell. Since expression of *P. furiosus* SOR in the Arabidopsis plants likely results in increased H_2O_2 production after an environmental stress due to the action of SOR (reduction of superoxide to two equivalents of H_2O_2), it is thought that the improved stress response of the SOR transgenics is the result of the SOR expression as well as induction of plant catalases/peroxidases (26). Future studies will evaluate whether expression and activities of plant catalases and peroxidases increase to compensate for the presumed increase in cellular H_2O_2 resulting from SOR activity following environmental stress.

Conclusion

Plants produce reactive oxygen species (ROS), such as superoxide and hydrogen peroxide as a response to environmental changes. Sudden increase of ROS production can cause significant damage, potentially leading to cell death. *P. furiosus* SOR, which has the function of detoxifying the superoxide molecules without producing of oxygen, was transformed into plant cells to function as an antioxidant enzyme. *P. furiosus* SOR was successfully expressed in both tobacco cell cultures as well as, Arabidopsis. Production of SOR in the tobacco cells provided some protection against heat exposure, while expression of SOR in Arabidopsis appeared to improve the plants' resistance to heat-stress and drought damage, presumably by limiting reactive oxygen production. Future studies are needed to more fully explore the changes in the transgenic plants that give rise to the significantly improved performance of the transgenic plants compared to wild type in response to various environmental stresses.

Table 4-1. SOR activity of transgenic tobacco cell culture strains

Sample	Specific activity (U/mg)		Percent heat stable activity	Fold increase in heat-stable activity relative to control*
	Untreated cell extract	Heat treated cell extract		
NT1 wild type	17.8+/-0.4	6.9+/- 0.9	39	5.0
NT1-GFP	3.7+/-0.2	1.4+/-0.7	38	1.0
NT1-SOR	28.3+/-6.6	23.8+/-3.5	84	17.5
NT2-SOR	30.7+/-12.3	19.6+/-4.5	64	14.0
NT3-SOR	37.9+/-10.6	37.9+/-5.6	100	27.1
NT4-SOR	39.5+/-4.3	42.1+/-1.9	106	30.1

The heat-treated cell extracts were incubated at 85^{o}C for 15 min and denatured protein was removed by high-speed centrifugation prior to the assay.

The specific activity is reported as the average ± deviation of 9 values from 3 separate experiments

*Calculated from heat-stable SOR activity relative to the NT1-GFP control.

Table 4-2. Reconstitution of heat-stable SOR activity from transgenic tobacco cell culture

Sample	Specific activity (U/mg)
NT1-GFP	1.6
NT1-GFP, HT[a]	0.23
NT1-GFP, HT + Rd, NROR, NADPH[b]	0.14
NT1-SOR3	17.2
NT1-SOR3, HT	0.12
NT1-SOR3, HT + Rd, NROR, NADPH	25.9

[a]The heat-treated cell extracts were incubated at 90^{o}C for 20 min and denatured protein was removed by high-speed centrifugation prior to the assay. The reported specific activity is the average of two values.

[b]For the reconstituted samples, 0.45 mM NADPH and 170 nM of both recombinant *P. furiosus* Rd and NROR were added to the assay mixture.

Table 4-3. SOR activity of transgenic Arabidopsis plants.

Samples	*P. furiosus* SOR in *E. coli* SodA, SodB mutant	Wild type Arabidopsis	*P. furiosus* SOR transgenic Arabidopsis (3-7)	*P. furiosus* SOR transgenic Arabidopsis (9-1)
Specific activity(U/mg) Non heat-treated	42.9	13.2	12.5	14.5
Specific activity(U/mg) Heat-treated for 15 min at 80^{o}C	N/A	19.83	50.5	47.72

The same samples that were used in Western analysis (Figure 8) were used for activity assays. The heat-treated cell extracts were incubated at 80^{o}C for 15 min and denatured protein was removed by high-speed centrifugation prior to the assay.

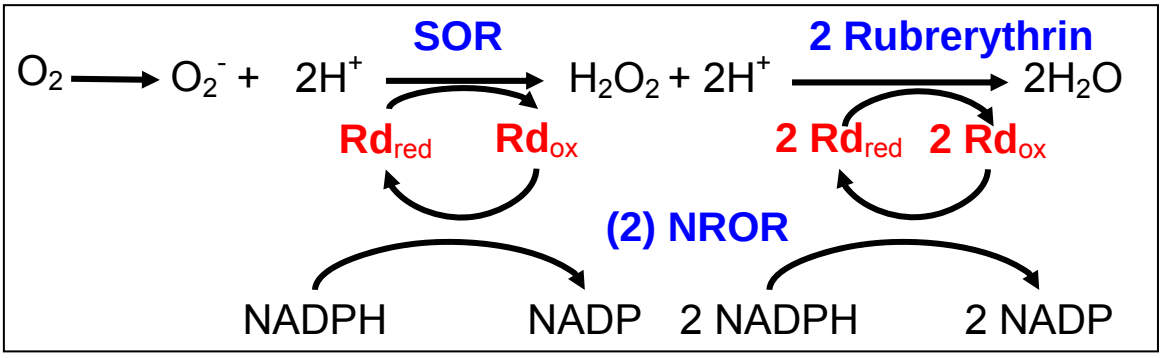

Figure 4-1. A model for the detoxification of oxygen in the hyperthermophilic, anaerobe *P. furiosus.* Figure from Grunden *et al*, (2005)

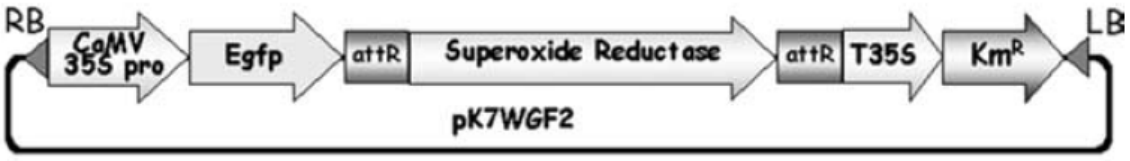

Figure 4-2. SOR expression construct used in this study. CaMV 35S Pro, 35S cauliflower mosaic virus promoter; SOR, superoxide reductase; T35S, terminator site; Km, kanamycin resistance selectable marker; GFP, green fluorescent protein.

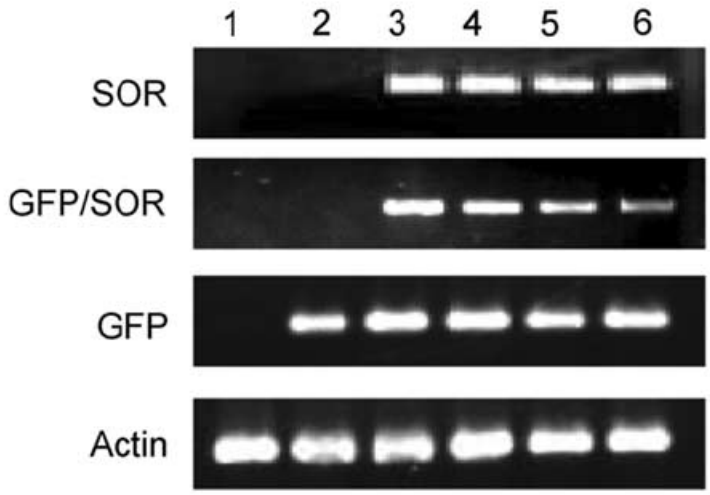

Figure 4-3. RT-PCR analysis shows that SOR mRNA is produced in the transgenic NT1 cells. Specific primers identified *P. furiosus* SOR, GFP, and tobacco cell actin (a loading control).

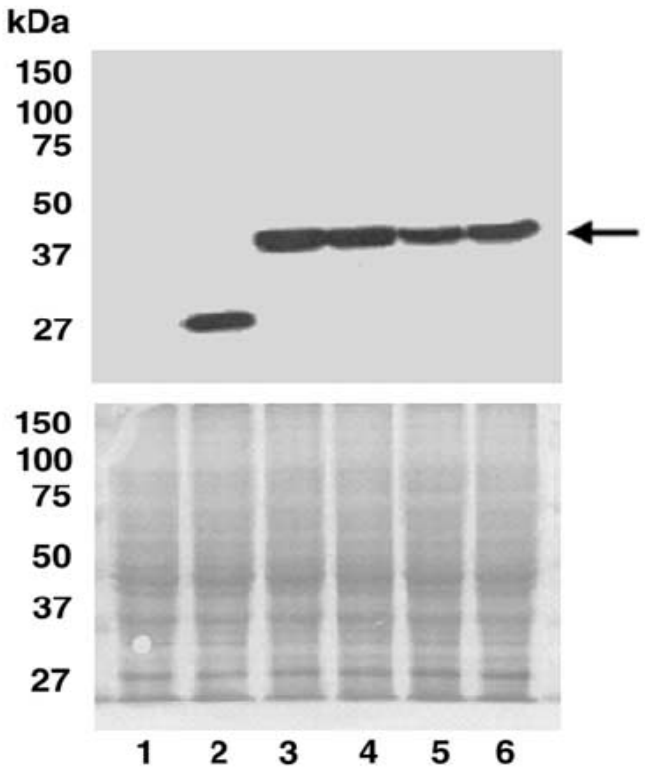

Figure 4-4. Western analysis indicates that the GFP–SOR fusion protein is produced in NT1 cell culture. Top panel is the immunoblot and lower panel is the amido black stained membrane that shows equal protein loading. Lane 1, wild-type NT1 tobacco cell sample; lane 2, NT1-GFP sample; lanes 3–6, NT1-SOR cell-lines 1–4, respectively. The predicted full length, 42-kDa GFP–SOR fusion protein was present in all transgenic SOR lines (arrow). Equal amounts of cellular protein (30 μg) were used in each lane.

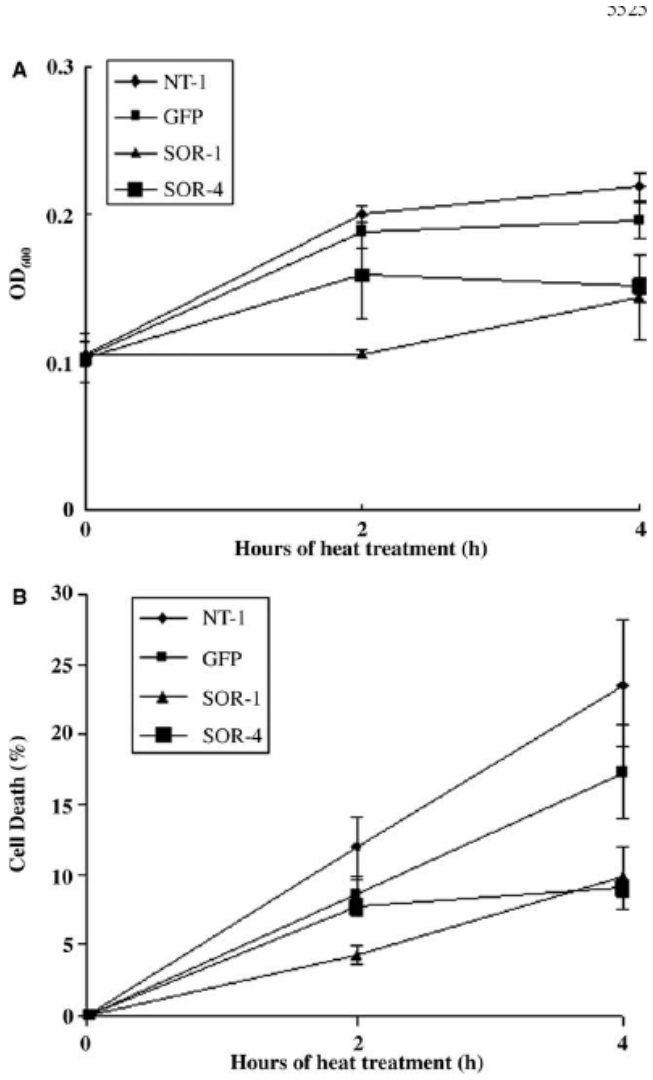

Figure 4-5. Heat resistance in suspension cultured cell lines of wild-type (NT1) and tobacco cells expressing either GFP or SOR. Freshly transferred suspension cells were cultured in NT1 medium at 40^{o}C for 2 and 4 h before staining cells with Evans Blue to detect dead cells. Cell death was quantified spectrophotometrically by measuring absorbance at 600 nm (A) and microscopically by counting the stained and unstained cells (B). The data presented are the result of three independent experiments.

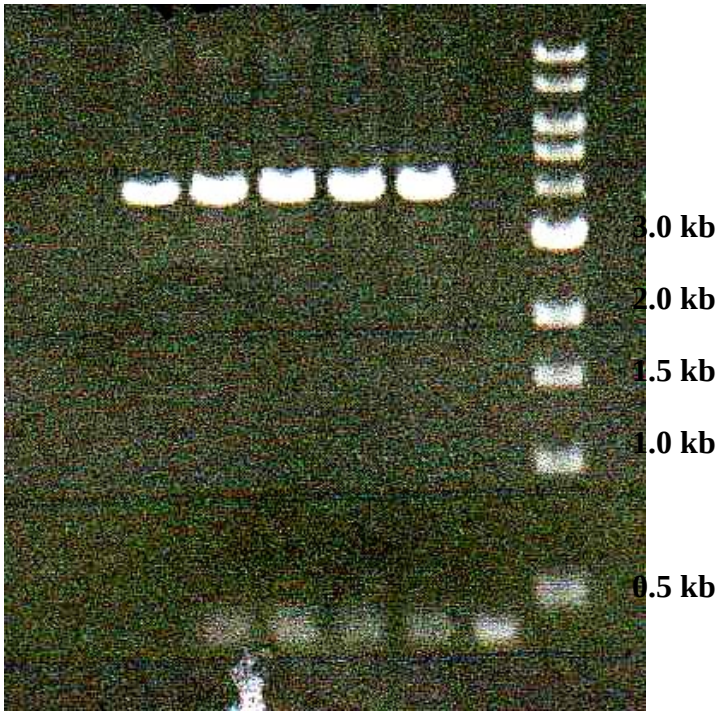

Figure 4-6. Restriction site analysis for the *P. furiosus* SOR expression plasmids. L: Molecular weight standard, Lane 1: pBAD/ HisA digested with *Xho*I and *Eco*RI,

Lane 2: clone #1 digested with *Xho*I and *Eco*RI, Lane 3: clone #2 digested with *Xho*I and *Eco*RI,

Lane 4: clone #3 digested with *Xho*I and *Eco*RI, Lane 5: clone #4 digested with *Xho*I and *Eco*RI,

Lane 6: SOR specific PCR product using *P. furiosus* genomic DNA as template

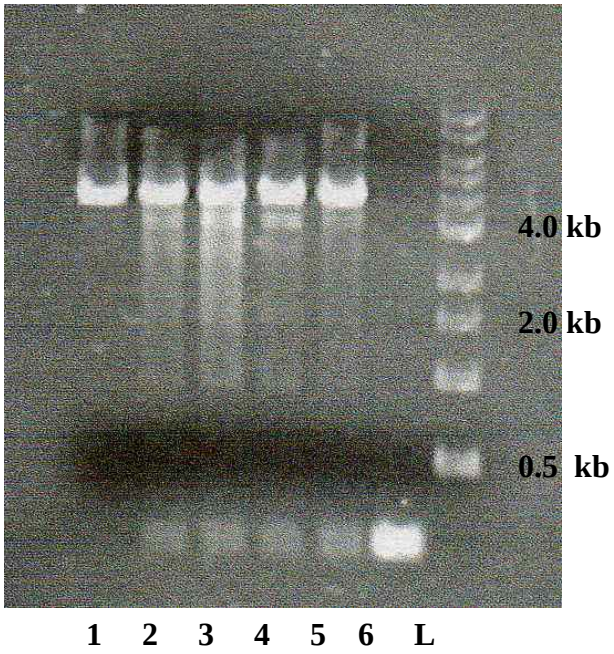

Figure 4-7. Restriction site analysis for the *P. furiosus* Rd expression plasmids.

L: Molecular weight standard, Lane 1: pBAD/ HisA digested with *Pst*I and *Sac*I, Lane 2: clone #1 digested with *Pst*I and *Sac*I, Lane 3: clone #2 digested with *Pst*I and *Sac*I, Lane 4: clone #3 digested with *Pst*I and *Sac*I, Lane 5: clone #4 digested with *Pst*I and *Sac*I, Lane 6: Rd specific PCR product using *P. furiosus* genomic DNA

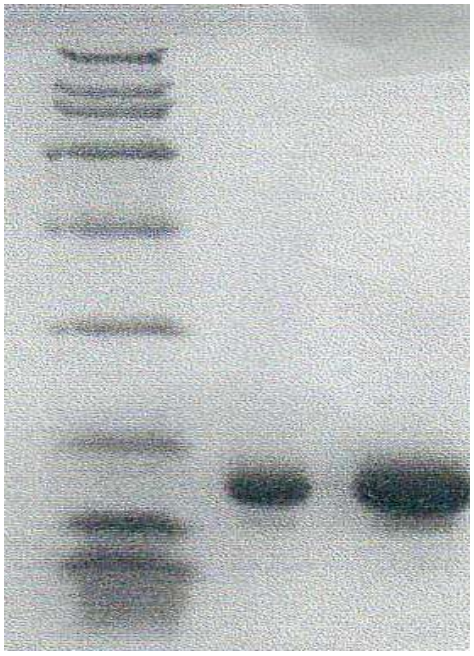

Figure 4-8. Protein purification of *P. furiosus* SOR. Expected molecular weight is ~ 17kDa. L: M.W. standard, Lane 1: 2µg of purified *P. furiosus* SOR protein, Lane 2: 5µg of purified *P. furiosus* SOR protein

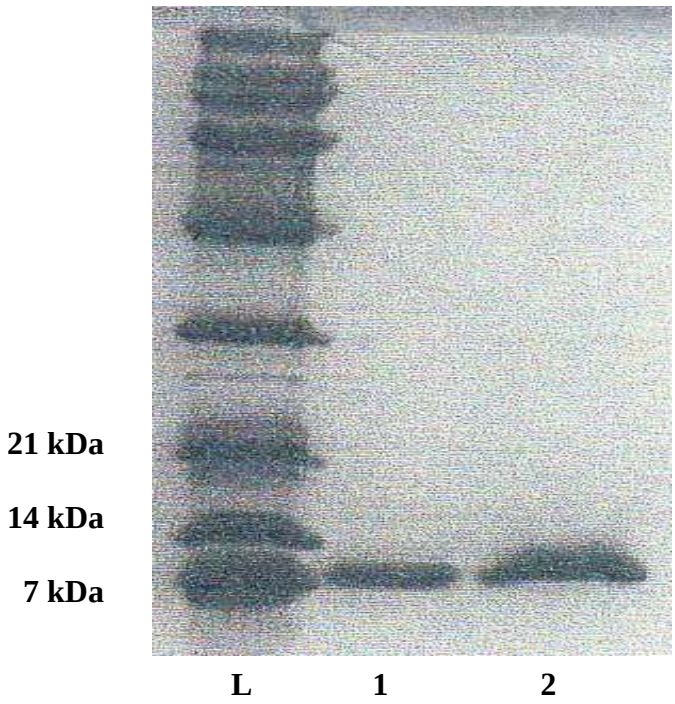

Figure 4-9. Protein purification of *P. furiosus* Rd. Expected molecular weight is ~ 8 kDa. L: M.W. standard, Lane 1: 2µg of purified *P. furiosus* Rd protein, Lane 2: 5µg of purified *P. furiosus* Rd protein

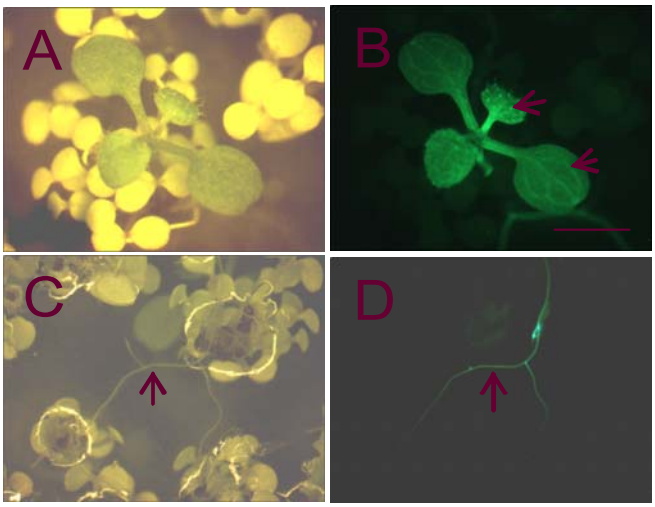

Figure 4-10. Detection of SOR expressed in Arabidopsis through visualization of GFP fluorescence (A) Plants that did not contain the SOR appeared dull yellowish, while the transgenic plant appeared healthy (green). (B) Leaves of plants producing SOR exhibited fluorescence because of the GFP-SOR fusion construct. (C) Roots of the transgenic plants also produced GFP-SOR; bright field image (D) fluorescence image of GFP-SOR in roots

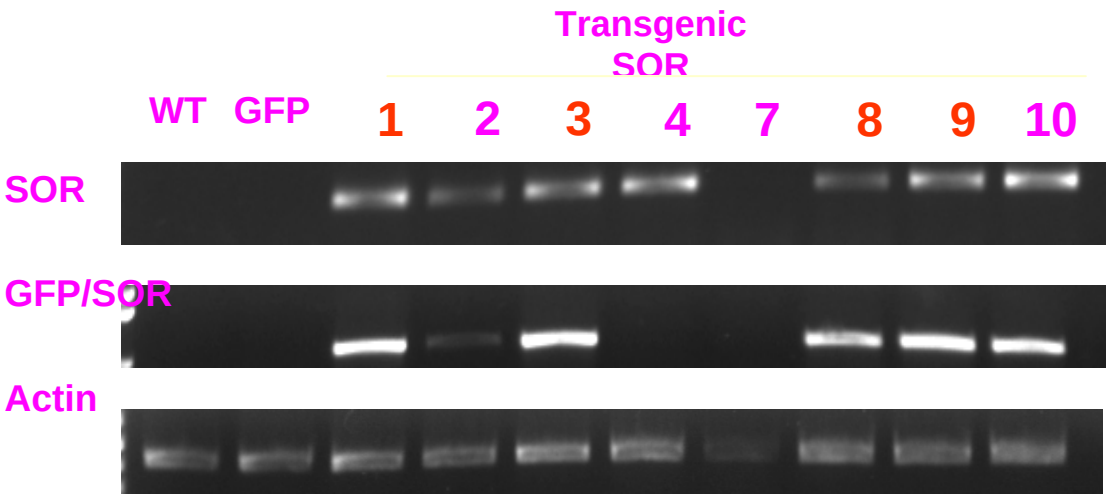

Figure 4-11. RT-PCR analysis showing that SOR mRNA is produced in the transgenic Arabidopsis

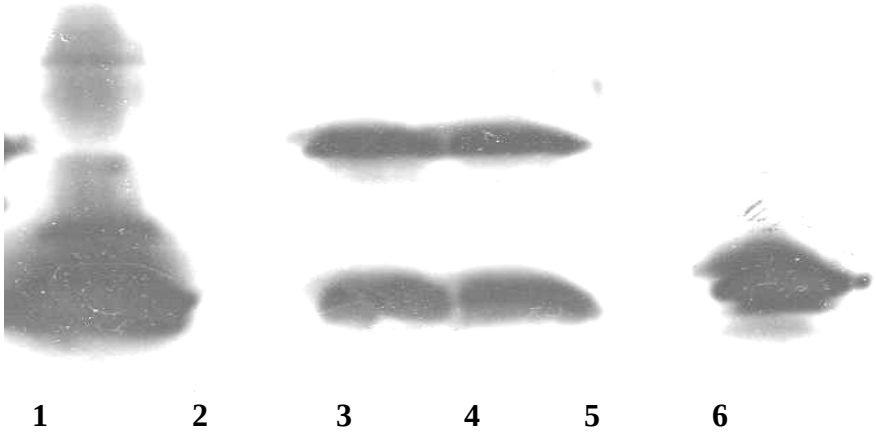

Figure 4-12. Western blot analysis for *P. furiosus* SOR in transgenic Arabidopsis plants Lane 1: Cell extract of *P. furiosus* SOR in *E. coli* SodA, SodB mutant, Lane 2: Cell extract of wild type Arabidopsis plant (heat treated), Lane 3: Cell extract of *P. furiosus* SOR transgenic Arabidopsis plant (3-7, heat treated), Lane 4: Cell extract of *P. furiosus* SOR transgenic Arabidopsis plant (9-1, heat treated), Lane 5: not loaded, Lane 6: Purified *P. furiosus* SOR protein (SOR is expressed as a six-histidine tagged fusion protein). Plant cell extracts were heated treated at 80^{o}C for 15 min. 27 μg of protein were loaded in lanes 1 through 4, and 50 ng was loaded in lane 6. The primary antibody used was anti-rabbit SOR at a dilution of 10,000

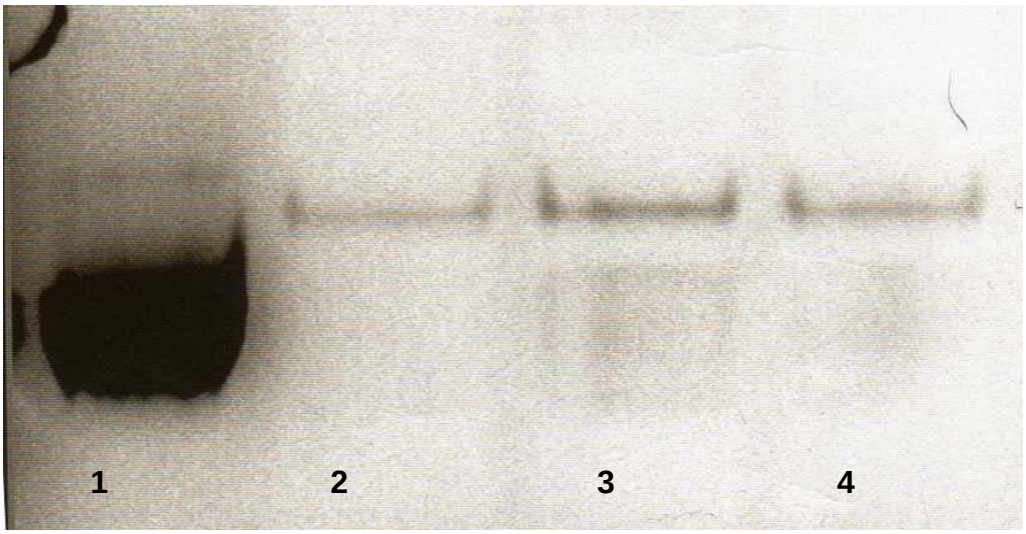

Figure 4-13. Gel for detection of *P furiosus* SOR activity in *N. crassa.* (Inverted Image) Lane 1: Purified *P furiosus* SOR (120 µg), Lane 2: Wild type (50 µg cell extract), Lane 3: *P furiosus* SOR transgenic line #6 (50µg cell extract), Lane 4: *P furiosus* SOR transgenic line #7 (50µg cell extract)

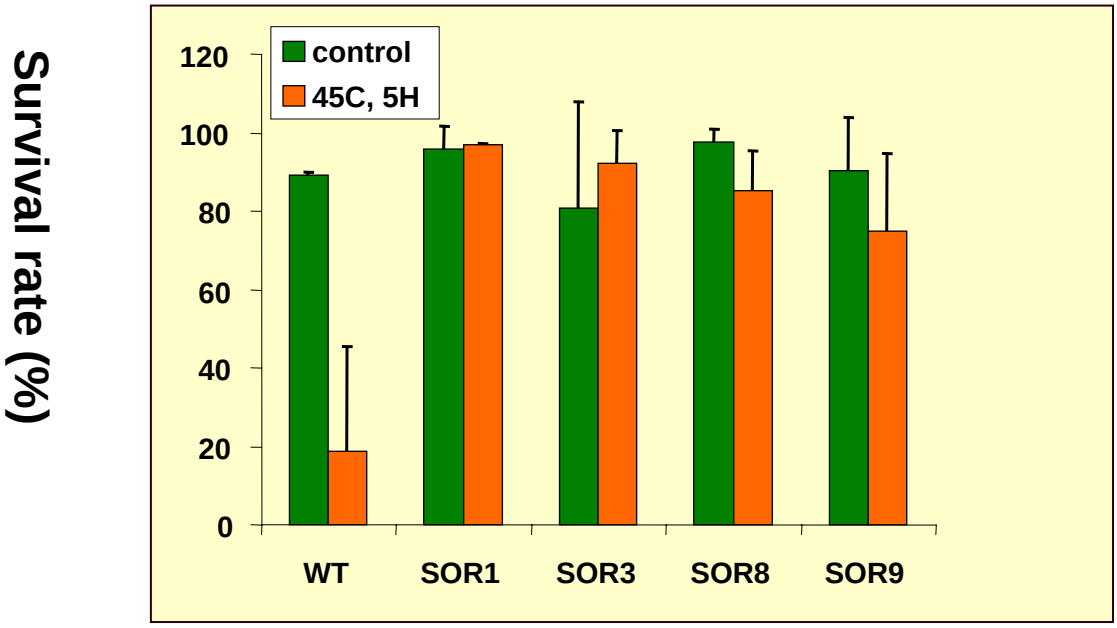

Figure 4-14. The effects of heat-stress on Arabidopsis seed germination. Heat stress at 45°C was applied to wild type and SOR-expressing transgenic Arabidopsis seeds for 5 hrs while control group seeds were incubated at 22°C. Following heat-stress, the experimental group was returned to the 22°C incubator and all plates were left at 22°C for 1 week. Germination rate was monitored after 2 days.

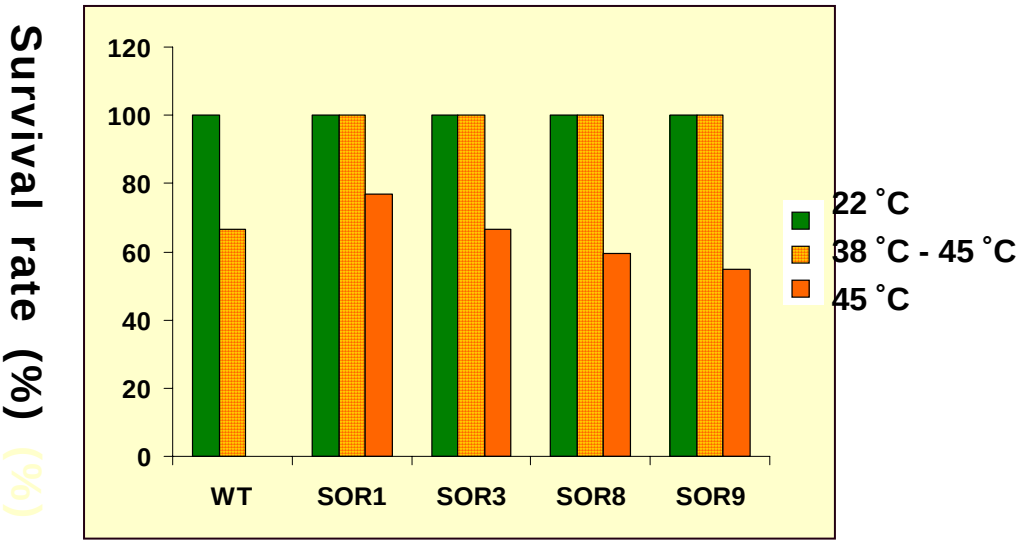

Figure 4-15. Survival rate of 10-day old Arabidopsis seedlings. Three groups of seeds were monitored for survival rate after heat stress. In the beginning, all seeds were left to germinate in a 22°C incubator for 10 days. The group 1 (control: green background) remained in the 22°C incubator. Group 2 (orange diamond in yellow background) were exposed to a temperature acclimation in seedlings were incubated at 38°C for 1.5 hours and then an additional 2 hour incubation at 45°C. Group 3 (orange background) were brought from the 22°C incubator and were directly exposed to 45°C for 2 hours. Following heat-stress, the experimental group was returned to the 22°C incubator and all plates were left at 22°C for 1 week. The number of seedlings that survived was counted after 7 days

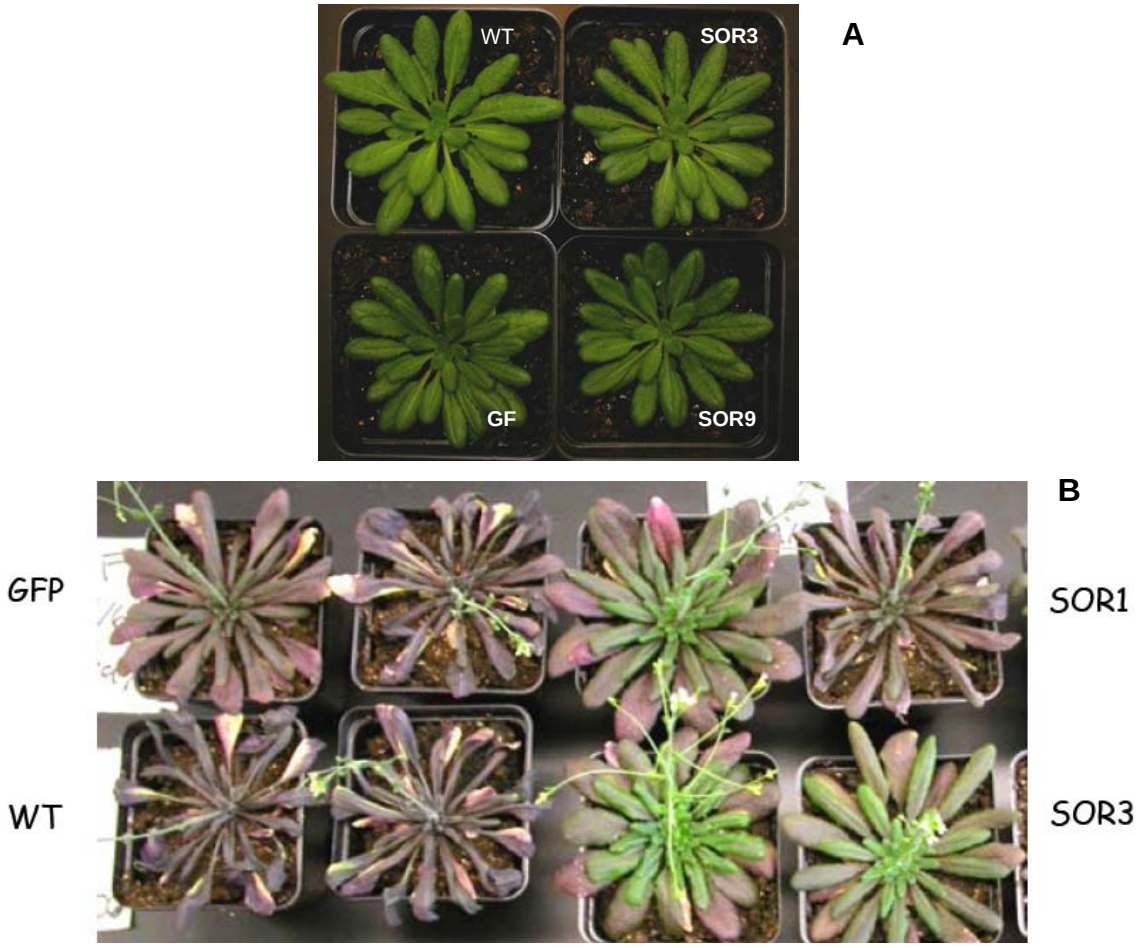

Figure 4-16. Responses of Arabidopsis plants to drought stress. Two-month old plants were grown under 8/16 h dark/light cycle in the Phytotron (A) and were not watered for the drought stress treatment (B). The photographs were taken 11 d later. GFP: vector control, WT: wild type, SOR1: SOR transgenic Arabidopsis clone #1, SOR3: SOR transgenic Arabidopsis clone #3,

Literature cited

1. **Allen, R. D.** 1995. Dissection of Oxidative Stress Tolerance Using Transgenic Plants. Plant Physiology **107:**1049-1054.

2. **Apel, K., and H. Hirt.** 2004. Reactive oxygen species: Metabolism, oxidative stress, and signal transduction. Annual Review of Plant Biology **55:**373-399.

3. **Arora, A., R. K. Sairam, and G. C. Srivastava.** 2002. Oxidative stress and antioxidative system in plants. Current Science **82:**1227-1238.

4. **Asada, K.** 1992. Ascorbate Peroxidase - a Hydrogen Peroxide-Scavenging Enzyme in Plants. Physiologia Plantarum **85:**235-241.

5. **Baker, C. J., and N. M. Mock.** 1994. An Improved Method for Monitoring Cell-Death in Cell-Suspension and Leaf Disc Assays Using Evans Blue. Plant Cell Tissue and Organ Culture **39:**7-12.

6. **Beauchamp, C., and I. Fridovich.** 1971. Superoxide dismutase: improved assays and an assay applicable to acrylamide gels. Anal Biochem **44:**276-87.

7. **Bowler, C., L. Slooten, S. Vandenbranden, R. Derycke, J. Botterman, C. Sybesma, M. Vanmontagu, and D. Inze.** 1991. Manganese Superoxide-Dismutase Can Reduce Cellular-Damage Mediated by Oxygen Radicals in Transgenic Plants. Embo Journal **10:**1723-1732.

8. **Bowler, C., M. Vanmontagu, and D. Inze.** 1992. Superoxide-Dismutase and Stress Tolerance. Annual Review of Plant Physiology and Plant Molecular Biology **43:**83-116.

9. **Bradford, M. M.** 1976. A rapid and sensitive method for the quantitation of microgram quantities of protein utilizing the principle of protein-dye binding. Anal Biochem **72:**248-54.

10. **Chen, H., R. S. Nelson, and J. L. Sherwood.** 1994. Enhanced Recovery of Transformants of Agrobacterium-Tumefaciens after Freeze-Thaw Transformation and Drug Selection. Biotechniques **16:**664-&.

11. **Foyer, C. H., and B. Halliwell.** 1977. Presence of Glutathione and Glutathione Reductase in Chloroplasts - Proposed Role in Ascorbic-Acid Metabolism. Planta **133:**21-25.

12. **Foyer, C. H., and B. Halliwell.** 1977. Purification and Properties of Dehydroascorbate Reductase from Spinach Leaves. Phytochemistry **16:**1347-1350.

13. **Foyer, C. H., and G. Noctor.** 2005. Oxidant and antioxidant signalling in plants: a re-evaluation of the concept of oxidative stress in a physiological context. Plant Cell and Environment **28:**1056-1071.

14. **Fridovich, I.** 1998. Oxygen toxicity: a radical explanation. J Exp Biol **201:**1203-9.
15. **Grunden, A. M., F. E. Jenney, Jr., K. Ma, M. Ji, M. V. Weinberg, and M. W. Adams.** 2005. In vitro reconstitution of an NADPH-dependent superoxide reduction pathway from Pyrococcus furiosus. Appl Environ Microbiol **71:**1522-30.

16. **Haseloff, J., and B. Amos.** 1995. Gfp in Plants. Trends in Genetics **11:**328-329.

17. **Hou, W. C., Y. L. Lu, S. Y. Liu, and Y. H. Lin.** 2003. Activities of superoxide dismutase and glutathione peroxidase in leaves of different cultivars of Liriope spicata L. on 10% SDS-PAGE gels. Botanical Bulletin of Academia Sinica **44:**37-41.

18. **Jenney, F. E., Jr., M. F. Verhagen, X. Cui, and M. W. Adams.** 1999. Anaerobic microbes: oxygen detoxification without superoxide dismutase. Science **286:**306-9.

19. **Ji, M. L.** 2003. Functional evaluation of the mechanisms of reactive oxygen detoxification in the hyperthermophilic archaeon Pyrococcus furiosus using complementation studies.

20. **McCord, J. M., and I. Fridovich.** 1969. Superoxide dismutase. An enzymic function for erythrocuprein (hemocuprein). J Biol Chem **244:**6049-55.

21. **Mittler, R.** 2002. Oxidative stress, antioxidants and stress tolerance. Trends in Plant Science **7:**405-410.

22. **Miyake, C., and K. Asada.** 1992. Thylakoid Bound Ascorbate Peroxidase Scavenges Hydrogen-Peroxide Photoproduced - Photoreduction of Monodehydroascorbate Radical. Photosynthesis Research **34:**156-156

23. **Noctor, G., A. C. M. Arisi, L. Jouanin, K. J. Kunert, H. Rennenberg, and C. H. Foyer.** 1998. Glutathione: biosynthesis, metabolism and relationship to stress tolerance explored in transformed plants. Journal of Experimental Botany **49:**623-647.

24. **Noctor, G., and C. H. Foyer.** 1998. Ascorbate and glutathione: Keeping active oxygen under control. Annual Review of Plant Physiology and Plant Molecular Biology **49:**249-279.

25. **Perl, A., R. Perltreves, S. Galili, D. Aviv, E. Shalgi, S. Malkin, and E. Galun.** 1993. Enhanced Oxidative-Stress Defense in Transgenic Potato Expressing Tomato Cu,Zn Superoxide Dismutases. Theoretical and Applied Genetics **85:**568-576.

26. **Rivett, A. J., J. E. Roseman, C. N. Oliver, R. L. Levine, and E. R. Stadtman.** 1985. Covalent modification of proteins by mixed-function oxidation: recognition by intracellular proteases. Prog Clin Biol Res **180:**317-28.

27. **Sengupta, A., R. P. Webb, A. S. Holaday, and R. D. Allen.** 1993. Overexpression of Superoxide-Dismutase Protects Plants from Oxidative Stress - Induction of Ascorbate Peroxidase in Superoxide Dismutase-Overexpressing Plants. Plant Physiology **103:**1067-1073.

28. **Suzuki, N., and R. Mittler.** 2006. Reactive oxygen species and temperature stresses: A delicate balance between signaling and destruction. Physiologia Plantarum **126:**45-51.

29. **Weinberg, M. V., F. E. Jenney, Jr., X. Cui, and M. W. Adams.** 2004. Rubrerythrin from the hyperthermophilic archaeon Pyrococcus furiosus is a rubredoxin-dependent, iron-containing peroxidase. J Bacteriol **186:**7888-95.

30. **Hames, B.D**. (1990) One-dimensional polyacrylamide gel electrophoresis. In Gel Electrophoresis of Proteins, a Practical Approach (Hames, B.D. & Rickwood, D., eds.), pp. 30-50. IRL Press, Oxford, UK

CHAPTER 5

Cloning, expression, and purification of recombinant *Colwellia psychrerythraea* glutathione reductase

Abstract

Under certain environmental stresses such as exposure to extreme temperatures, radiation, and dehydration, plants face the challenges of protecting protein structure and preventing cellular damage. Glutathione reductase (GR) from *Colwellia psychrerythraea*, which is a psychrophilic marine bacterium, is stable at low temperature and could be engineered into plants to aid in combating damage from rapid changes in temperature and to protect against freezing and oxidative stress. Two different constructs were designed to express the recombinant GR protein. In the first construct, GR was cloned into the pBAD/HisA expression vector, generating a recombinant *C. psychrerythraea* GR protein with an N-terminal tag consisting of 6 histidine residues (His_6-GR). The other expression construct used the IMPACT (Intein Mediated Purification with an Affinity Chitin-binding Tag) system, and enabled the purification of an untagged version of the recombinant protein. Both of the His_6-tagged and untagged recombinant *C. psychrerythraea* GOR proteins were purified and enzyme assays were performed to measure activity. Significant levels of activity (> 100 U/mg) were observed for the untagged *C. psychrerythraea* GR when assays were conducted at low temperature (4°C).

5.1. Introduction

Glutathione (abbreviated GSH) is a tripeptide composed of glutamate, cysteine and glycine that has numerous important functions within cells. It contains an unusual peptide linkage between the amine group of cysteine and the carboxyl group of the glutamate side chain (Figure 5-1) (31). Glutathione is ubiquitous in animals, plants, and microorganisms, and being water soluble is found mainly in the cell cytosol and other aqueous phases of the living system (22, 23, 29). It protects cells from toxins such as free radicals by serving as a reductant (14). The sulfhydryl group of GSH can be used to reduce peroxides. The resulting oxidized form of GSH consists of two molecules of disulfide bonded together (GSSG). Utilization of GSH results in its conversion to the disulfide form, (GSH), the major non-protein sulfhydryl in living organisms (2, 25). Glutathione often attains millimolar levels inside cells, which makes it one of the most highly concentrated intracellular antioxidants (19). GSH takes part in many different intra-cellular processes, including maintenance of reduced thiol groups, protection from oxygen-induced cell damage, and generation of deoxyribonucleotide precursors for DNA synthesis (18, 19). It is regenerated in an NADPH-dependent reaction catalyzed by glutathione reductase (13).

Glutathione reductase catalyzes the reduction of oxidized glutathione according to the reaction: $GSSG + NADPH + H^+ \rightarrow 2GSH + NADP^+$. The enzyme is important in maintaining a reducing environment within the cell (1). Glutathione reductase together with NADPH, glutathione and glutaredoxin make up a second hydrogen transport system in *Escherichia coli* in addition to thioredoxin. The active site of glutathione reductase is a redox-active disulfide bond which acts with the bound FAD (18). In *E. coli*, glutathione reductase is a member of the dimeric FAD-containing thiol reductase family. It shares significant homology with the thioredoxin reductases from higher eukaryotes (29). One interesting aspect of glutathione metabolism in *E.*

coli is that the ratio of reduced to oxidized glutathione does not appear to change significantly in mutants that lack glutathione reductase (33).

In plants, numerous functions of GSH have been identified. It regulates sulfur allocation and acts as a regulator of gene expression (28). The reduced form of GSH may act as an important redox buffer, preventing enzyme inactivation by protecting protein thiol groups (12, 16). The ascorbate-glutathione cycle has been demonstrated to remove hydrogen peroxide via the activity of ascorbate peroxidase in the chloroplast stroma and so protect the thiol-modulated enzymes of the Benson-Calvin cycle from oxidative inactivation (12, 15, 20). In this pathway, glutathione acts as a recycled intermediate in the reduction of H_2O_2 using electrons derived from H_2O (12). Efficient recycling of glutathione is ensured by GR activity.

Protein mixed disulfide formation, which may also occur with cysteine or other non-physiological thiols, is generally referred to as S-thiolation. To specifically indicate mixed disulfide formation with GSH, the term S-glutathionylation or S-glutathiolation is used. Protein S-glutathiolation has been implicated in buffering against oxidative stress, stabilization of extracellular proteins, protection of proteins against irreversible oxidation of critical cysteine residues, and regulation of enzyme activity (21). H_2O_2 inactivates yeast glyceraldehyde 3-phosphate dehydrogenase, whether GSH is present or absent, but the inhibition was reversible only in the presence of GSH (14). This shows that glutathionylation protects the protein from fatal inactivation due to irreversible oxidation.

Colwellia psychrerythraea belongs to a group of strictly psychrophilic gamma proteobacteria, which thrive at temperatures below 5^{o}C. It has been obtained from stably cold marine environments, including deep sea and Arctic and Antarctic sea ice. *C. psychrerythraea*

can be exposed to high levels of reactive oxygen species (ROS) through their own metabolism as well as by exposure to its environment, which can be a high UV-light environment. The production of extra polyunsaturated fatty acids can result in lipid peroxidation of membrane. The environmental source of ROS such as high concentrations of hydrogen peroxide (500 nmol l^{-1}) within brine channels of sea ice and increased solubility of oxygen at low temperature (3, 27) can cause enhanced oxidative stress compared to mesophilic organisms. In order to cope with the oxygen toxicity, several antioxidants are present in *C. psychrerythraea* including SODs and catalases that have been identified in its genome (26). In the work described here, one of the antioxidant enzymes produced in *C. psychrerythraea*, glutathione reductase, is being characterized. The rationale for this study is that we are interested in determining whether *C. psychrerythraea* GR, when expressed in plants, may have utility in improving the protection of protein structure and prevention of cellular damage from certain environmental stresses such as exposure to extreme temperatures, radiation, and dehydration. There have been several studies of over-expressing GRs of bacterial origin in plants. The studies showed function in the chloroplasts of plant cells to increase both the GSH/GSSG ratio and the total glutathione pool. NADPH-dependent inhibition of GR activity in the stroma does not negate the effects of increased GR activity (28). These data are in agreement with results obtained for tobacco transformed to express the bacterial GR in the chloroplast (8). *C. psychrerythraea* GR, which is stable under cold temperature and responsible for continuous production of the reduced glutathione (GSH), could be engineered into plants to aid in combating oxidative stress under low-temperature/freezing conditions. Therefore, the study of the GR of *C. psychrerythraea* would certainly yield crucial information related to plants' responses to reduce cellular damage caused by exposure to extreme environments. In the study described in this chapter, the

glutathione reductase gene from *C. psychrerythraea* was cloned into *E. coli.* The GR gene was over-expressed in *E. coli* and small amounts of recombinant *C. psychrerythraea* GR protein was purified and used for characterization of the protein. Two different methods were used to clone *C. psychrerythraea* GR into *E. coli*. The first attempt was the production of *C. psychrerythraea* GR fused with an N-terminal His_6-tag by cloning the GR gene into the pBAD-HisA vector (pBAD system, Invitrogen). The second method used was generating a GR-intein-chitin-binding domain fusion using the IMPACT vector system (New England BioLab). The recombinant GR produced using the IMPACT system was purified and had significant activity at low temperature. In addition, a GR deficient *E. coli* strain was generated to remove any background GR activity from the host cell to simplify downstream protein purification.

5.2. Materials and Methods

5.2.1 Cloning of Glutathione Reductase (GR) into the pBAD (His_6 tag) plasmid

The marine psychrophilic *Colwellia psychrerythraea* (Cps) 34H strain was obtained from ATTC and grown in marine broth 2216 (Difco laboratories) at 4°C according to the supplier's protocol. Genomic DNA was isolated using the Ultra Clean Microbial DNA Isolation Kit (MO BIO Laboratories, California). The *C. psychrerythraea* glutathione reductase gene was amplified with PCR using the following primers targeted to Cps 34H: forward primer containing an *XhoI* site 5'-CGTTAACTCGAGAGTGAAACCATGACA-3' and the reverse primer containing a *KpnI* site 5'-GGCATAGGTACCAACATTCAGCTTGCT-3'. The following PCR amplification program was used: 40 cycles consisting of denaturation at 95°C for 1 min, annealing at 56°C for 2 min, and extension at 72°C for 2 min. The GR gene was amplified using *Pfu* polymerase. The GR PCR product was subcloned into the *Dra*I site of pACYC184 (New England Bio Lab). The subcloned GR gene was digested with *Xho*I and *Kpn*I restriction enzymes and purified by gel extraction (Qiagen), and finally ligated into the *Xho*I-*Kpn*I site of plasmid pBADHisA (Invitrogen) downstream of araBAD promoter. The resulting plasmid construct was transformed into *E. coli* Mach chemically competent cells (Invitrogen). Plasmid DNA was isolated from the transformants using Qiagen Minipreps, and the plasmids were screened for inserts by visualization of DNA agarose gels. The cloned GR gene sequence was verified by MWG-Biotech (High Point, NC).

5.2.2 Protein over-expression and purification of the recombinant His_6-tagged *C. psychrerythraea* GR

The recombinant form of His_6-GR was over-expressed into *E. coli* Top 10 cultures incubated at temperatures from 4°C to 37°C during the induction period to optimize the GR

expression. For the initial experiment, 30 ml cultures were grown at 37^{o}C. When the cultures had reached an optical density between 0.6 and 0.8, induction of GR was initiated by adding either 0.2% or 0.02% arabinose, and the cultures were incubated at either 37^{o}C for 3h, at 30^{o}C for 5h, at room temperature for 8h, or at 4^{o}C 36h. For each expression sample after the appropriate induction period, 1 ml aliquots of the cultures were collected and the OD_{600} was measured. The samples were centrifuged and the resulting pellets were then resuspended in the appropriate amount of 2X protein denaturing dye (0.125 M tris-Cl, 4% SDS, 20% v/v glycerol, 0.2M DTT, 0.02% bromophenol blue, pH 6.8) according to the O.D. by normalizing cell density at the time of the arabinose induction. The samples were loaded on 12.5% polyacrylamide SDS gels, and the protein expression was evaluated using visual detection of Coomassie Blue-stained gels.

For large-scale protein over-expression, the recombinant form of His_6-GR was induced in a 2 L culture by adding of 0.02 % arabinose when the $O.D._{600}$ reached about 1. The induced culture was incubated at room temperature for 6 h prior to harvesting the cells for protein purification. A pellet from 500 ml of the 2 L expression culture was resuspended in 20 mM sodium phosphate, pH 8 containing 1mM benzamidine and the cell suspension was passed through a French press cell (20000 lb/in^2) twice. The lysed cell suspension was centrifuged in a Sorval ss-34 rotor spun at 40,000 g for 30 min. to remove any cell debris. The cell extract was applied to a 5 ml Ni affinity column (HiTrap Chelating HP, GE Healthcare, New Jersey). Since it was determined that the His_6-GR failed to bind the metal chelation column well, the column flow through was collected and was subsequently applied to a 5mL Q column (HiTrap Q FF, GE Healthcare, New Jersey). Fractions containing the GR protein were collected and applied to a 1 ml phenyl sepharose column (HiTrap Phenyl FF, GE Healthcare, New Jersey) for further purification. The GR-containing fractions were then applied to a second Ni affinity column (1 ml,

HiTrap Chelating HP by GE Healthcare). Since the binding affinity to the metal chelation column was still poor the flow through containing most of the recombinant GR was collected and the protein was concentrated using a Centriplus concentrator (Amicon). A total of 1.2 mg recombinant *C. psychrerythraea* His_6-glutathione reductase was purified from 500 ml of over-expression culture.

5.2.3 Cloning of *C. psychrerythraea* glutathione reductase into the IMPACT expression system vector

5.2.3.1 PCR amplification and cloning: PCR amplification of the *C. psychrerythraea* GR gene for cloning into the IMPACT system vector was performed using the following primers: forward primer containing an *Nde*I site 5'-ttaactaatgagtgaacatatgacacaacat-3' and reverse primer containing a *Sma*I site 5'-atcaacattcagcttcccgggcatagtgacaaa-3' The following PCR amplification program was used: 40 cycles consisting of denaturation at 95°C for 1 min, annealing at 56°C for 1 min, and extension at 72°C for 2 min. The GR gene was amplified using *Pfu* polymerase. The Amplified GR DNA was digested with *Nde*I and *Sma*I and purified by gel extraction (Qiagen), then ligated into *Nde*I-*Sma*I site of plasmid pTYB2 (New England Biolab) downstream of the T7 promoter. The resulting plasmid construct was transformed into *E. coli* XL1 Blue cells (Stratagene, California). Plasmid DNA was isolated from the transformants using Qiagen Minipreps and the presence of insert was screened for by visualization of the plasmids on DNA agarose gels. Restriction site analysis was additionally performed to select the clones containing the GR genes. The cloned GR gene sequence was verified by MWG-Biotech.

5.2.3.2. Protein over-expression and purification of GR using the IMPACT system.

The verified clone was transformed into the *E. coli* Artic strain (Stratagene, California) to over-express the protein. 1 L of cell culture was grown at 12^oC for 36 hours in lactose auto-induction

media (32) that was supplemented with gentamycin (20mg/ml). Over-expressed cell cultures were harvested and cell pellets were frozen at -80^{o}C until used. The cell pellets were resuspended in Cell Lysis Buffer (20 mM Tris pH 8.00, 500 mM NaCl, 0.1 % Triton X-100, 1 mM EDTA) and the cell suspensions were passed through a French press cell (20000 lb/in2) twice. The lysed cell suspension was centrifuged in a Sorval ss-34 rotor at 40,000 g for 30 min. to remove any cell debris. The cell extract was applied to a 20 ml chitin column (New England Biolabs) for the purification. After loading the column with the protein extract, cleavage buffer containing reducing agent (50 mM Dithiothreitol) to induce the self cleavage of the intein fusion and 50 µM FAD (flavin adenine dinucleotide) to reconstitute the GR cofactor was added to the column. The column was then stored at4^{o}C for 48 hours to allow for cleavage of the intein and release of recombinant GR protein. The column was then eluted with cleavage buffer (20 mM Tris pH 8.00, 500 mM NaCl, 1 mM EDTA, 50 mM Dithiothreitol), and fractions containing protein at the expected size of GR were collected.

5.2.4 Enzyme assay of *C. psychrerythraea* glutathione reductase

The GR enzyme activity was detected using a previously described protocol (24). To evaluate whether the protein functioned at low temperature as would be expected for a psychrophilic enzyme, GR assays were conducted at 5^{o}C and 25^{o}C. For the assay, a 3 ml reaction mix containing 75 mM potassium phosphate, 2.6 mM ethylenediaminetetraacetic acid, 1 mM glutathione, 0.09 mM ß-nicotinamide adenine dinucleotide phosphate (NADPH, reduced form), 0.13% (w/v) bovine serum albumin, was prepared. Activity was monitored following the addition of purified glutathione reductase to the reaction mix. The GR activity was monitored by oxidation of NADPH to $NADP^{+}$ at the absorbance of 340 nm for 5 min. One unit is defined as the reduction of 1.0 µmole of oxidized glutathione per minute at pH 7.6. All reagents were

purchased from Sigma and the assay was performed at 25°C and 5°C using a thermostatted Shimadzu UV-2401 spectrophotometer. Protein concentration was measured by the Bradford method (5)

5.2.5 *E. coli gor* mutant strain construction.

For disrupting *gor* (glutathione reductase), which is homologous to *C. psychrerythraea* GR in *E. coli*, the PCR-based one step inactivation of chromosomal gene method by Datsenko & Wanner (10) was used. Plasmid, pKD3, which contains a chloramphenicol resistance gene cassette, is used as the template for generation of PCR fragments encoding the chloramphenicol resistance marker and homologous DNA regions for the target gene (*gor*). The primers consist of 60 bases, which include 40 that are homologous to the flanking region of the target genes and 20 bases that are complementary to the chloramphenicol resistance cassette (see Table 5-1). The PCR products were gel purified (Qiagen, Valencia, CA). pKD46 is a helper plasmid that carries the phage λ Red recombinase that is L-arabinose inducible. pKD46 is cured from cells when the incubation temperature is raised to 37°C. Three strains of *E coli* were transformed: ER2566, and BL21 (DE3), and JM105. The JM105/pKD46, ER2566/pKD46, and BL21 (DE)/pKD46 were plated in LB + ampicillin + 0.3% glucose agar and incubated overnight at 30°C. Transformants carrying pKD46 were grown in 10 ml SOB medium containing 0.2% of L-arabinose and ampicillin at 30°C until the O.D.600 reached 0.6. The cultures were spun down at 9,500 rpm in a Beckman C1015 rotor for 10 min. and washed three times with ice-cold 10% glycerol in order to make the cells electrocompetent. The cells carrying pKD46 were suspended in 100 µl of 10% glycerol and 50 µl aliquots were placed into two separate microfuge tubes. The *gor* specific PCR products (concentration ~1 µg) were added to the 50µl of the suspended cells and no DNA was added to the other 50 µl of cells as a negative control. Electroporation was

done by using a Gene Pulser (Bio Rad, Hercules, CA) set at 2.5V, 200Ω, and 25μF according to the manufacturer's instructions. Shocked cells were added to 1 ml of pre-warmed SOC medium and incubated for 1-hour at 37°C. 10% of the electroporated cells were employed in mutant strain construction. The cells were plated onto LB+ chloramphenicol agar and incubated at 37°C overnight. The remainder of the cells were incubated overnight at room temperature before plating the next day. JM105 (wild type) and its *gor* deficient strain genomic DNAs were purified using the GNOME DNA Kit (Bio 101, Carlsbad, CA) and the isolated DNA was sheared with *Bst*EII. Verification of the gor mutant was performed by using the respective genomic DNAs as the templates and the primers that are specific to the outer region of the genes as well as the primers specific to the disrupted genes (see Table 5-2 for primers).

5.3. Results and discussions

5.3.1 Cloning the *C. psychrerythraea* strain 34H glutathione reductase gene into the pBAD-HisA vector

We initially tried direct cloning of the *Xho*I and *Kpn*I-restricted GR gene into the pBAD vector, but no insert-containing constructs were successfully obtained. In a second effort to clone the GR gene into the pBAD vector, the GR gene (as a blunt-ended PCR product) was subcloned into the *Dra*I site in plasmid pACYC184 (Tet^r and Cm^r; New England BioLabs). Digestion of plasmid pACYC184 with *Dra*I resulted in disruption of the chloramphenicol resistance gene. The plasmids were screened by selecting the transformed colonies that failed to grow in both tetracycline and chloramphenicol containing media, while transformed colonies that had vector with no insert that could grow on both tetracycline and chloramphenicol-containing media were excluded. The GR-containing pACYC184 plasmids were subsequently digested with *Xho*I and *Kpn*I to provide appropriate insert for cloning into the pBAD-HisA expression vector. Two

clones were selected and analyzed using restriction enzyme and PCR analysis to confirm the presence of the GR gene in the pBAD-HisA vector. The expected sized DNA fragment (~1400bp) was observed for both of the clones when they were cut with *Xho*I and *Kpn*I. Additional restriction enzyme analysis was performed using *EcoR*I and *Sap*I. The expected fragment sizes of ~1.1 kb and ~4.4 kb for *EcoR*I site digestion and 1.4kb, 1.4K, 2.7kb (the band near at 4.1kb region is presumed to be the partial digestion of 1. 4kb and 2.7 kb) for *Sap*I digestion were observed after electrophoresis of the DNA in 1% agarose gels (Figure 5-2). PCR analysis was performed for the clones, which showed restriction analysis patterns consistent with GR cloned into the *Xho*I and *Kpn*I sites of pBAD-HisA, and the GR gene was successfully amplified from these plasmids (Figure 5-3). The correct sequence for the GR gene in the pBAD-HisA construct was verified by sequencing both of the strands (MWG-Biotech).

5.3.2. Over-expression of recombinant *C. psychrerythraea* His_6-GR in *E. coli* at various induction temperatures

The *C. psychrerythraea* pBAD/hisA-GR construct was transformed into *E. coli* Top 10 cells for the protein over-expression. 30 ml cultures were grown to optimize the protein expression at various temperatures. Whole cell pellets were obtained at various time points after induction with 0.2% or 0.02% arabinose at 4^{o}C for 36 hours, room temperature for 9 hours, 30^{o}C for 4 hours, and 37^{o}C for 3 hours. In most of the cases, the expected size of the protein bands (~53KDa) was observed except for the case of the culture induced for 2 or 3 h at 37^{o}C with 0.2% arabinose (Figure 5-4). GR protein expression was induced after 1 hour but exhibited instability as the induction time at 37^{o}C was increased to 2 or 3 hours. One of the general aspects of cold-active enzymes is their thermolability at moderate temperatures (30). It is known that psychrophilic, cold-adapted enzymes have an intrinsic temperature-dependent relationship

between the activity, stability, and flexibility of the protein (9, 11). High activity at low temperature is directly related to structural stability of the protein and in general an increased flexibility of the structure at low temperature. It is possible that the thermolability of *C. psychrerythraea* GR at 37°C may be explained from the structural instability of the cold-adapted enzymes at higher temperature (6).

5.3.3 Purification and activity analysis of recombinant *C. psychrerythraea* His_6-GR Protein

Protein extracts derived from large scale cultures (1L) grown at room temperature were applied to Ni affinity columns with the expectation that the GR protein with the N-terminal six-histidine tag would be tightly bound to the metal affinity resin. However, the His-tagged GR protein did not bind well to the Ni-affinity resin, and an alternate multiple column chromatography purification scheme was used instead. After passage of the GR-containing cell extract on an anion exchange column (Q column), a hydrophobic interaction column (phenyl sepharose) and metal affinity column, a relatively pure GR protein was obtained (~53 kDa of > 90% purity by visual inspection on Coomassie Blue-stained 12.5% polyacrylamide gels, (Figure 5-5). A total of 1.23 mg of rHis_6-GR was obtained from 500 ml of the culture.

Enzyme assays were then performed at 25°C and 5°C to measure the activity of the rHis_6-GR protein. No significant activity was observed for this recombinant version of *C. psychrerythraea* GR (Table5-3). One possible reason why this recombinant form of GR is inactive is that the His tag could have significantly modified the structure of *C. psychrerythraea* GR, thereby reducing its activity (7). It is possible that poor binding of the His-tagged GR protein to the Ni-affinity column could be the result of the tag having been folded into the core of the protein , making it surface-inaccessible (4). The other possibility is that multi-step chromatography can affect the activity of the enzyme because prolonged exposure to non-native

conditions can lead to reversible/irreversible denaturation of the protein or weakening of the cofactor binding to the enzyme. Cold-active enzymes are readily affected by higher temperature, often resulting in significantly reduced activity levels. One known example of the thermolability of a cold-active enzyme, is the case of β-galactosidase that is present in an Antarctic *Arthrobactor* strain which is a tetramer at low temperature, but dissociated to inactive monomers at moderate temperatures (7). Another potential problem for the recombinant GR is that deflavination of the required FAD cofactor during the purification process can be induced by high salts, such as the ammonium sulfate used in the hydrophobic interaction chromatography, exposure to temperatures >5°C for the heat-labile psychrophilic enzyme, and as a result of dialysis (17). As a result of these complications, a different GR expression method was designed which had the advantages of producing an unmodified (untagged) recombinant form of the purified protein which required fewer purification steps and enabled a low-temperature on-column cofactor reconstitution

5.3.4 Purification and enzyme activity analysis of an unmodified recombinant *C. psychrerythraea* GR

Due to the very low enzyme activity (5.3 U/mg) observed for the His_6-GR tagged protein, a second *C. psychrerythraea* GR expression construct, using the IMPACT (Intein Mediated Purification with an Affinity Chitin-binding Tag) system, which produces an unmodified recombinant protein, was generated. The IMPACT system vector (pTYB2) features an inducible self-cleavage activity of a protein-splicing element (termed intein) to separate the target protein from the affinity tag, resulting in the purification of an untagged recombinant protein in a single chromatographic step. The *C. psychrerythraea* GOR was cloned into the pTYB2 vector and restriction site analysis was performed to screen the clones (Figure 5-6). One of the plasmids

(#1-4), had an identical-sized DNA fragment as the *Colwellia psychrerythraea* GR PCR product (~1.37 kb) released after digestion with the restriction enzymes *Sma*I and *Nde*I. The intein-fused *C. psychrerythraea* GR sequence was verified by MWG-Biotech.

The recombinant GR protein was over-expressed in the *E. coli* Artic strain (Figure 7, Lane 1). It was observed that the expected size of the fusion protein (~ 105 kDa) was not significantly over-expressed but instead, a strong single band approximately the size of the non-fused GR protein (~ 50 kDa) was obtained after the induction, indicating the possibility of significant self-cleavage of the fusion protein either within the cells or in the cell extract prior to induction of cleavage on the column with the addition of the reducing agent. For the purification, cell extracts of the over-expressed intein-fused recombinant *C. psychrerythraea* GR protein was applied to the chitin column for binding prior to adding the cleavage buffer containing deducting agent (DDT) and storing at 4°C for 48 h to allow cleavage of the protein fusion. Inspection of the protein in the flow-though fraction of the protein extract that was initially applied to the chitin column did not show significant retention of the fusion protein on the chitin column as expected, instead a thick band of ~50 kDa area was observed (Figure 5-7, Lane 2). However, eluted fractions after the cleavage (Figure 5-7, Lane 3 to 8), were shown to contain small amounts of protein at the expected size of *C. psychrerythraea* GR (~50 kDa).

Enzyme assays were performed at 4^{o}C, 12^{o}C and 25^{o}C to measure the activity of the purified protein (Table 5-4). Significant levels of activity were observed for the untagged *C. psychrerythraea* GR even at 4^{o}C as is expected for enzymes from a psychrophilic source. Despite the good activity determined for the recombinant *C. psychrerythraea* GR, there were a few problems encountered during the purification of the protein in terms of its quality and quantity. The over-expressed fusion protein did not appear to remain intact because of the

possible self cleavage of the fusion *in vivo* prior to the induction of the cleavage with reducing agent, which limited the binding of the target protein to the chitin column. Additionally, it was observed that the fusion protein that remained intact bound inefficiently to the chitin affinity column. Over-expression and protein processing protocols need to be further optimized to increase the yield of purified *C. psychrerythraea* GR to enable a full biochemical characterization of the enzyme. The other disadvantage observed during purification is a contaminating band in the eluted fractions. One possibility of the contaminated protein is the *E. coli* host cell GR. The molecular weight of *E. coli* GR is 48.77 kDa, which is an indistinguishable size from the GR of C. *psychrerythraea*. Contamination of purified *C. psychrerythraea* GR with *E. coli* GR would compromise the biochemical analysis of the *C. psychrerythraea* GR enzyme.

The enzyme glutathione reductase (GR) is a member of the pyridine nucleotide-disulfide oxidoreductase family of flavoenzymes, containing two active-site electron acceptors, FAD and a redox-active disulfide (25). GR of *C. psychrerythraea* was compared with other GR sequences from various sources including bacteria, plant, and human (blood cell) using the Clustal W program (Figure 5-8), in order to identify sequence similarities. *C. psychrerythraea* GR showed a high degree of sequence identity with GR sequences from *E. coli* (66 %) and human (44%), but showed the least identity to Arabidopsis (36%). It has conserved sequences of the FAD binding motif (C_XCxxC) and NAD(P)H binding motif ($G_XGYIA_{X18}R_X5R$) that are present in the other GR homologs and characteristic of flavoenzymes in general.

5.3.5. Construction of the *E. coli* GR (glutathione reductase) mutant strains.

In an effort to prevent contamination of recombinant *C. psychrerythraea* GR with *E. coli* GR, the *E. coli* GR gene was disrupted on the chromosome. Three strains of E. coli were chosen

to disrupt the GR gene (Table 5-1). For construction of the *gor* specific gene disruption, 4 colonies from overnight-incubated cells were isolated on LB+ Cm selection plates, which were putative *gor* specific mutants (*gor* deficient in *E. coli* strain). These two isolates for each strain (along with the parental type strain) were subjected to PCR analysis for verification of the targeted gene disruption. For the PCR analysis, sheared genomic DNA from each isolate and the control strain were used as the DNA templates and primers that are specific to either the outer region of the genes or located within the disrupted genes were used (Table 5-2). The different primer combinations would yield different sized PCR products. Only the JM105 strain showed expected sized DNA fragments. The expected sizes of the GR-disrupted DNA in the JM105 strain are 1.1 kb, 1.35 kb, 1.45 kb, and 1.9 kb when the following primer combinations are used: 5' *gr*:Cm specific and 3' *gr*:Cm specific primers, 5' outer region and 3' *gr*:Cm specific primers, 5' *gr*:Cm specific and 3' outer region primers, and 5' outer region and 3' outer region primers, respectively. The expected DNA size when using the wild type DNA as the template DNA and the 5' outer region and 3' outer region primers is about 2.0 kb. PCR analysis of one of the two isolates did result in the production of PCR fragments that matched the expected sizes (Figure 5-9). The verified stain was designated as MJ500.

5.4 Conclusion

For this project, we successfully isolated and amplified the GR gene sequence from *C. psychrerythraea* 34H using designed primers. The GR gene was inserted into two different expression vectors, which supported the over-expression of *C. psychrerythraea* GR. His-tagged GR (His_6-GR) proteins were purified by multiple-column chromatography and had low enzyme activities. The untagged GR protein expressed using the IMPACT system exhibited high activity even at 4^oC indicating that the untagged recombinant version of *C. psychrerythraea* GR has activity at low temperature as is expected for enzymes from a psychrophilic source.

5.5 Future Work

In order to improve the protection of protein structure and prevention of cellular damage from cold and rapid temperature fluctuations, plants must be redesigned using synthetic biology approaches to express psychrophilic proteins to aid in combating oxidative stress under low-temperature/freezing conditions. A complete biochemical characterization of the *C. psychrerythraea* GR will be performed in the near future and transformation into of the *C. psychrerythraea* GR gene in Arabidopsis will be the next step to test the functionality of the GR protein in plants. Combined expression of the *C. psychrerythraea* GR with superoxide reductase (SOR), rubredoxin (Rd), and rubrerythrin (Rr) from *Pyrococcus furiosus* will be the eventual goal of this project to provide improved protection against damage inflicted by reactive oxygen species that are generated when plants are exposed to environmental stress.

Table 5-1. *E. coli* strains used for GR disruption

E. coli strains	genotype	properties
JM105	(*end*A1, *thi*, *rps*L, *sbc*B15, *hsd*R4, ¢(*lac-pro*AB), [F', *tra*D36, *pro*AB, *lac*IqZDM15])	General purpose host for trc promoter expression
ER2566	F– λ– fhuA2 [lon] ompT lacZ::T7 gene1 gal sulA11 Δ(mcrC-mrr)114::IS10 R(mcr-73::miniTn10–TetS)2 R(zgb-210::Tn10)(TetS) endA1 [dcm]	Host for expression of the fusion protein from pTYB vector in IMPACT T7 system. A derivative of BL21(DE)
BL21(DE)	F-, *omp*T, *hsd*S_β(r_β-m_β-), *dcm*, *gal*, (DE3) tonA.	General purpose host for T7 vector protein expressions.

Table 5-2. The sequences and features of primers used in construction of the disrupted GR mutation in the *E. coli* strains.

E.coli gr (outer region)	Forward 5'-TGGGTCAGCGGATAGCAGAAGG-3'	outer region of the gene (-388 to -366)
	Reverse 5'-CAGTGGATGAGTAAGCGGATGC-3'	outer region of the gene (+624 to +649)
PCR product (*gr*-Cm specific) used in JM105 strain	Forward 5'-CGCTACAATCGCGGTAATCAACGATAAGG-ACACTTTGTCATGTAGGCTGGAGCTGCTTCG-3'	*Homologous region of the gene *chloramphenicol gene cassette region
	Reverse 5'-TTTTGGTTGCCCCCATCTTCAGCG CCACCG-CGAAGCCCTGCATATGAATATCCTCCTTAG-3'	
PCR product (*gr*-Cm specific) used in BL21(DE) strain	Forward 5'-CGCTACAATCGCGGTAATCAACGATAAGG-ACACTTTGTCATGTAGGCTGGAGCTGCTTCG-3'	*Homologous region of the gene *chloramphenicol gene cassette region
	Reverse 5'-CCCTTTAACATTTAACGCATTGTCACGAAC-TCTTCTGCCGCATATGAATATCCTCCTTAG-3'	
PCR product (*gr*-Cm specific) used in ER2566 strain	Forward 5'-GTGATGTGGCACGCGGCGCAAATCCGTGA-AGCGATCCATATGTAGGCTGGAGCTGCTTCG-3'	*Homologous region of the gene *chloramphenicol gene cassette region
	Reverse 5'-TTTTGGTTGCCCCCATCTTCAGCG CCACCG-CGAAGCCCTGCATATGAATATCCTCCTTAG-3'	

Table 5-3. His_6-GR enzyme activity.

Sample	Protein con. (mg/ml)	Sample amount (μL)	mABS/min	Blank (BSA only)	Specific activity (units/mg)
GR at 25°C	1.23	200	-3.1507	-0.4319	5.34
GR at 4°C	1.23	100	-0.9575	0.2038	3.0

The assay was based on the oxidation of NADPH to $NADP^+$ catalyzed by glutathione reductase**.** One GR activity unit is defined as the amount of enzyme catalyzing the reduction of one micromole of GSSG (oxidized GR) per minute.

Table 5-4. Enzyme activity for the unmodified recombinant *C. psychrerythraea* GR

Sample	Protein con. (mg/ml)	Sample amount (μL)	mABS/min	Blank (BSA only)	Specific activity (units/mg)
GR at 25°C	0.075	10	-223	-1.2	142.64
GR at 12°C	0.075	10	-158	-1.2	100.84
GR at 4°C	0.075	10	-93.78	-1.2	59.54

. The assay was performed as described in Table 1.

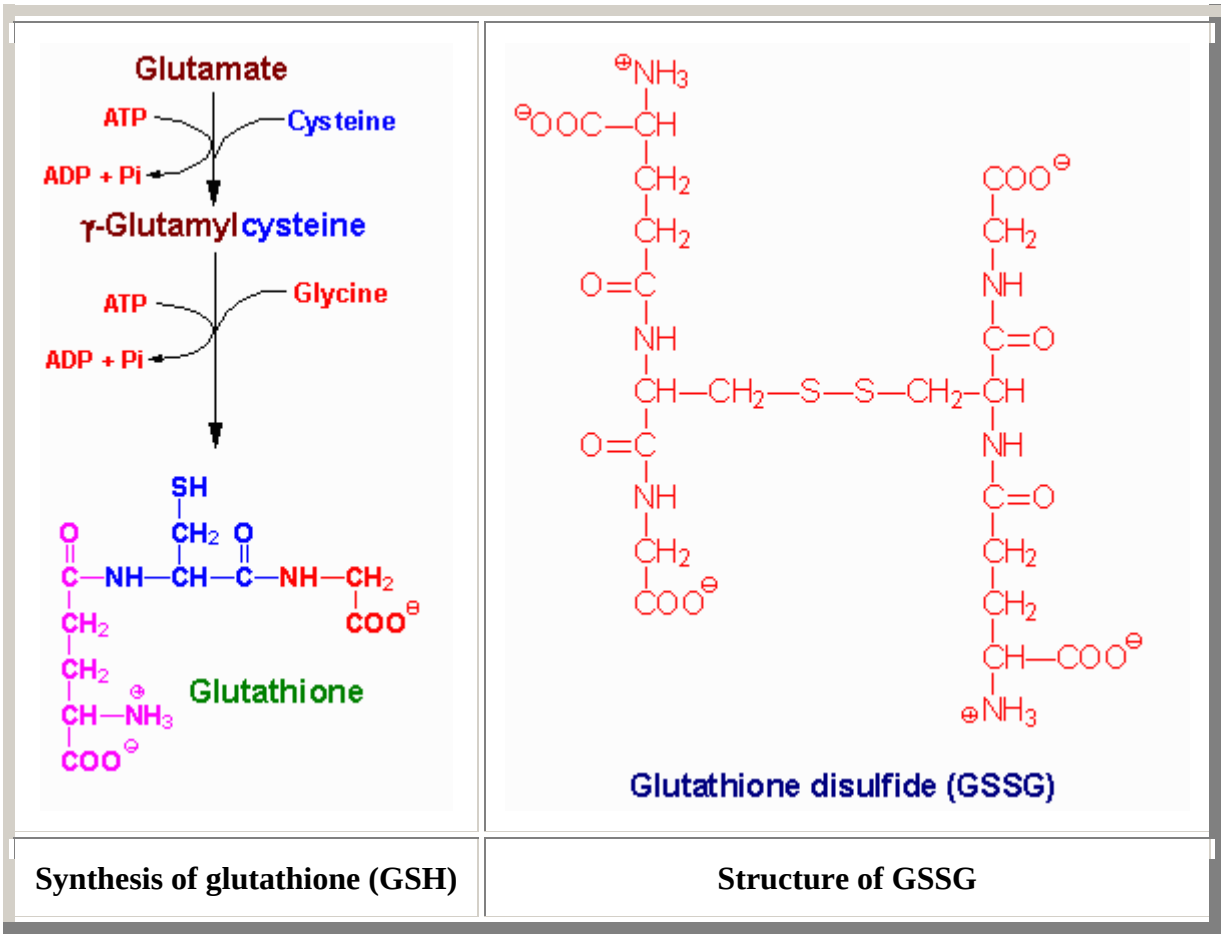

Figure 5-1. The synthesis and structure of GSH (reduced glutathione, left) and structure of GSSG (oxidized glutathione, right). Adapted from 'Medical Biochemistry Page' (34).

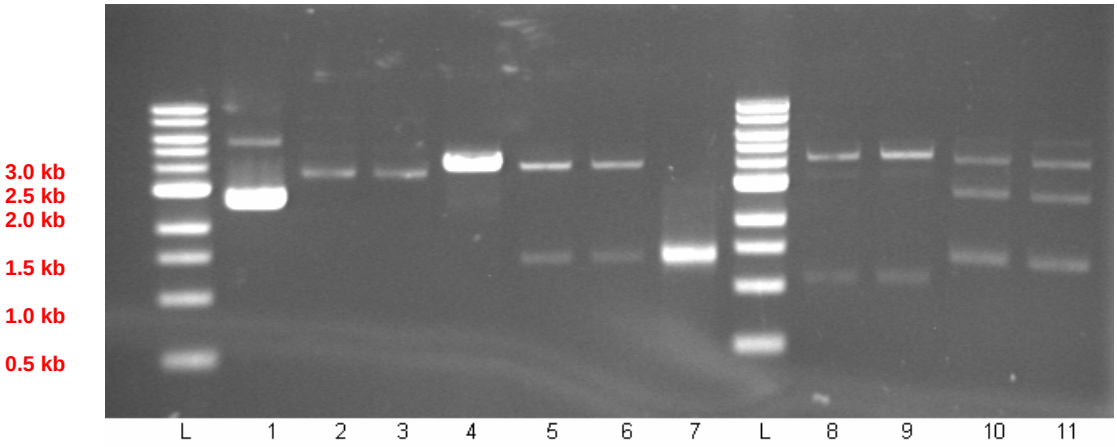

Figure 5-2. Restriction enzyme analysis of glutathione reductase from *C. psychrerythraea 34H* cloned into the pBAD-HisA vector

L : M.W, Lane 1: pBAD/HisA (supercoiled.), 2.Lane 2: Clone #1 (supercoiled), Lane 3: Clone #2 (supercoiled), Lane 4: pBAD/ His A digested with *Xho*I/ *Kpn*I, Lane 5: Clone #1 (digested with *Xho*I and *Kpn*I), Lane 6: Clone # 2 (digested with *Xho*I and *Kpn*I), Lane 7: PCR Product of *C. psychrerythraea* GR, Lane 8. Clone #1 (digested with *EcoR*I), Lane 9: Clone #2 digested with *EcoR*I, Lane 10: Clone # 1 digested with *Sap*I, Lane 11: Clone #2 digested with *Sap* I

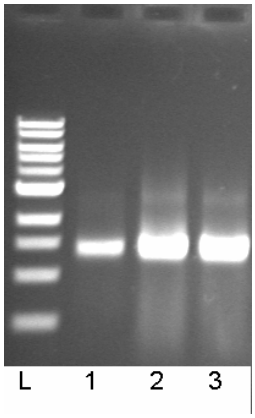

Figure 5-3. PCR verification of *C. psychrerythraea* GR insert in the pBAD-HisA vector. Lane 1: PCR product of *C. psychrerythraea* GR (~1.4 kb), Lane 1:PCR product using clone #1 as template, Lane 2:PCR product using clone #2 as template, L:Molecular weight.

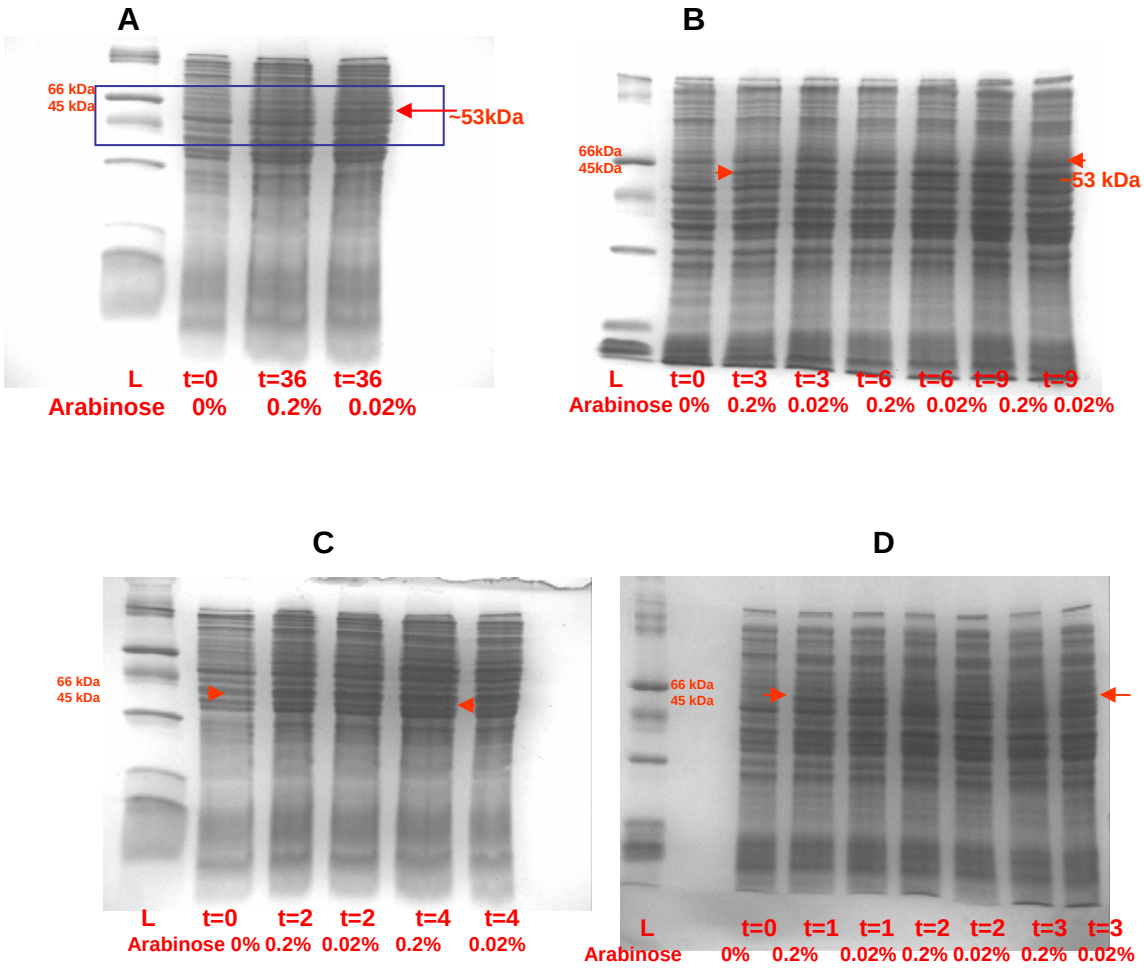

Figure 5-4. *C. psychrerythraea* His_6-GR tagged protein over-expression analysis for protein expression induced at various temperatures. Whole cell pellets were obtained at various time points after induction with 0.2% or 0.02% arabinose. Resuspended cells were denatured at 100°C for 4 min. Expected molecular weight of the protein is ~50kDa. A) *C. psychrerythraea* GR protein expression at 4°C, B) *C. psychrerythraea* GR protein expression at room temperature, C) *C. psychrerythraea* GR protein expression at 30°C, D) *C. psychrerythraea* GR protein expression at 37°C

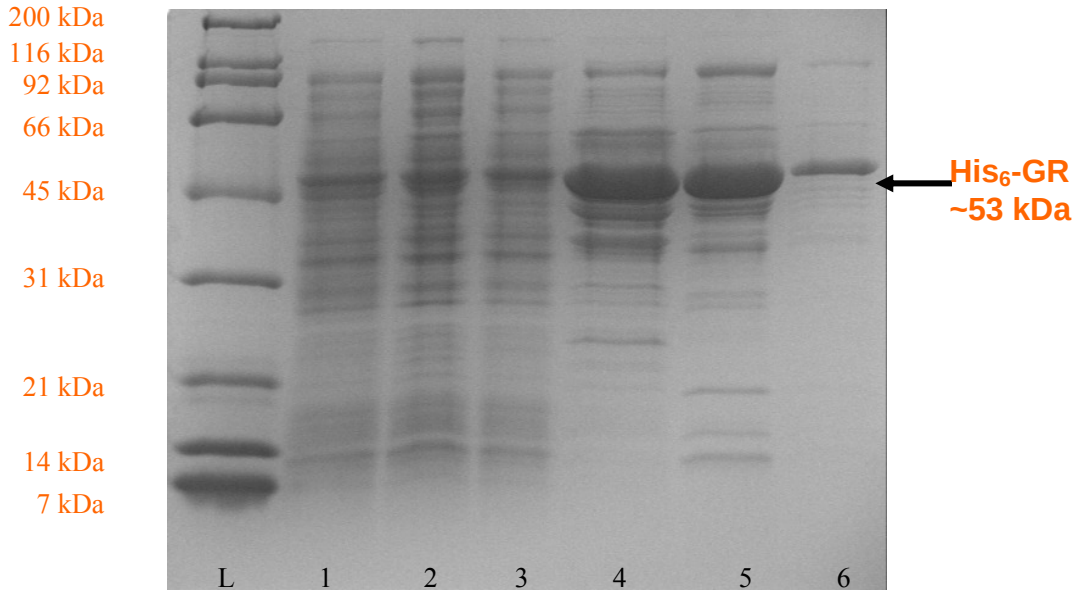

Figure 5-5. Protein purification of the recombinant form of *C. psychrerythraea* His_6-GR. L: Molecular weight marker, Lane 1: Crude cell-free extract, Lane 2: Flow through of first Ni-affinity column, Lane 3: Sample loaded onto Q column, Lane 4: Pooled GR containing fractions from Q column, Lane 5: Pooled GR containing fractions from phenyl sepharose column, Lane 6: Flow though of the second Ni-affinity column

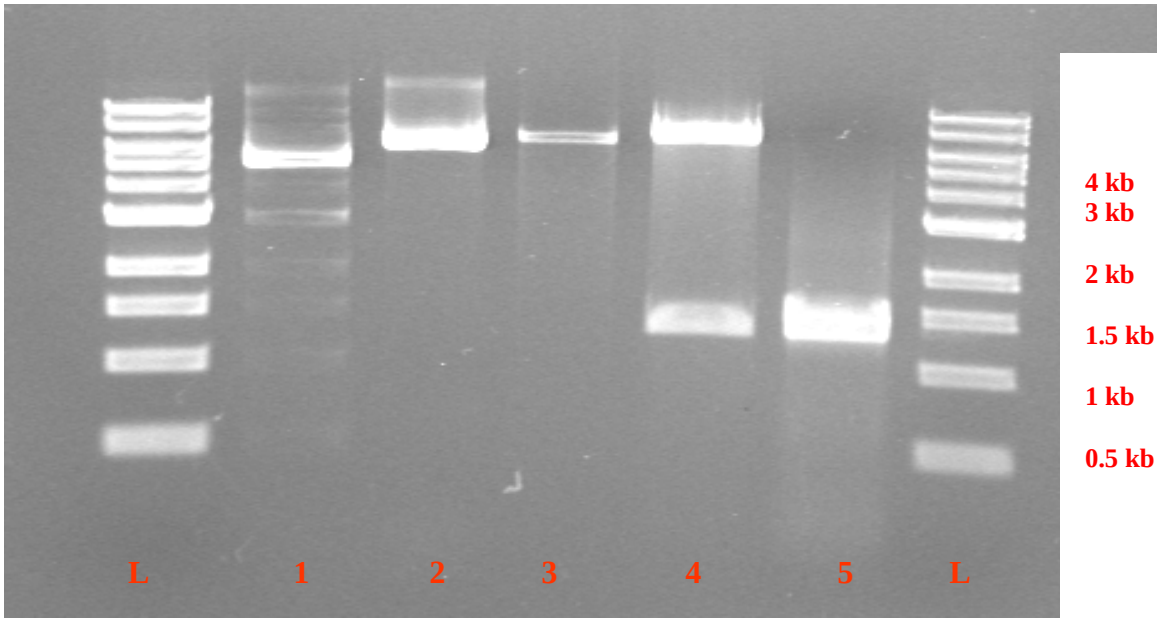

Figure 5-6. Restriction enzyme analysis of glutathione reductase from *C. psychrerythraea* 34H cloned into the in IMPACT vector. L: Molecular weight, Lane 1: pTYB2 (supercoiled), Lane 2:Clone #1-4 (supercoiled), Lane 3. pTYB2 digested with *Sma*I and *Nde*I, Lane 4. Clone #1-4 digested with *Sma*I and *Nde*I, Lane 5. PCR product of GR using *C. psychrerythraea* 34H genomic DNA as template

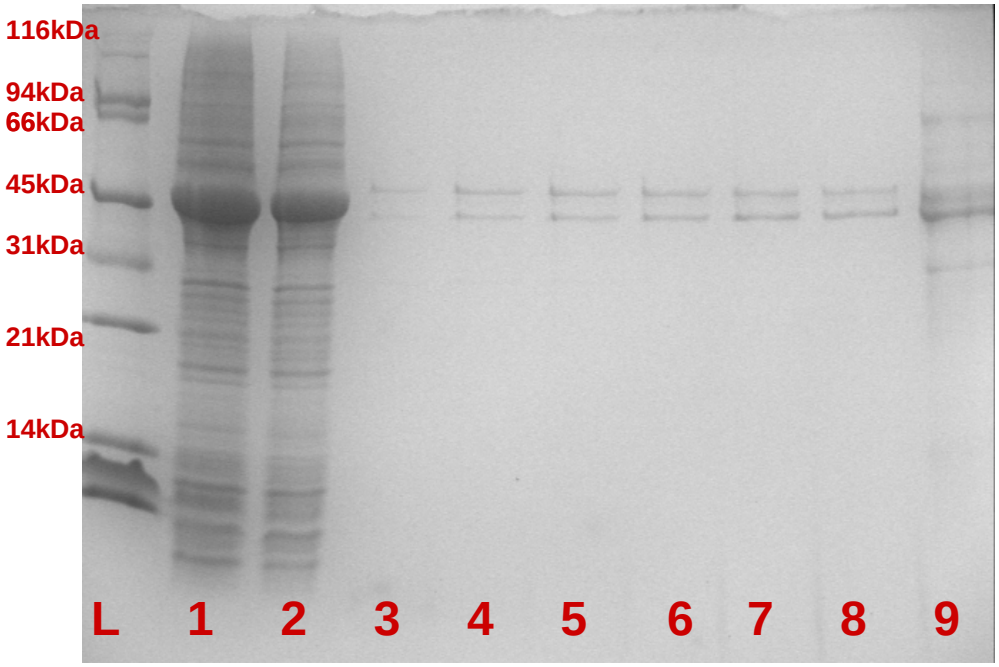

Figure 5-7. Protein purification of the recombinant form of *C. psychrerythraea* GR expressed using the IMPACT system (untagged GR). L: Molecular weight marker, Lane 1: Crude cell free extract, Lane 2: Flow through after chitin column, Lane 3-8: Elution fractions after stopping column flow and inducing a self-cleavage reaction at 4°C for 36 hours., Lane 9: After stripping of remaining proteins bound to chitin column

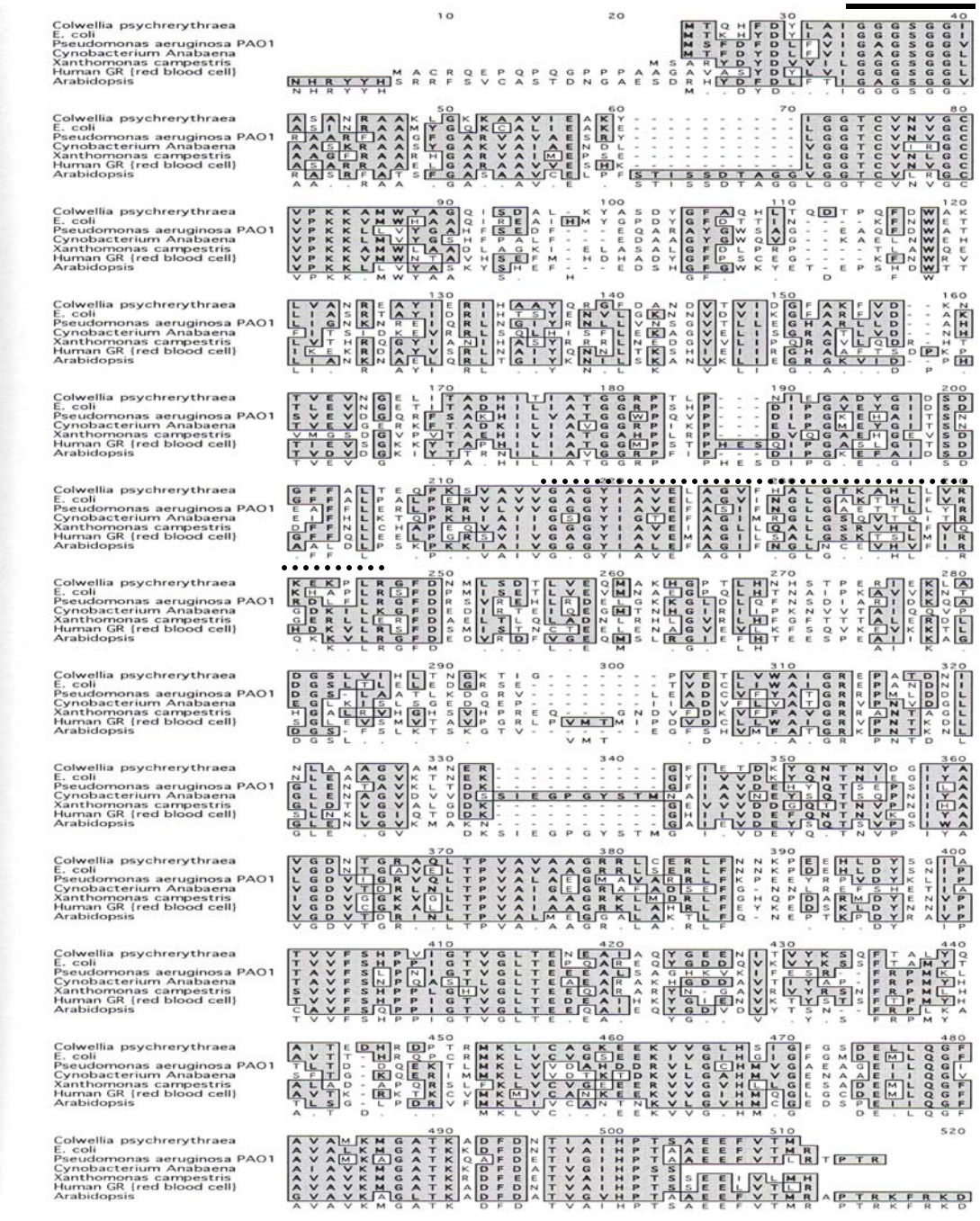

Figure 5-8. Alignment of the amino acid sequence of *C. psychrerythraea* GR with other Grs from other organisms. Solid line indicates the conserved motif for FAD binding, and dotted line indicates the NAD(P)H binding motif.

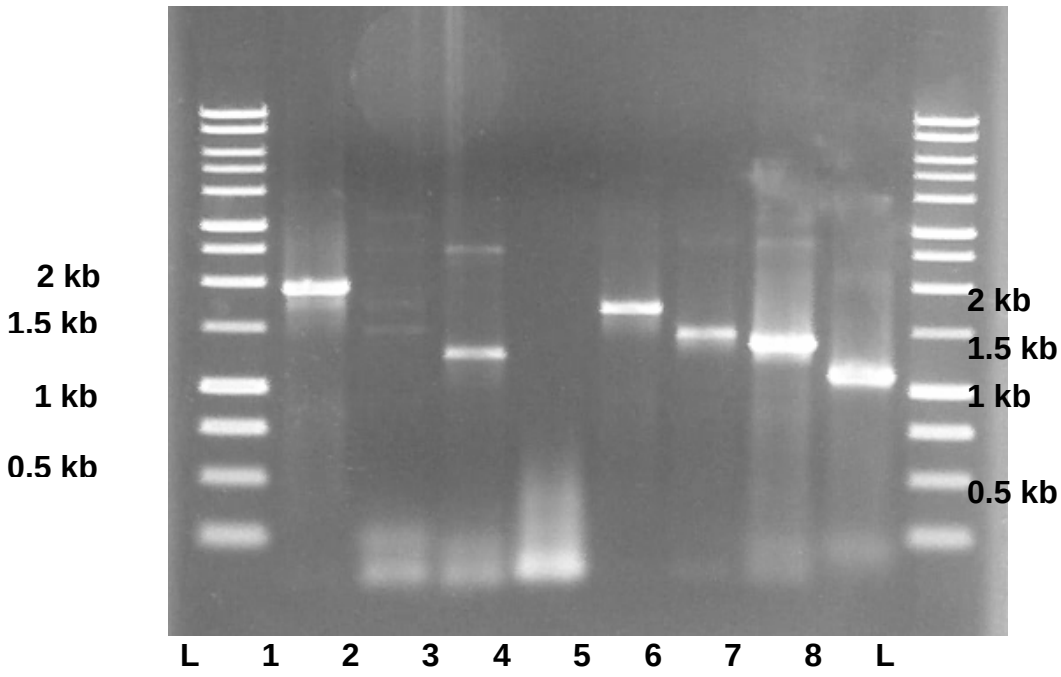

Lanes	Template used	Primers used	Expected sizes
1	JM105 (Parental strain)	5' GR outer region 3' GRouter region	1.95kb
2	JM105 (Parental strain)	5' GR outer region 3' *gr-cm* specific	No DNA
3	JM105 (Parental strain)	5' *gr-cm* specific 3' GR outer region	No DNA
4	JM105 (Parental strain)	5' *gr-cm* specific 3' *gr-cm* specific	No DNA
5	MJ500 *gr* deficient JM105	5' GR outer region 3' GR outer region	1.9 kb
6	MJ500 *gr* deficient JM105	5' GR outer region 3' *gr-cm* specific	1.45 kb
7	MJ500 *gr* deficient JM105	5' *gr-cm* specific 3' GR outer region	1.35 kb
8	MJ500 *gr* deficient JM105	5' *gr-cm* specific 3' *gr-cm* specific	1.1 kb

Figure 5-9. PCR verification of *E. coli gor* mutant (MJ500) using different combinations of gene-Cm specific or outer gene specific primers.

Literature cited

1. **Akerboom, T. P., M. Bilzer, and H. Sies.** 1982. The relationship of biliary glutathione disulfide efflux and intracellular glutathione disulfide content in perfused rat liver. J Biol Chem **257:**4248-52.

2. **Alscher, R. G.** 1989. Biosynthesis and Antioxidant Function of Glutathione in Plants. Physiologia Plantarum **77:**457-464.

3. **Baker, C. J., and N. M. Mock.** 1994. An Improved Method for Monitoring Cell-Death in Cell-Suspension and Leaf Disc Assays Using Evans Blue. Plant Cell Tissue and Organ Culture **39:**7-12.

4. **Bornhorst, J. A., and J. J. Falke.** 2000. Purification of proteins using polyhistidine affinity tags. Methods Enzymol **326:**245-54.

5. **Bradford, M. M.** 1976. A rapid and sensitive method for the quantitation of microgram quantities of protein utilizing the principle of protein-dye binding. Anal Biochem **72:**248-54.

6. **Chattopadhyay, M. K.** 2006. Mechanism of bacterial adaptation to low temperature. Journal of Biosciences **31:**157-165.

7. **Coker, J. A., P. P. Sheridan, J. Loveland-Curtze, K. R. Gutshall, A. J. Auman, and J. E. Brenchley.** 2003. Biochemical characterization of a beta-galactosidase with a low temperature optimum obtained from an Antarctic arthrobacter isolate. J Bacteriol **185:**5473-82.

8. **Creissen, G., P. Broadbent, R. Stevens, A. R. Wellburn, and P. Mullineaux.** 1996. Manipulation of glutathione metabolism in transgenic plants. Biochemical Society Transactions **24:**465-469.

9. **D'Amico, S., T. Collins, J. C. Marx, G. Feller, and C. Gerday.** 2006. Psychrophilic microorganisms: challenges for life. EMBO Rep **7:**385-9.

10. **Datsenko, K. A., and B. L. Wanner.** 2000. One-step inactivation of chromosomal genes in Escherichia coli K-12 using PCR products. Proc Natl Acad Sci U S A **97:**6640-5.

11. **Feller, G.** 2003. Molecular adaptations to cold in psychrophilic enzymes. Cell Mol Life Sci **60:**648-62.

12. **Foyer, C. H., and B. Halliwell.** 1977. Presence of Glutathione and Glutathione Reductase in Chloroplasts - Proposed Role in Ascorbic-Acid Metabolism. Planta **133:**21-25.

13. **Grant, C. M., and I. W. Dawes.** 1996. Synthesis and role of glutathione in protection against oxidative stress in yeast. Redox Report **2:**223-229.

14. **Grant, C. M., F. H. MacIver, and I. W. Dawes.** 1996. Glutathione is an essential metabolite required for resistance to oxidative stress in the yeast Saccharomyces cerevisiae. Curr Genet **29:**511-5.

15. **Groden, D., and E. Beck.** 1979. H2O2 Destruction by Ascorbate-Dependent Systems from Chloroplasts. Biochimica Et Biophysica Acta **546:**426-435.

16. **Halliwell, B., and C. H. Foyer.** 1978. Properties and Physiological Function of a Glutathione Reductase Purified from Spinach Leaves by Affinity Chromatography. Planta **139:**9-17.

17. **Hefti, M. H., J. Vervoort, and W. J. van Berkel.** 2003. Deflavination and reconstitution of flavoproteins. Eur J Biochem **270:**4227-42.

18. **Holmgren, A.** 1976. Hydrogen Donor System for Escherichia-Coli Ribonucleoside-Diphosphate Reductase Dependent Upon Glutathione. Proceedings of the National Academy of Sciences of the United States of America **73:**2275-2279.

19. **Kehrer, J. P., and L. G. Lund.** 1994. Cellular reducing equivalents and oxidative stress. Free Radic Biol Med **17:**65-75.

20. **Kelly, G. J., and E. Latzko.** 1979. Soluble Ascorbate Peroxidase - Detection in Plants and Use in Vitamin-C Estimation. Naturwissenschaften **66:**617-618.

21. **Klatt, P., and S. Lamas.** 2000. Regulation of protein function by S-glutathiolation in response to oxidative and nitrosative stress. Eur J Biochem **267:**4928-44.

22. **Kosower, N. S., and E. M. Kosower.** 1978. The glutathione status of cells. Int Rev Cytol **54:**109-60.

23. **Lomaestro, B. M., and M. Malone.** 1995. Glutathione in health and disease: pharmacotherapeutic issues. Ann Pharmacother **29:**1263-73.

24. **Mavis, R. D., and E. Stellwagen.** 1968. Purification and subunit structure of glutathione reductase from bakers' yeast. J Biol Chem **243:**809-14.

25. **Meister, A., and M. E. Anderson.** 1983. Glutathione. Annual Review of Biochemistry **52:**711-760.

26. **Methe, B. A., K. E. Nelson, J. W. Deming, B. Momen, E. Melamud, X. Zhang, J. Moult, R. Madupu, W. C. Nelson, R. J. Dodson, L. M. Brinkac, S. C. Daugherty, A. S. Durkin, R. T. DeBoy, J. F. Kolonay, S. A. Sullivan, L. Zhou, T. M. Davidsen, M. Wu, A. L. Huston, M. Lewis, B. Weaver, J. F. Weidman, H. Khouri, T. R. Utterback,**

T. V. Feldblyum, and C. M. Fraser. 2005. The psychrophilic lifestyle as revealed by the genome sequence of Colwellia psychrerythraea 34H through genomic and proteomic analyses. Proc Natl Acad Sci U S A **102:**10913-8.

27. **Neftel, A., P. Jacob, and D. Klockow.** 1984. Measurements of Hydrogen-Peroxide in Polar Ice Samples. Nature **311:**43-45.

28. **Noctor, G., A. C. M. Arisi, L. Jouanin, K. J. Kunert, H. Rennenberg, and C. H. Foyer.** 1998. Glutathione: biosynthesis, metabolism and relationship to stress tolerance explored in transformed plants. Journal of Experimental Botany **49:**623-647.

29. **Ritz, D., and J. Beckwith.** 2001. Roles of thiol-redox pathways in bacteria. Annual Review of Microbiology **55:**21-48.

30. **Russell, N. J.** 2000. Toward a molecular understanding of cold activity of enzymes from psychrophiles. Extremophiles **4:**83-90.

31. **Stryer, L.** 1995. Biochemistry, 4th ed. W.H. Freeman, New York.

32. **Studier, F. W.** 2005. Protein production by auto-induction in high density shaking cultures. Protein Expr Purif **41:**207-34.

33. **Tuggle, C. K., and J. A. Fuchs.** 1985. Glutathione reductase is not required for maintenance of reduced glutathione in Escherichia coli K-12. J Bacteriol **162:**448-50.

APPENDIX

Evaluation of the impact of small affinity tags on the expression and activity of recombinant *P. furiosus* NAD(P)H:rubredoxin Oxidoreductase (NROR)

A1. Introduction

The production of recombinant proteins as fusions of the protein of interest with affinity tags is an increasingly popular method for recombinant protein expression, since the affinity tags generally aid in downstream protein isolation. The most widely used affinity tag method is based on the interaction between the side chains of certain amino acids, particularly histidines, on a protein surface and immobilized transition metal ions, and is today known as immobilized metal ion affinity chromatography (IMAC) (15). The metal ions are immobilized on a matrix and interact with imidazole rings of polyhistidine residues that are fused with recombinant proteins. Proteins containing sequences of consecutive histidine residues are efficiently retained on IMAC column matrices, and they can be easily eluted by either adjusting the pH of the column buffer or by adding free imidazole to the column buffer (2).

The most commonly used affinity tag in IMAC is one containing multiple histidine peptides arrayed at either the N- or C-terminus of the recombinant protein (4). IMAC-based purifications in general are simple, one step purification processes that can withstand denaturing conditions (5). The IMAC affinity tag normally is comprised of 6-10 histidines, which are small enough to be incorporated easily into any expression vector. These tags can be added onto target genes by site-directed mutagenesis or by polymerase chain reaction methods (16). DNA fragments coding for the polyhistidine affinity tag can also be created from synthetic oligonucleotides and cloned into an appropriate location in the desired plasmid (6, 18).

Despite its popularity, there are drawbacks to the polyhistidine affinity tag purification approach. One disadvantage of the traditional His tag is that during affinity purification, other proteins (especially those containing several histidines) may bind nonspecifically to the metal

matrix resulting in contamination of unwanted proteins. In mammalian systems in particular there is a higher natural abundance of proteins containing consecutive histidine residues (2, 5). A second potential problem is that the His tag may affect the properties of the recombinant protein. There is a known example where histidine residues in the tag may influence the binding of recombinant DNA-binding proteins to its target DNA, as it has been documented that the His-tag can interfere with the fidelity of the analysis of essential contacts (4). A third potential problem arises when the protein tag is inaccessible to the immobilized metal due to occlusion of the tag in the folded protein (2).

There has been a study that the addition of a C terminal poly-His tag, designed to facilitate purification, resulted in a modified processing of the N terminus of the protein (12). The presence of an N-terminal His-tag can cause the protein to aggregate and prevent ligand binding. Recent estimates indicate that perhaps one-third to one-half of all prokaryotic proteins cannot be over-expressed in bacteria in soluble form using a His-tag (1, 7). Three recent high-throughput studies have indicated that this number is even higher for eukaryotic proteins (3, 10, 17), particularly larger multi-domain proteins. If the problem of insoluble expression of the His-tagged protein in *E. coli* is encountered, one or more of the following options are typically explored. It is known that the affinity tags including His tag can influence the recombinant protein structure, and it is worthwhile to investigate the impact of the affinity tag to the activity of the recombinant protein.

NAD(P)H:rubredoxin oxidoreductase (NROR) from *P. furiosus* is characterized as a monomeric, flavin adenine dinucleotide (FAD)-containing protein catalyzing the NADPH-dependent reduction of rubredoxin , a small (5.3-kDa) iron-containing redox protein (13). A recombinant form of *P. furiosus* NROR was obtained and was use to demonstrate the function of

the *P. furiosus* oxygen detoxification pathway *in vitro* in which superoxide is reduced to hydrogen peroxide in a multi-step process (9). SOR reduces the superoxide using electrons donated from Rd, which is reduced by NROR in an NAD(P)H-dependent reduction (9, 11). The N terminal amino acid sequence of *P. furiosus* NROR has been determined (13) and has the signature sequence of an FAD binding moiety (GXGXXG): MKVVIVGNGPGGFELAKQLSQTYEV (8, 13). It is presumed that the FAD binding pocket presumably will be present in the N-terminal portion of the protein.

Although affinity tags have been employed frequently in purification of recombinant protein, there is no significant data about the impact of small affinity tags, such as the $(His)_6$-tag, on the protein conformation. The influence of affinity tags on recombinant protein structure and stability is not clearly defined. In this study, the impact of the small affinity tags was investigated by attaching various tags in front of the recombinant form of *P. furiosus* NROR protein to determine the resulting affect on the structure.

Three different tags were fused onto the N terminus of the rNROR protein by modifying the multiple cloning region of pET24 (Novagen). pET24dBam was constructed (Mike Weinberg) by replacing the T7 region of pET24d with sequence encoding six histidine residues resulting in the fusion of the $(His)_6$-tag to the N terminus of the *P. furiosus* rNROR (Figure A1, Figure A2). Two additional constructs were developed in this study. pET24dAla was obtained by substituting the 6 histidine residues of pET24dBam with 6 alanine residues. The pET24dMAGS construct was made by deleting the 6 histidine residues of pET24dBam. These 3 different recombinant forms of the *P. furiosus* NROR proteins were purified to investigate the impact of the tags on the structure and activity of the protein.

A2. Methods and Materials

A2.1 Construction of Tagged NROR Vectors

A2.1.1 pET24dBam construction. Novagen's pET24d (FigureA1) was modified by Mike Weinberg by inserting a short piece of DNA between the *Nco*I (CCATG) and *Bam*HI (GGATCC) sites (Figure A2). It was constructed based on substitution of the T7 tag region with 6 histidine residues to investigate the impact of the histidine tag on the NROR activity.

CC-ATG-GCT-CAT-CAC-CAT-CAC-CAT-CAC-GGA-TCC

Met- Ala - His- His- His- His –His---His---Gly---Ser –NROR:start from 2nd A.A.

A2.1.2 pET24dAla and pET24dMAGS construction. Two more different tagged NROR were designed by replacing the six histidine residues of pET24dBam with six alanine residues or by removing them. For these constructs, the following DNA primers were ordered from MWG:

For the Ala tag construct,

5'-CAT-GCC-ATG-GCT-GCG-GCC-GCG-GCG-GCG-GCC-GGA-TCC-CGC-3'

5'-GCG-GGA-TCC-GGC-CGC-CGC-CGC-GGC-CGC-AGC-CAT-GGC-ATG-3'

To give: Met- Ala- Ala- Ala- Ala- Ala- Ala- Ala- Gly- Ser-NROR

For MAGS tag construct,

5'-CAT-GCC-ATG-GCT-GGA-TCC-CGC-3'

5'-GCG-GGA-TCC-AGC-CAT-GGC-ATG-3'

To give: Met- Ala- Gly- Ser-NROR

The complementary oligos for the Ala and MAGS tags of the NROR expression vector were diluted to 100 pmole/μL and heated at 94°C for 4 min. to remove the secondary structure of the DNA fragments. These were slowly cooled and cleaned by ethanol precipitation followed by digesting with *NcoI* and *BamH*I. The vector pET24dBam was also cleaved with *NcoI* and

*BamH*I. Ligation mixes were prepared and incubated overnight at 16^{o}C followed by transformation into the XL1-Blue using conventional $CaCl_2$ treatments. Colonies were picked, and the plasmids were isolated using Qiagen mini preps.

A2.2 Screening the clones. Due to the similar sizes of the inserts compared to pET24dBam, restriction enzyme and PCR verification analyses were performed to select the appropriate clones. For the pET24dAla expression vector, the clones were analyzed by digestion at the *BglI* site, which is present in the middle of the Ala tag-encoding region while pET24dBam does not contain a *Bgl*I restriction site in this area of the vector. For the pET24dMAGS construct, PCR verification using different priming sequences between the tagged regions of pET24dBam and pET24dAla was performed to screen the clones. The forward primer specific for the 'MAGS' region in the pET24dMAGS vector , (5'-AGATATACCATGGCTGGATCCGAA-3') and the forward primer specific for the six-histidine-encoding region in the pET24dBam vector (5'TCATCACCATCACCATCACGG-3') were used for the PCR analysis. . The reverse primer, 5'-GGGTTGAGTGTTGTTCCAGTTTG-3' was designed for use with both of the expression vectors. Temperature gradient PCR was performed to screen the fine fixed position for annealing of the primers to pET24dMAGS vector. The cycles used for the amplification were the following: 30 cycles consisting of denaturation at 95°C for 30 sec., annealing at 70.5°C for 30 sec., and extension at 72°C for 1.5 min. using Pfu polymerase for amplification.
Selected clones for both expression vectors were sequenced (MWG) and their inserts verified.

A2.3 Cloning *P. furiosus* NROR into the pET24sMAGS and pET24dAla vectors. The *P. furiosus* NROR gene from pET24dBam (designated pNROR-His, from Mike Adams lab) was digested using the restriction enzymes *Not*I and *BamH*I, which are located in the multiple cloning site in the pET24dBam vector. The resulting NROR DNA fragments were purified and

ligated into the *Not*I and *BamH*I sites in multiple cloning sites of pET24dMAGS. For the cloning of *P. furiosus* NROR in pET24dAla, the vector was restricted at the *BamH*I and *Xho*I sites and the resultant fragments were ligated with T4 ligase at 16^{o}C during an overnight incubation. These ligation mixes were transformed into XL1-Blue cells using conventional $CaCl_2$ methods and Qiagen Mini-preparations were used to isolate the plasmid DNA. The presence of the *P. furiosus* NROR inserts were screened based on visualization of the migration of the plasmids on DNA-agarose gels. Restriction enzyme digestion analysis was done to verify the NROR insert of the MAGS and Ala tagged expression vectors (pET24dMAGS and pET24dAla, respectively).

A2.4 NROR protein over-expression in BL21(DE3). The cloned NROR in the His-, MAGS- and Ala-tagged vectors were transformed into BL21(DE3) and 30 ml cultures of cells transformed with each of the tagged clones were prepared. The cultures were grown in 30 ml of LB supplemented with 50 mg/L kanamycin (LB + Kan) and were incubated at 37^{o}C with shaking. A total concentration of 0.4mM of IPTG was added when the $O.D._{.600}$ reached about 0.8 for each culture. The cultures were then incubated an additional 3 hours before harvesting the cells. The cultures were centrifuged to collect the cells and the resulting pellets were frozen at –20°C until used. The cell pellets were resuspended in lysozyme buffer (0.03mg/ml lysozyme in 50 mM Tris, pH 8) and sonicated on ice for bursts of 45 sec, 5 times. The cell extracts were centrifuged at 15,000 rpm for 20 min. and supernatants were heat treated at 80^{o}C for 20 min. and centrifuged again at 15,000 rpm to remove the denatured *E. coli* proteins. Protein concentration was determined based on the Bradford method (include reference here). 2X protein loading dye (0.125 M tris-HCl, 4% SDS, 20% v/v glycerol, 0.2MDTT, 0.02% bromophenol blue, pH6.8) was added and the samples were boiled at 100^{o}C for 5 min. Samples (3-5µg) were loaded onto 12.5% polyacrylamide SDS gels. Protein detection was done by staining the gels with Coomassie-Blue.

A2.5 Large-scale NROR purification using anion exchange columns. Each of BL21(DE3) strains containing rNROR in the His-, MAGS-, and Ala-tagged expression vectors were cultured in 2 L LB+Kan. at 37^{o}C with shaking. 0.4mM IPTG was added to the cultures when the O.D.$_{600}$ reached about 0.8 to induce expression of the rNROR proteins. Cells were grown 3 additional hours before harvesting. The cells were collected by centrifugation at 6,000 rpm for 20min. The resulting pellets were stored at –80^{o}C until used. Frozen cells were resuspended in buffer A (50mM Tri, pH 8) and broken with passage through a French Press cell twice (20,000 lb/in^{2}**)**. A cell free extract was obtained by centrifugation of the broken cell suspension at 20,000 rpm for 30 min. The cell free extract was filtered using a 0.4 μm filter and was subsequently vacuum sparged and heat-treated for 30 min. at 80^{o}C anaerobically with continuous stirring. The denatured *E. coli* proteins were pelleted using the same conditions as described above. The heat-treated cell extract was applied to a HiTrap 5mL Q sepharose column (Amersham) at a flow rate of 1 ml/min equilibrated with column buffer A (50 mM tris, pH 8). The loaded column was washed with 3 column volumes of buffer A to remove any loosely bound protein. For purification of the rNROR protein, Buffer A was used for binding the sample and Buffer B (50 mM tris, 1M NaCl, pH 8) was used for the elution. rNROR was eluted at a flow rate of 1 ml/min into 2 ml fractions. Fractions containing rNROR were determined by SDS-PAGE and concentrated with YP-30 Centricon concentrators. The rNROR was stored anaerobically at -80^{o}C until used.

A2.6 rNROR Enzyme Assay. For the FAD reconstitution of rNROR proteins with the three different fusion tags, a 10-fold molar excess of FAD was added to each protein and the protein-FAD mixtures were heat-treated at 85^{o}C for 15min to aid in FAD incorporation into rNROR proteins. The excess FAD was removed by gel filtration. rNROR was stored in a buffer (20mM

Tris-HCl, 200mM NaCl, 1 mM DDT, pH 8) before the rNROR enzyme assays were performed. rNROR activity was determined anaerobically at both 23^{o}C and 80^{o}C using benzyl viologen (BV) as electron acceptor and NADH as an electron donor. The reaction mixture (2 ml) containing 50mM CAPS [3-(cyclohexamino)-1-propanesulfonic acid] buffer, pH 10.2, 1mM Benzyl Viologen, and 0.3 ml NADH was prepared anaerobically and was incubated either at 23^{o}C or 80^{o}C. The enzyme assay was initiated by adding the rNROR and the reaction was followed for 5 min. The reaction involved measuring the reduction rate of BV at 598 nm using a Shimadzu UV-2401 PC spectrophotometer**.**

A2.7 Purification of recombinant Ala-tagged-NROR (rNROR in pET24dAla). The Ala-tagged rNROR was expressed from a 4L LB-Kan culture and was purified using multi-step chromatography. A heat-treated cell free extract was prepared as described above. This cell free extract was applied to a 5mL anion exchange column (HiTrap Q column, Amersham) equilibrated with buffer A (50mM Tris-HCl, pH 8, 1mM DTT, 10% glycerol) and eluted with buffer B (50mM Tris-HCl pH 8, 1M NaCl, 1mM DTT, 10% glycerol) as described above. The flow-through containing the rNROR protein was collected and this was reapplied to 5ml anion exchange column (HiTrap Q column, Amersham) equilibrated with binding buffer (20mM ethanolamine, pH 10, 1mM DTT, 10% glycerol) and eluted with elution buffer (20mM ethanolamine pH10, 1M NaCl, 1mM DTT, 10% glycerol). The flow-through was collected and concentrated using a YP30 Centricon concentrator. The concentrated sample was applied to a 5mL cation exchange column (HiTrap S column, Amersham) equilibrated with buffer A (20 mM MOPS, pH 6.5, 1 mM DTT) and eluted with buffer B (20mM MOPS, pH 6.5, 1M NaCl, 1mM DTT). The flow-through was collected and concentrated using a YP-30 Centricon concentrator. The concentrated sample was made anaerobic using the vacuum-sparge system and was reduced

with the addition of 1 mM DT and 1mM DTT. This sample was sent to University of Georgia for X-ray crystal structure analysis.

A3. Results and Discussion

A3.1 Cloning and screening the pET24dAla and pET24dMAGS expression vectors. The newly constructed expression vectors that have the six histidine residues in pET24dBam either replaced by six alanine residues (pET24dAla) or removed altogether (pET24dMAGS) were screened. Since pET24dAla has a *Bgl*I restriction site in the region coding for the six alanine residues, restriction enzyme analysis was performed to screen the clones (Figure A3). Plasmid pET24Ala has a total of two *Bgl*I sites and its digestion with *Bgl*I resulted in the release of two DNA fragments having the expected sizes of ~3.4 kb and 1.9 kb. On the other hand, plasmid pET24dBam contains only one *Bgl*I site and its digestion with *Bgl*I yielded a single DNA fragment of ~5.3 kb. For the screening of the pET24dMAGS, PCR verification was used to select the clone. Two different kinds of forward primers, specific to the tagging regions, were designed to distinguish between the pET24dMAGS construct and the pET24dBam expression vector. The amplified PCR products that contained the correct priming sites were expected to support amplification. Under stringent amplification conditions, in this case, high annealing temperatures (70.5^{o}C), clone #3 exhibited amplification of the correct PCR product (Figure A4). For this construct, no PCR product was observed when the histidine tag-specific forward primer was used, while the expected size PCR product was obtained when the MAGS specific region forward primer was used. The screened clones for pET24dAla and pET24dMAGS were verified by sequencing (MWG).

A3.2 *P. furiosus* NROR can be expressed as fusions with different types of tags. The previously constructed *P. furiosus* rNROR expression vector, in which rNROR is produced as a His_6-rNROR fusion (pNROR-His), was digested with *BamH*I and *Not*I. This restriction reaction released the *P. furiosus* NROR DNA, which was subsequently purified and ligated into the

corresponding restriction sites in pET24dMAGS. The resulting plasmid was named pNROR-MAGS, and the correct insert was verified by restriction analysis (Figure A5). Expected sizes of DNA fragments were observed (Lane 4, ~1100bp), which has the similar size of DNA as that shown from the digestion of pNROR-His (Lane 2). The same methods were applied to rNROR cloned in to the Ala_6-tag expression vector except for the restriction sites used. For pNROR-Ala plasmid, *BamH*I and *Xho*I restriction sites were used to clone the NROR DNA. The resulting plasmid was named pNROR-Ala and restriction analysis was adapted to ensure the presence of the correct insert DNA (Figure A6). Each of the three plasmids was transformed into BL21(DE3) to observe rNROR protein expression. The expected sizes (~40k Da) of the expressed rNROR fused with the His_6 or MAGS tag were shown in figure 7. The molecular mass of the rNROR protein containing the His_6-fusion tag was slightly greater than that observed for the rNROR-MAGS tagged protein due to the extra six histidine residues in present in the His_6-NROR protein. For rNROR expression from the Ala_6-tag expression vector, the expression of rNROR was showed a different trend than either the His_6-NROR or MAGS-rNROR (Figure A7). The amount of the expressed Ala_6-NROR protein was significantly less compared to either His_6-NROr or MAGS-rNROR, and the Ala_6-rNROR had the tendency to aggregate, especially after heat-treatment for 20 min at 80^{o}C. It is assumed that the hydrophobic amino acid, alanine caused the change if protein expression levels and quality. Six residues of alanine can affect the structure of the recombinant form of *P. furiosus* NROR and cause the protein to fold inappropriately.

A3.3 Enzyme activity for the various tagged forms of *P. furiosus* rNROR. Large scale (2L) cultures of *E. coli* expressing the three different tagged forms of rNROR (His_6-rNROR, Ala_6-rNROR, or MAGS-rNROR) were prepared. Harvested cells were broken into buffer A (50mM

Tris pH 8, 1mM Dithiothreitol) the resulting cell extracts were heat-treated under anaerobic conditions for 20 min at 80^{o}C, and the purification of the various forms of rNROR was performed using anion exchange column (5ml Q column) by eluting the samples with buffer B (50mM Tris pH 8, 1mM Dithiothreitol, 1M NaCl). Fractions that contained the major portions of rNROR were collected and concentrated (Figure A8). From the results, it was observed that major bands are the recombinant forms of *P. furiosus* NROR as the His6 and MAGS-fusion forms. For the purification of the Ala_6-rNROR, considerable contamination with other proteins was observed since the Ala_6-rNROR failed to bind well to the HiTrap Q anion exchange columns. Actually, most of the Ala_6-rNROR protein remained in flow-through after the Q column application at pH 8.0.

The partially purified His_6-rNROR, Ala_6-rNROR, and MAGS-rNROR proteins were reconstituted with FAD followed by heat-treatment for 15 min at 85^{o}C to aid in the incorporation of the FAD (elevated temperature is required to provide flexibility to the hyperthermophile protein to enable efficient binding of cofactor). For heat treatment with FAD, a 10-fold molar excess FAD was added to each protein preparation. Unbound FAD was removed by gel filtration. Quantification of the FAD bound to rNROR was calculated in Table A1. For each tagged rNROR protein, activity assays were performed under anaerobic conditions at 80°C by measuring the reduction rate of benzyl viologen (BV) with NADH serving as the electron donor (Table A2). From the tables, the His_6-rNROR and MAGS-rNROR showed a high ratio of FAD incorporation and significant enzyme activities after reconstitution with FAD. On the other hand, the Ala_6-rNROR protein exhibited low levels of FAD binding a poor enzyme activity even after the FAD reconstitution. From the overall results in this study, it is presumed that alanine tag is inhibiting the FAD binding to rNROR protein resulting in the low observed activity of the

protein. It is known that alanine, which has a small, uncharged side chain, fits well into the α-helical conformation (14). It is possible that the stretch of six alanine residues forms an α-helix, and this can hinder the contact between FAD and the binding pocket of rNROR protein. It was determined that the histidine tag in the His_6rNROR protein does not seem to affect to the FAD binding to the FAD binding region. The results of the table indicated that there is no significant difference in terms of FAD incorporation and enzyme activity between the short tag MAGS-rNROR and the histidine tag His_6-rNROR versions of the recombinant *P. furiosus* NROR.

A3.4 Large-scale purification of recombinant *P. furiosus* NROR. In order to investigate the impact of the alanine tag on the FAD binding pocket of rNROR, large scale of purification of the proteins was performed for X-ray crystal structure analysis. Heat-treated, anaerobic cell extracts derived from 4L expression cultures were applied to multiple chromatography columns for purification (Figure A9). During the purification, it was found that Ala_6-rNROR did not bind to any of the column matrices and that it formed protein aggregates after heat treatment as observed in Figure A9 and Figure A10b. When the concentration of the protein was high (> 1.0 mg/ml) and the protein preparation was maintained at low temperature (~ 4°C), protein aggregation was significantly enhanced. To reduce the observed aggregation, 5% glycerol was added to the purification buffers, the entire purification scheme was conducted as quickly as possible, and a lower temperature heat-treatment was used (75°C). Even with these steps, aggregation still occurred. Since the Ala_6-rNROR protein has the PI value of ~8, storing the protein in buffers with pH values significantly lower than the pI was attempted. Storing the Ala_6-rNROR protein at room temperature in 50mM MOPS buffer pH at 6.5 showed lower levels of protein aggregation compared to the protein stored in 50mM Tris buffer pH at 8, or 20mM ethanolamine buffer pH at 9.5 (Figure A10a). It was concluded that the stretch of six alanine residues at the N terminus of

the rNROR protein are responsible for the enhanced aggregation, poor FAD-binding and low activity of the recombinant *P. furious* NROR. A total of 5mg of the Ala_6-rNROR protein was purified and sent to the University of Georgia for crystallization in order to investigate the influence the alanine tag on the structure of the *P. furiosus* NROR protein.

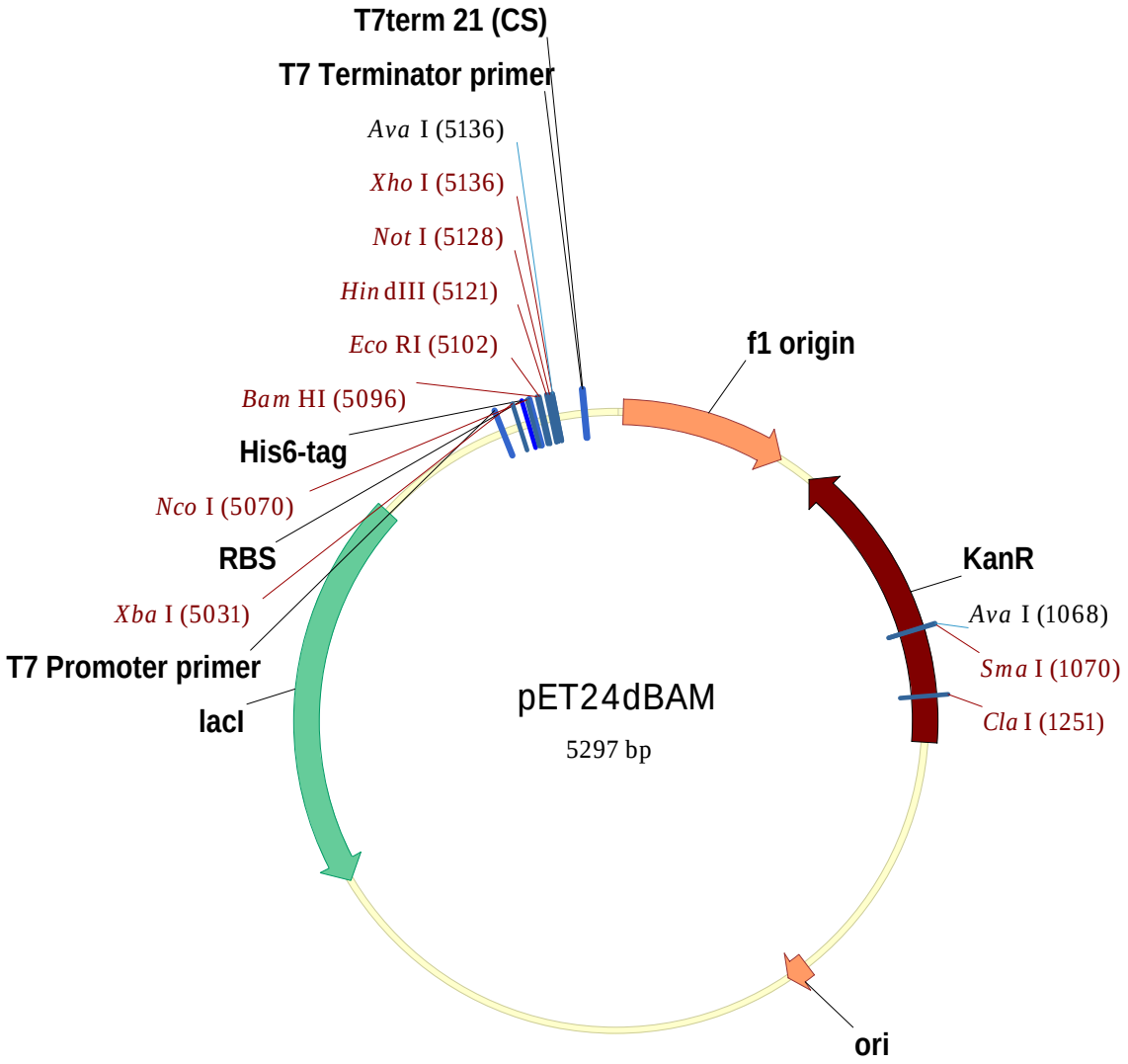

Figure A1. pET24dBam expression vector map. The vector is modified from pET24d (Novagen) by deleting the T7 tag region between the *Nco*I and *BamH*I sites in the multiple cloning sites and replacing with this region with a $(His)_6$-tag encoding region..

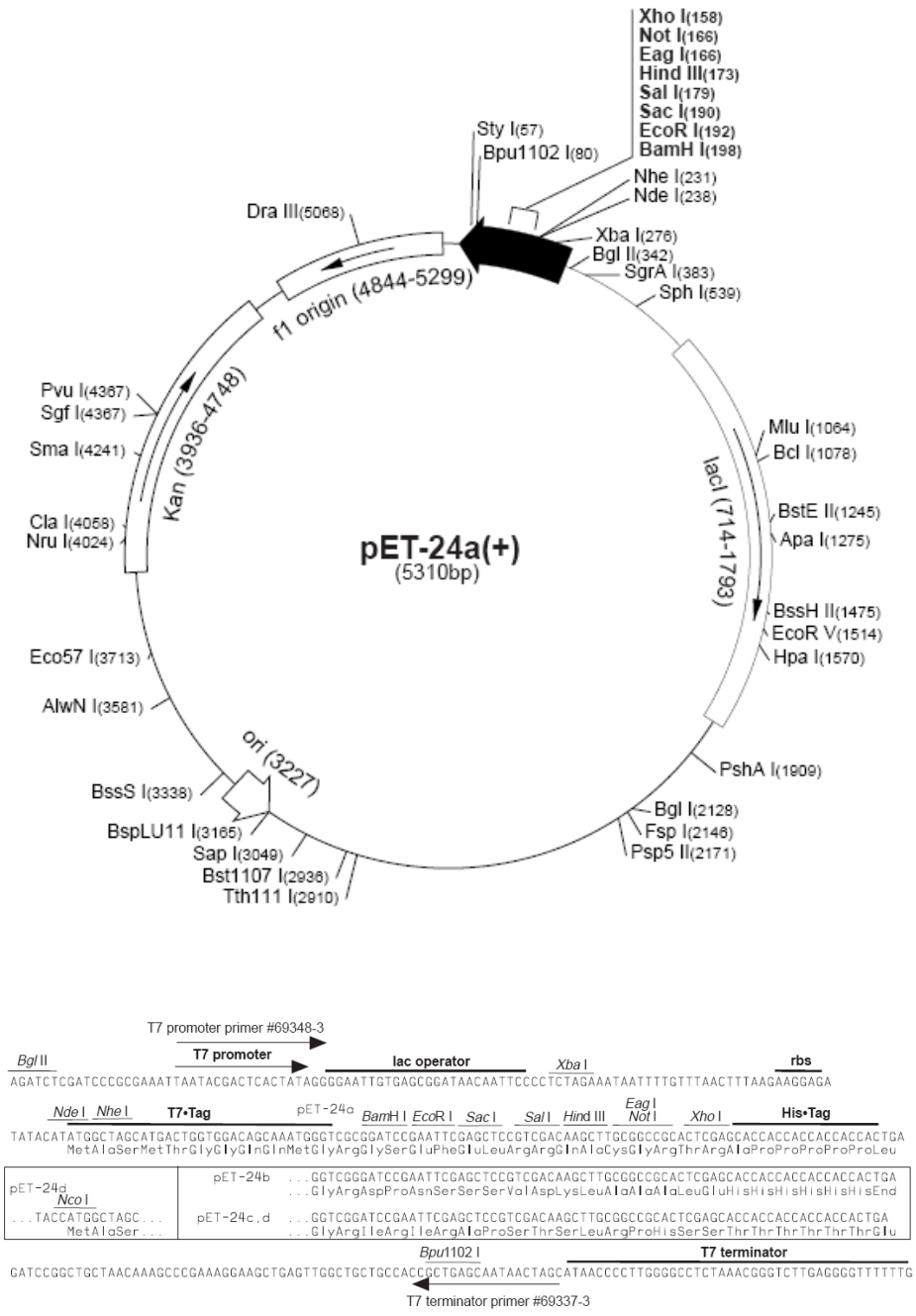

Figure A2. pET24(a-d) vector map and cloning/expression region (Novagen, Germany)

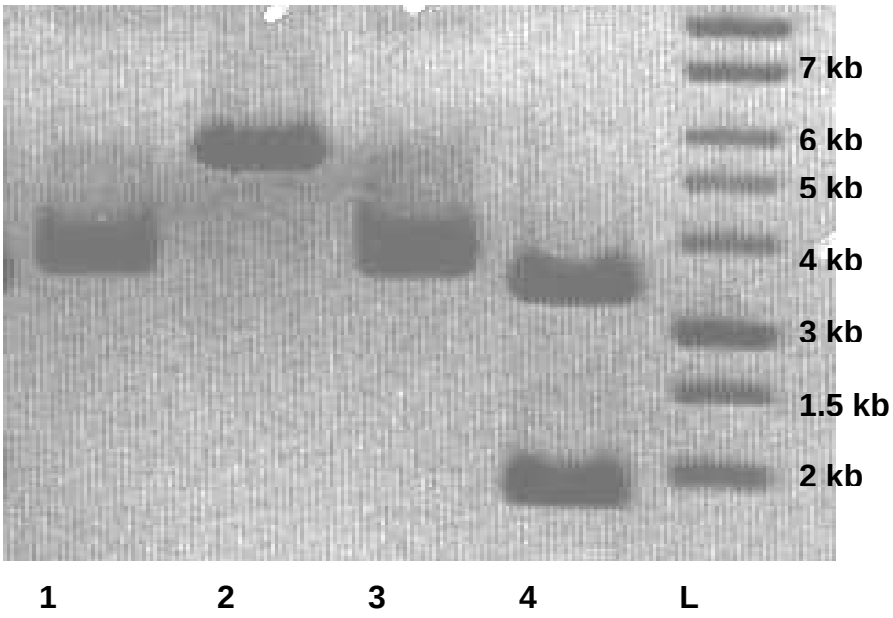

Figure A3. Restriction site analysis for pET24dAla. L: M.W. standard, Lane 1: pET24dBam (supercoiled), Lane 2: pET24dBam (digested with *Bgl*I), Lane 3: pET24dAla (supercoiled), Lane 4: pET24dAla (digested with *Bgl*I)

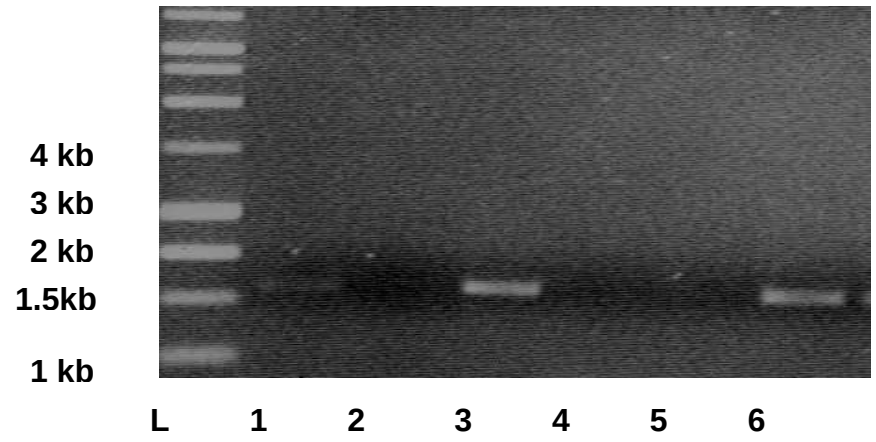

FigureA4. PCR verification to screen the pET24MAGS construct. L: M.W. standard, Lane 1: PCR product using clone #1 as template and (His_6) tag specific forward primer, Lane 2: PCR product using clone #1 as template and MAGS tag specific forward primer, Lane3: PCR product using clone #2 as template and (His_6) tag specific forward primer, Lane 4: PCR product using clone #2 as template and MAGS tag specific forward primer, Lane 5: PCR product using clone #3 as template and (His_6) tag specific forward primer, Lane 6: PCR product using clone #3 as template and MAGS tag specific forward primer. For the reverse primers, same sites are used for the clones. A 70.5^{o}C annealing temperature and Pfu polymerase were used for the amplification of the products.

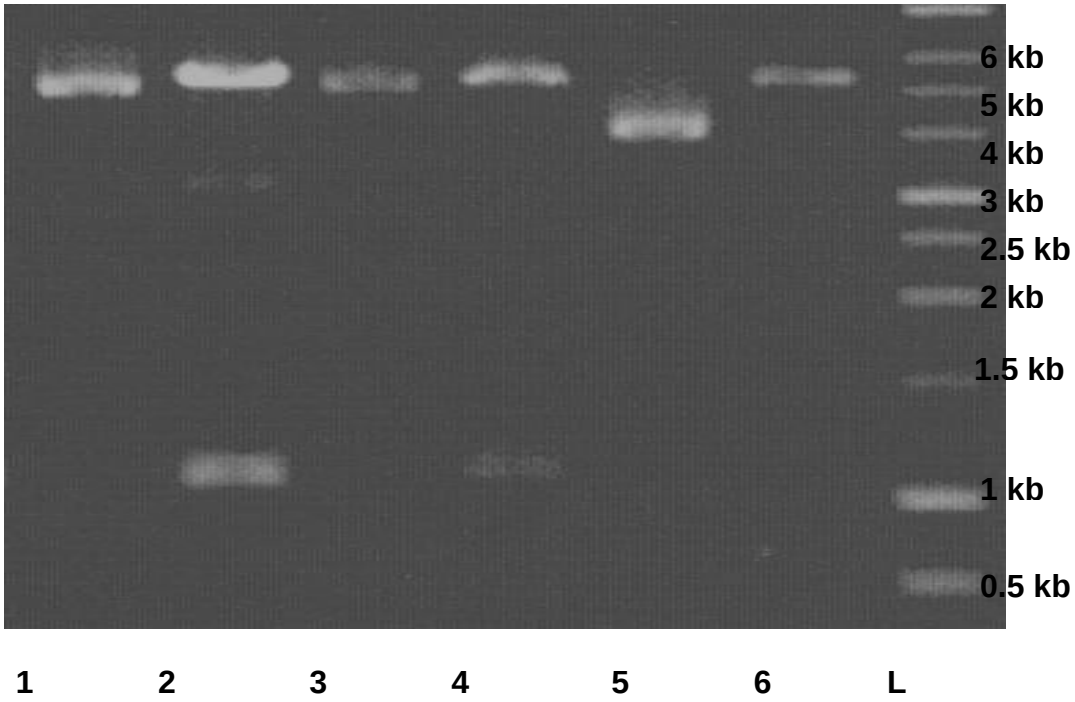

Figure A5. Restriction site analysis for pNROR-MAGS clone**.** L: M. W. standard, Lane 1: pNROR-His (supercoiled), Lane 2: pNROR-His (digested with *BamH*I and *Not*I), Lane 3: pNROR-MAGS clone #1 (supercoiled), Lane 4: pNROR-MAGS clone #1 (digested with *BamH*I and *Not*I), Lane 5: pET24dMAGS (supercoiled), Lane 6: pET24dMAGS (digested with *BamH*I and *Not*I).

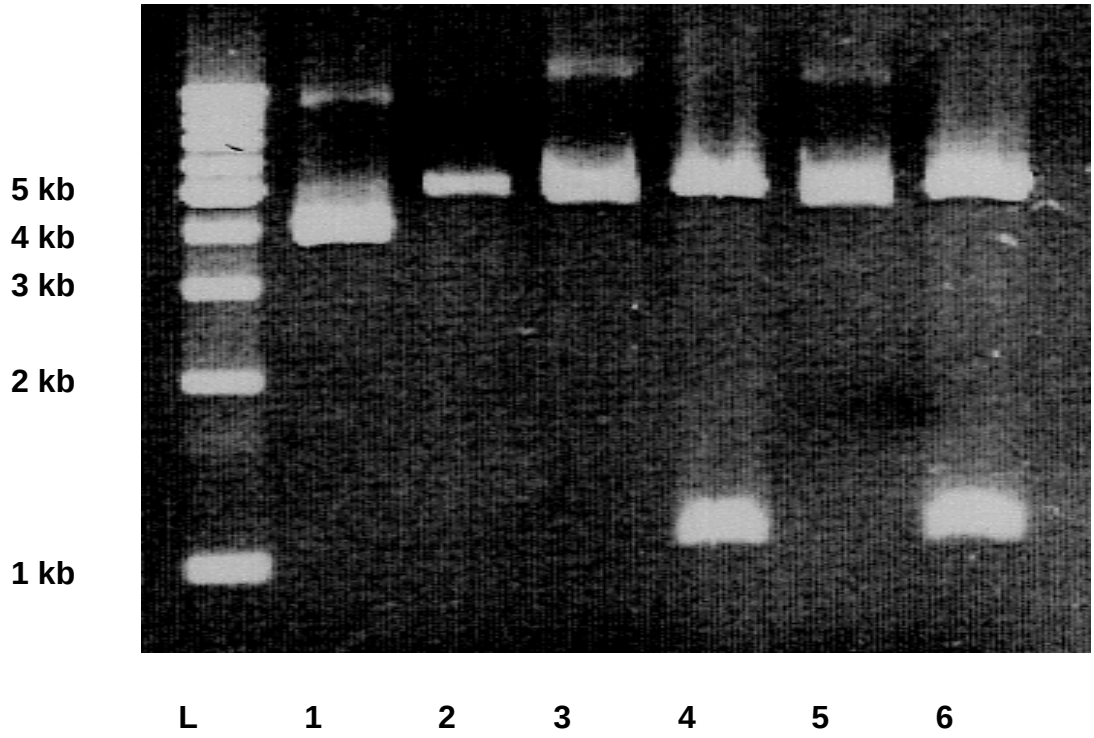

Figure A6. Restriction analysis for pNROR-Ala clone**.** L: M. W. standard, Lane 1: pET24dAla (supercoiled), Lane 2: pET24dAla (digested with *BamH*I and *Xho*I), Lane 3: pNROR-His (supercoiled), Lane 4: pNROR-His (digested with *BamH*I and *Xho*I), Lane 5: pNROR-Ala clone #1 (supercoiled), Lane 6: pNROR-Ala clone #1 (digested with *BamH*I and *Xho*I)

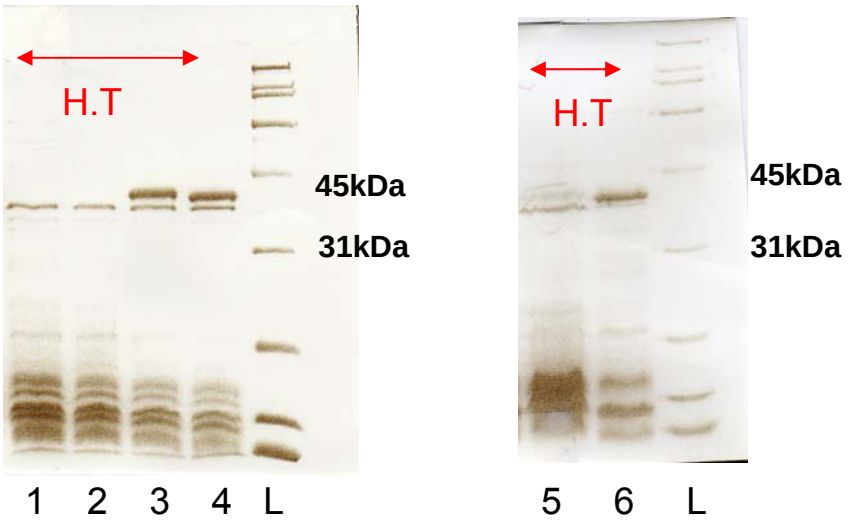

Figure A7. Protein over-expression of *P. furiosus* His_6-NROR, MAGS-NROR, and Ala_6-NROR in *E. Coli* strain BL21(DE3). Expected molecular weigh is about 40k Da. H.T.: heat treated at 80^{o}C for 20min. L: M. W. standard, Lane 1: pET24dBam, cell free extract (5µg), Lane 2: pET24dMAGS, cell free extract, (5µg), Lane 3: *P. furiosus* NROR in (His_6) tag**,** cell free extract (5 µg), Lane 4: *P. furiosus* NROR in MAGS tag**,** cell free extract, (5 µg), Lane 5: pET24dAla, cell free extract (5 µg), Lane 6: pET24dAla, cell free extract (5 µg).

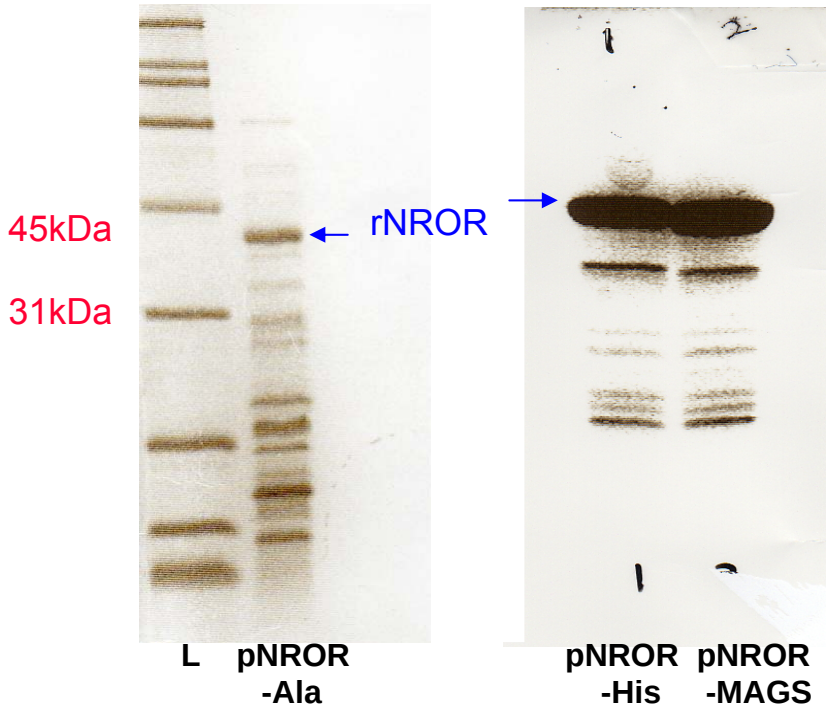

Figure A8. Protein purification of the various recombinant forms of *P. furiosus* NROR. Over-expressed recombinant NROR variant was partially purified using an initial heat-treatment of the crude cell extract followed by anion exchange chromatography (Q column). Fractions containing the rNROR were collected. L: M. W. standard, pNROR-Ala: *P. furiosus* NROR in pET24dAla, pNROR-His: *P. furiosus* NROR in pET24dBam, pNROR-MAGS: *P. furiosus* NROR in pET24dMAGS,

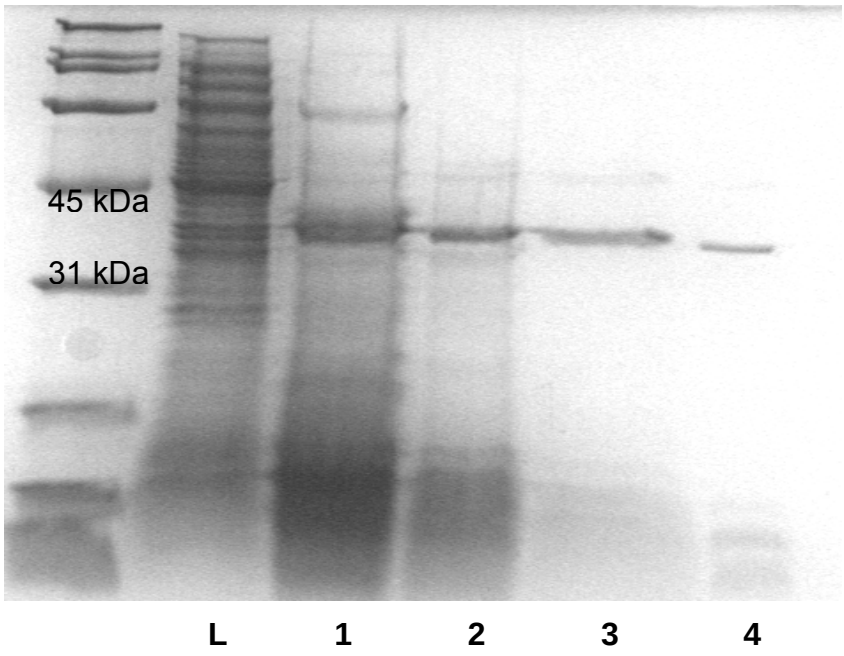

Figure A9. Stages of purification Ala_6-rNROR.

Lane 1: M.W. standard, Lane 1: crude cell extract, Lane 2: cell free extract (Heat-treated), Lane 3: Flow-through after 1st Q column at pH 8, Lane 4: Flow-through after 2nd Q column at pH10, Lane 5: Flow-though SP column at pH 6.5.

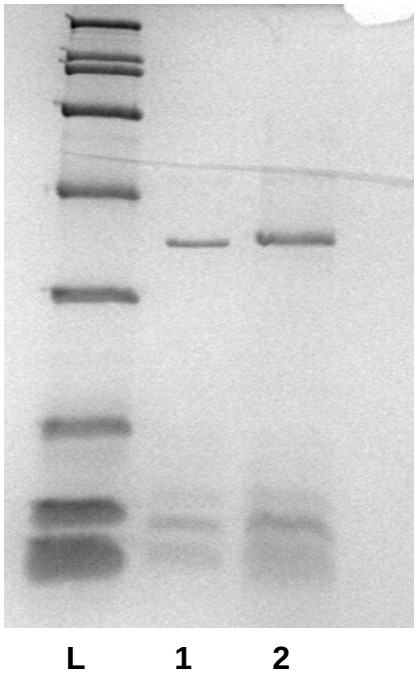

Figure A10a. Purified *P. furiosus* Ala_6-rNROR stored in 50mM MOPS buffer pH at 6.5.

L: M.W. standard, Lane 1: 2 μg, Lane 2: 5 μg

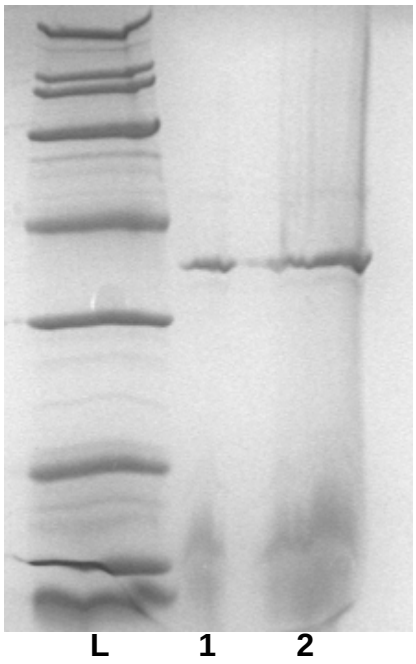

Figure A10b. Purified *P. furiosus* Ala_6-rNROR stored in 50mM Tris buffer pH at 8.

L: M.W. standard, Lane 1: 2 μg, Lane 2: 5 μg

Table A1. Quantification of FAD content of the different tagged recombinant NROR enzymes

RNROR Protein	FAD Conc. (μM)	rNROR Conc. (μM)	% rNROR bound with FAD
MAGS-NROR	1.17	2.7	43.3%
MA(His_6)GS-NROR	0.78	1.3	60.0%
MA(Ala_6)GS-NROR	0.39	4.5	8.7%

Notes for the data table:

FAD was quantified for the same samples heat-treated with FAD used in the various tagged rNROR reconstitution experiments. The FAD content of the rNROR enzymes was determined using the difference absorbance of FAD at 450 nm when oxidized or reduced using a molar coefficient of 10,300 $M^{-1} \bullet cm^{-1}$ at 450 nm for FAD.

Table A2. Reconstitution of the different recombinant tagged-NROR proteins

Sample	Sp. Activity (U/mg)
MAGS-NROR	
As purified apoenzyme	1.4
Heat-treated without FAD	31.2
Heat-treated with FAD	150.7
MA(His_6)GS-NROR	
As purified apoenzyme	0.8
Heat-treated without FAD	19.8
Heat-treated with FAD	185.6
MA(Ala_6)GS-NROR	
As purified apoenzyme	4.3
Heat-treated without FAD	8.6
Heat-treated with FAD	16.3

For heat treatment with FAD, a 10-fold molar excess FAD was added to each protein preparation followed by incubating the indicated proteins at 85 °C for 15 minutes. Unbound FAD was removed by gel filtration. Activity assays were performed at 80°C using reaction mixtures (2 ml) containing 50 mM CAPS buffer, pH 10.2, 0.3 mM NADH, and 1mM BV. The assay was initiated by the addition of rNROR and a molar absorbance of 7,800 $M^{-1} \bullet cm^{-1}$ at 598 nm was used to calculate the rate of BV reduction.

Literature cited

1. **Baek, M. G., R. C. Stevens, and D. H. Charych.** 2000. Design and synthesis of novel glycopolythiophene assemblies for colorimetric detection of influenza virus and E-coli. Bioconjugate Chemistry **11:**777-788.

2. **Bornhorst, J. A., and J. J. Falke.** 2000. Purification of proteins using polyhistidine affinity tags. Methods Enzymol **326:**245-54.

3. **Braun, P., Y. Hu, B. Shen, A. Halleck, M. Koundinya, E. Harlow, and J. LaBaer.** 2002. Proteome-scale purification of human proteins from bacteria. Proc Natl Acad Sci U S A **99:**2654-9.

4. **Buning, H., U. Gartner, D. von Schack, P. A. Baeuerle, and H. Zorbas.** 1996. The histidine tail of recombinant DNA binding proteins may influence the quality of interaction with DNA. Anal Biochem **234:**227-30.

5. **Crowe, J., H. Dobeli, R. Gentz, E. Hochuli, D. Stuber, and K. Henco.** 1994. 6xHis-Ni-NTA chromatography as a superior technique in recombinant protein expression/purification. Methods Mol Biol **31:**371-87.

6. **David, N. E., M. Gee, B. Andersen, F. Naider, J. Thorner, and R. C. Stevens.** 1997. Expression and purification of the Saccharomyces cerevisiae alpha-factor receptor (Ste2p), a 7-transmembrane-segment G protein-coupled receptor. J Biol Chem **272:**15553-61.

7. **Edwards, D. R., and D. T. Denhardt.** 1985. A study of mitochondrial and nuclear transcription with cloned cDNA probes. Changes in the relative abundance of mitochondrial transcripts after stimulation of quiescent mouse fibroblasts. Exp Cell Res **157:**127-43.

8. **Eppink, M. H., H. A. Schreuder, and W. J. Van Berkel.** 1997. Identification of a novel conserved sequence motif in flavoprotein hydroxylases with a putative dual function in FAD/NAD(P)H binding. Protein Sci **6:**2454-8.

9. **Grunden, A. M., F. E. Jenney, Jr., K. Ma, M. Ji, M. V. Weinberg, and M. W. Adams.** 2005. In vitro reconstitution of an NADPH-dependent superoxide reduction pathway from Pyrococcus furiosus. Appl Environ Microbiol **71:**1522-30.

10. **Hammarstrom, M., N. Hellgren, S. van Den Berg, H. Berglund, and T. Hard.** 2002. Rapid screening for improved solubility of small human proteins produced as fusion proteins in Escherichia coli. Protein Sci **11:**313-21.

11. **Jenney, F. E., Jr., M. F. Verhagen, X. Cui, and M. W. Adams.** 1999. Anaerobic microbes: oxygen detoxification without superoxide dismutase. Science **286:**306-9.

12. **Ledent, P., C. Duez, M. Vanhove, A. Lejeune, E. Fonze, P. Charlier, F. Rhazi-Filali, I. Thamm, G. Guillaume, B. Samyn, B. Devreese, J. Van Beeumen, J. Lamotte-Brasseur, and J. M. Frere.** 1997. Unexpected influence of a C-terminal-fused His-tag on the processing of an enzyme and on the kinetic and folding parameters. FEBS Lett **413:**194-6.

13. **Ma, K., and M. W. Adams.** 1999. A hyperactive NAD(P)H:Rubredoxin oxidoreductase from the hyperthermophilic archaeon Pyrococcus furiosus. J Bacteriol **181:**5530-3.

14. **Monera, O. D., F. D. Sonnichsen, L. Hicks, C. M. Kay, and R. S. Hodges.** 1996. The relative positions of alanine residues in the hydrophobic core control the formation of two-stranded or four-stranded alpha-helical coiled-coils. Protein Eng **9:**353-63.

15. **Nilsson, J., S. Stahl, J. Lundeberg, M. Uhlen, and P. A. Nygren.** 1997. Affinity fusion strategies for detection, purification, and immobilization of recombinant proteins. Protein Expr Purif **11:**1-16.

16. **Nygren, P. A., S. Stahl, and M. Uhlen.** 1994. Engineering proteins to facilitate bioprocessing. Trends Biotechnol **12:**184-8.

17. **Shih, Y. P., W. M. Kung, J. C. Chen, C. H. Yeh, A. H. Wang, and T. F. Wang.** 2002. High-throughput screening of soluble recombinant proteins. Protein Sci **11:**1714-9.

18. **Skerra, A.** 1994. A general vector, pASK84, for cloning, bacterial production, and single-step purification of antibody Fab fragments. Gene **141:**79-84.